AN INVESTIGATION INTO THE EFFECTS OF ALTERATIONS IN RIBOSOMAL PROTEINS S4 AND S5 ON TRANSLATIONAL ACCURACY, RIBOSOMAL RNA PROCESSING, AND RIBOSOME ASSEMBLY

A DISSERTATION IN
Molecular Biology and Biochemistry
and
Cell Biology and Biophysics

Presented to the Faculty of the University
of Missouri-Kansas City in partial fulfillment of
the requirements for the degree

DOCTOR OF PHILOSOPHY

by
DIVYA KAMATH

M.S., University of Missouri-Kansas City, 2013

Kansas City, Missouri

2016

©2016

DIVYA VIJAYVINAYAK KAMATH

ALL RIGHTS RESERVED

AN INVESTIGATION INTO THE EFFECTS OF ALTERATIONS IN RIBOSOMAL PROTEINS S4 AND S5 ON TRANSLATIONAL ACCURACY, RIBOSOMAL RNA PROCESSING, AND RIBOSOME ASSEMBLY

Divya Kamath, Candidate for the Doctor of Philosophy Degree

University of Missouri-Kansas City, 2016

ABSTRACT

Accurate translation of genetic message is an essential step in gene expression and is carried out by the ribosome. Ribosomal proteins S4 and S5 are critical for the decoding and the assembly processes on the ribosome. The interaction between residues in the S4-S5 interface region is crucial for the large scale conformational changes occurring on the ribosome during decoding. Earlier studies predominantly isolated S4 and S5 mutations located near the S4-S5 interface. However, recent studies show that ribosomal proteins S4 and S5 affect translational accuracy to a larger extent than previously realized.

To understand the diverse ways by which mutation in S4 and S5 can affect translational accuracy, we generated and studied a wide array of S4 and S5 mutants with altered accuracy phenotypes, that were located not only at the interface but also distributed

throughout the protein. We also generated a collection of mutants with alteration in the loop 2 region of S5 protein. As the loop 2 region is away from the interface, it modulates accuracy by mechanisms different than disruption of the S4-S5 interface. The C-terminal region of S4 protein interacts extensively with the S5 protein and C-terminal truncated mutants are temperature sensitive, have a ribosome assembly defect and are error-prone. We obtained temperature insensitive S4 mutants with restored C-termini that partially rescued miscoding but almost completely rescued the ribosome assembly defect at 42˚C. Finally, in the process of exploring interactions of S4 and S5 with other regions in the ribosome, we discovered that accuracy can be altered indirectly by affecting amino acid pools or tRNA modification.

APPROVAL PAGE

The faculty listed below, appointed by the Dean of the School of Graduate Studies, have examined a dissertation titled "An Investigation into the Effects of Alterations in Ribosomal Proteins S4 and S5 on Translational Accuracy, Ribosomal RNA Processing, and Ribosome Assembly", presented by Divya Kamath, candidate for the Doctor of Philosophy degree, and certify that in their opinion it is worthy of acceptance.

Supervisory Committee

Michael O'Connor, PhD., Committee Chair
Department of Molecular Biology and Biochemistry

Samuel Bouyain, DPhil.
Department of Molecular Biology and Biochemistry

Leonard Dobens, PhD.
Department of Molecular Biology and Biochemistry

Thomas Menees, PhD.
Department of Cell Biology and Biophysics

Michael D. Plamann, PhD.
Department of Cell Biology and Biophysics

CONTENTS

ABSTRACT iii
LIST OF ILLUSTRATIONS viii
LIST OF TABLES xi
LIST OF SUPPLEMENTAL ILLUSTRATIONS xii
LIST OF SUPPLEMENTAL TABLES xiii
LIST OF ABBREVIATIONS xiv
ACKNOWLEDGEMENTS xvi
Chapter
1. INTRODUCTION 1
1.1 Overview of Bacterial Translation Process 1
1.2 Cellular Machinery Involved in the Elongation Cycle 4
1.3 The Elongation Cycle 18
1.4 Genetic Studies on Translational Accuracy 30
1.5 References 38
2. MODULATION OF DECODING FIDELITY BY RIBOSOMAL PROTEINS S4 AND S5 45
2.1 Abstract 45
2.2 Introduction 46
2.3 Materials and Methods 49
2.4 Results 53
2.5 Discussion 66
2.6 Acknowledgements 71
2.7 References 72
2.8 Supplemental Information 76
2.9 References for Supplemental Information 88
3. THE LOOP 2 REGION OF RIBOSOMAL PROTEIN uS5 INFLUENCES SPECTINOMYCIN RESISTANCE, TRANSLATIONAL FIDELITY AND RIBOSOME BIOGENESIS 90

3.1 Abstract 90
3.2 Introduction 91
3.3 Materials and Methods 93
3.4 Results 97
3.5 Discussion 109
3.6 Acknowledgements 111
3.7 References 112
3.8 Supplemental Information 116
3.9 References for Supplemental Information 122
4. THE C-TERMINUS OF RIBOSOMAL PROTEIN S4 CONTRIBUTES TO 30S SUBUNIT ASSEMBLY AND FIDELITY OF TRANSLATION 123
4.1 Abstract 123
4.2 Introduction 124
4.3 Materials and Methods 126
4.4 Results 131
4.5 Discussion 151
4.6 References 155
4.7 Supplemental Information 157
5. INDIRECT INTERACTIONS OF S4 AND S5 RIBOSOMAL PROTEINS AFFECTING TRANSLATIONAL FIDELITY 159
5.1 Abstract 159
5.2 Introduction 160
5.3 Materials and Methods 161
5.4 Results 166
5.5 Discussion 180
5.6 References 183
5.7 Supplemental Information 186
6. CONCLUSIONS AND FUTURE DIRECTIONS 190
VITA 196

LIST OF ILLUSTRATIONS

Figure Page

1.1 The bacterial translation process....2
1.2 The structure of bacterial 16S rRNA....5
1.3 The structure of bacterial tRNA....6
1.4 The secondary structure of bacterial elongation factors....8
1.5 The structure of bacterial ribosomes....10
1.6 Maturation of ribosomal RNAs in bacteria....12
1.7 Assembly map of SSU r-proteins on 16S rRNA....14
1.8 Interaction of tRNA and mRNA in the A, P, and E site....16
1.9 The bacterial elongation cycle....18
1.10 Formation of an aminoacylated-tRNA molecule....19
1.11 Kinetic scheme for decoding....20
1.12 Large subunit structure showing L7/L12 stalk....21
1.13 Recognition of minor groove geometry by 16S rRNA....23
1.14 Cross section of 30S subunit in the region of the decoding center....24
1.15 Role of His84 of EF-Tu during GTPase activation and GTP hydrolysis....26
1.16 Dynamics of translocation....28
2.1 Effects of selected mutations in ribosomal proteins S5 and S4 on growth on solid medium at 20˚C, 37˚C, and 42˚C....59
2.2 Effects of altered ribosomal proteins S4 and S5 on missense decoding and UGA readthrough....62
2.3 Ribosome profiles of a wild type strain and selected S4 and S5 mutants that displayed altered profiles....64
2.4 rRNA processing in wild-type (WT) and selected S4 and S5 mutant strains....65
2.5 Prediction of structural effects of amino acid substitutions and termination mutants on the basis of the wild-type *E.coli* 70S ribosome crystal structure....69

3.1 Location of ribosomal protein S5 amino acid substitutions in the ribosome three-dimensional structure. 100
3.2 Effects of selected ribosomal proteins uS5 mutations on growth at 20˚C and 37˚C .102
3.3 Effects of altered ribosomal proteins uS5 on UAG readthrough 104
3.4 Effects of altered uS5 ribosomal proteins on missense decoding....105
3.5 Ribosome profiles of a wild-type strain and uS5 mutant strains grown at 37˚C 106
3.6 rRNA processing in wild-type (WT) and selected uS5 mutant strains....108
4.1 Effects of ribosomal proteins S4 mutations on growth at 20˚C, 37˚C and 42˚C 136
4.2 Effects of altered ribosomal proteins S4 on UGA readthrough 137
4.3 Ribosome profiles of a wild-type strain and S4 mutant strains grown at 37˚C and 42˚C....138
4.4 rRNA processing in wild-type (WT) and S4 mutant strains grown at 37˚C and 42˚C 140
4.5 Effects of reconstructed altered ribosomal protein S4 (containing wild-type S17) on growth on solid media at 20ºC, 37ºC, and 42ºC 144
4.6 Effects of reconstructed altered ribosomal protein S4 (containing wild-type S17) on UGA (top) and UAG (bottom) readthrough at 37˚C and 42˚C 145
4.7 Ribosome profiles of a wild-type strain and S4 mutant strains (containing wild-type S17) grown at 37˚C and 42˚C 146
4.8 rRNA processing in wild-type (WT) and reconstructed S4 mutant strains (containing wild-type S17) grown at 37˚C (top) and 42˚C (bottom) 147
4.9 Effects of altered *E.coli* and *Salmonella* ribosomal protein S4 on UGA (top) and UAG (bottom) readthrough 149
4.10 Ribosome profiles of a wild-type and altered S4 mutants at 37˚C for *E.coli* and *Salmonella* ribosomal protein 150
5.1 Transposition and isolation of Tn10 linked to suppressors 164
5.2 Complementation experiments using *E.coli* genomic libraries. 167
5.3 Isolation and identification of unknown secondary mutation in Hss. 169
5.4 Hydroxyurea sensitivity testing 173

5.5 Isolation and identification of unknown secondary mutation in Sup2 and Sup3. 174
5.6 Isolation of suppressor of cold sensitivity 176
5.7 Isolation and identification of unknown secondary mutation in Evo4 and Evo5. 178

LIST OF TABLES

Table Page

1.1 Accuracy altering mutations in r-proteins.....33

2.1 Effects of altered S4 and S5 ribosomal proteins on growth and antibiotic sensitivity 55

3.1 Spectinomycin resistance, decoding, cold sensitivity phenotypes and doubling times of uS5 mutants. 98

4.1 Alterations in the C-terminal *rpsD* mutant strain 133

5.1 Characteristics of the strains used for isolation of secondary mutation in an error-prone mutant strain 165

5.2 Characteristics of the strains used for isolation of secondary mutation in an error-restrictive mutant strain.....171

5.3 Characteristics of the strains used for isolation of secondary mutation that increase fitness in the selected mutant strain 177

LIST OF SUPPLEMENTAL ILLUSTRATIONS

Figure Page

S2.1 Intersubunit bridge B8 76

S3.1 Effects of altered ribosomal protein uS5 on UGA readthrough. 120

LIST OF SUPPLEMENTAL TABLES

Table		Page
S2.1	Previously reported alterations affecting ribosomal proteins S4 and S5	77
S2.2	Distance measurements of residues involved in protein-protein and protein –rRNA contacts	84
S2.3	Summary of probable structural effects of amino acid substitutions	85
S2.4	Oligonucleotides used in chapter 2	87
S3.1	Method of isolation, spectinomycin resistance, decoding and cold sensitivity phenotypes and doubling times of uS5 mutants	118
S3.2	Oligonucleotides used in chapter 3	121
S4.1	Oligonucleotides used in chapter 4	157
S5.1	Oligonucleotides used in chapter 5	186

LIST OF ABBREVIATIONS

aaRS	aminoacyl-tRNA synthetase
aa-tRNA	Aminoacyl transfer RNA
AMP	Adenosine monophosphate
ASL	Anticodon Stem Loop
ATP	Adenosine Triphosphate
BLAST	Basic Local Alignment Search Tool
DNA	Deoxyribose Nucleic Acid
EF-G	Elongation Factor-translocase
EF-Tu	Elongation Factor- Thermounstable
FRET	Forster Resonance Energy Transfer
GAC	GTPase Activation Factor
GDP	Guanine Diphosphte
GTP	Guanine Triphosphate
IF	Initiation Factor
IPTG	Isopropyl-β-d-thiogalacopyranoside
Kb	Kilobase
LSU	Large subunit
MDa	Mega Dalton
MM	Minimal Media
MOI	Multiplicity of Infection
mRNA	Messenger RNA
PPi	inorganic pyrophosphate
PTC	Peptidyl transferase center
Ram	ribosomal ambiguity mutant
RF	Release factor
Rim	Ribosomal modification
RNA	Ribose Nucleic Acid
RRF	Ribosome recycling factor

Rrn	ribosomal RNA
SmD	Streptomycin dependent
SmI	Streptomycin independent
SmR	Streptomycin resistant
SRL	Sarcin-Ricin Loop
SSU	Small Subunit
tRNA	Transfer RNA
X-Gal	5-bromo-4-chloro-3-indolyl-β-D-galactopyranoside

ACKNOWLEDGEMENTS

I would like to thank my advisor Dr. Michael O'Connor for his guidance, patience, and support throughout the course of my Ph.D. I would like to extend my sincere gratitude to the members of my committee Dr. Samuel Bouyain, Dr. Leonard Dobens, Dr. Thomas Menees and Dr. Michael Plamann for not only their scientific comments and insights but also for the constant support and encouragement. I would also like to thank Dr. Brian Geisbrecht and Dr. Sean Yu for the interactions I had with them during my laboratory rotation. Special thanks to Dr. Karen Bame, for making sure everything goes smoothly for all the students. Her constant help, guidance, and support definitely made our life here easier.

I am grateful for the wonderful friends that I have made during the past few years. I would especially like to thank Anna Shipman, Kristen Nondorf, Christopher Nauman, Somanon Bhattacharya, Zach Fisher, and Brooke Esquivel. I also want to extend my thanks to Benjamin Allgeyer, who has been part of the lab for past few semesters and always made the lab fun and lively.

I would not be where I am today without my family. First, I would like to thank my Father Vijayvinayak Kamath, Mother Vinaya Kamath, my sister Vidya and brother-in-law Ravi for their unwavering love, belief and support. I would like to thank my in-laws (Vijay Thakur, Snehal Thakur and Sonal Thakur) for their love and support. I would also like to extend my gratitude to my husband Abhishek Thakur, without whom this journey would not have been possible. Thank you, Abhishek, for your unconditional love and support and for being my pillar of strength.

Finally, I would like to thank the School of Graduate Studies and Women's Council for their funding support.

CHAPTER 1

INTRODUCTION

1.1 Overview of Bacterial Translation Process

Protein synthesis is a complex process wherein triplets of codon on the mRNA are translated into amino acids to form a protein (1). Bacterial translation process and can be divided into four major steps (Initiation, Elongation, Termination, and Recycling) as shown in Figure 1.1.

Translation begins with a multistep process of translation initiation that culminates in the formation of 70S ribosome. During the initiation process, the mRNA, the aminoacylated and formylated initiator tRNA (fMet-tRNA^{fMet}) and the initiation factors (IF) come together to form a 30S initiation complex. This is followed by binding of the 50S large subunit to the 30S initiation complex to form a 70S initiation complex. Initiation factors IF1, IF2, and IF3 that direct assembly of the initiation complexes dissociate allowing binding of the large and small subunit to form an intact 70S ribosome ready to proceed to the next step. The elongation cycle converts the mRNA codons into the amino acid sequence of the protein. It involves four major steps; delivery of a ternary complex of aminoacyl-tRNA (aa-tRNA) with GTP and EF-Tu to the A site of the ribosome, decoding, peptide bond formation, and translocation. In contrast to the binding of the charged initiator tRNA^{fMet} to the start codon on the P site of the ribosome during initiation, the aa-tRNA ternary complex is delivered to

the A site of the ribosomes during elongation. Successive codon triplets are decoded during the elongation cycle until a stop codon (UAG, UGA or UAA) is encountered. In bacteria, the stop codon UAG is recognized by release factor 1 (RF1), UGA is recognized by RF2 and UAA is recognized by both RF1 and RF2. The release factors hydrolyze the peptidyl-tRNA bond releasing the polypeptide chain. The tRNA and mRNA are then removed from the post-termination complex in the recycling step so that the large and small subunits can dissociate and be recycled. Ribosome recycling factors (RRF) along with EF-G and IF3 aid to recycle the ribosomes for the next round of translation (2,3).

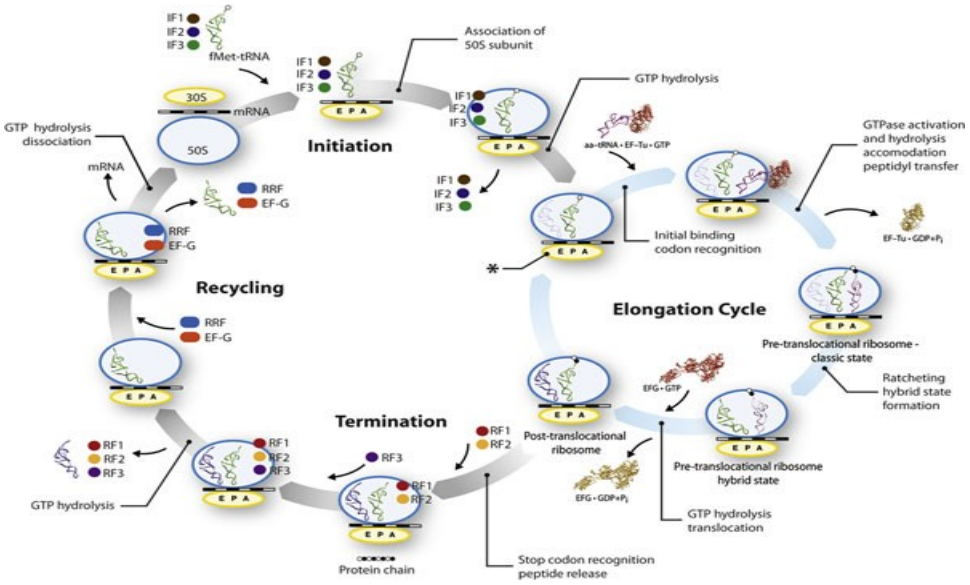

Figure 1.1 The bacterial translation process. During the initiation step of the bacterial translation process, the 30S and 50S subunit associate to form the 70S ribosome with fMet-tRNA^{fMet} at the P site. This is followed by the elongation cycle that adds an amino acid to the C-terminus of the growing polypeptide chain based on the mRNA codon. The termination step ensues when a stop codon is encountered on the mRNA. On termination, the nascent peptide is released and the ribosomal subunits disassemble to be recycled for the next cycle of translation (4). Figure from *Agirrezabala et al 2010.*

Translation is a fundamental process that is energetically costly to the cell and hence is highly regulated. Accurate translation of the genetic code depends on several sequential steps, each with its inherent error rate (5). The estimated range of translational error rate is 10^{-5} to 10^{-3}. Elongation of an average 330 amino acid long protein is completed in about 10-80 seconds with an average rate of elongation being 4-22 amino acids per second at 37˚C, making it rate limiting (6,7). The work in this thesis focuses on a part of the elongation cycle and hence only the key players involved in this process are described.

1.2 Cellular Machinery Involved in the Elongation Cycle

The elongation process requires the efficient and accurate interaction of the ribosome with a multitude of cellular components, including messenger RNA (mRNA) and transfer RNA (tRNA). Some of the key cellular components relevant to the work in this thesis are described below.

1.2.1 16S Ribosomal RNA (rRNA)

16S rRNA is a 1542 nucleotide long RNA on which the 30S subunit is assembled. The secondary structure of 16S rRNA can be distinguished into three compact domains (5', central and 3') and one extended 3' minor domain as shown in Figure 1.2. The 5' domain with 18 double stranded helices (H1-H18) and its associated r-proteins make up the body of the 30S subunit. The central domain corresponds to the shoulder/platform of the 30S subunit and has 9 helical elements (H20-H27) folded into a W-shape. The shoulder domain is crucial for binding of P site tRNA and subunit association (8). The 3' major domain is a component of the head and contains 16 helical elements (H28-H43) while the 3' minor domain consists of helix H44. H44 is the longest single helix and is stretched from the bottom of the head to the bottom of the body (9).

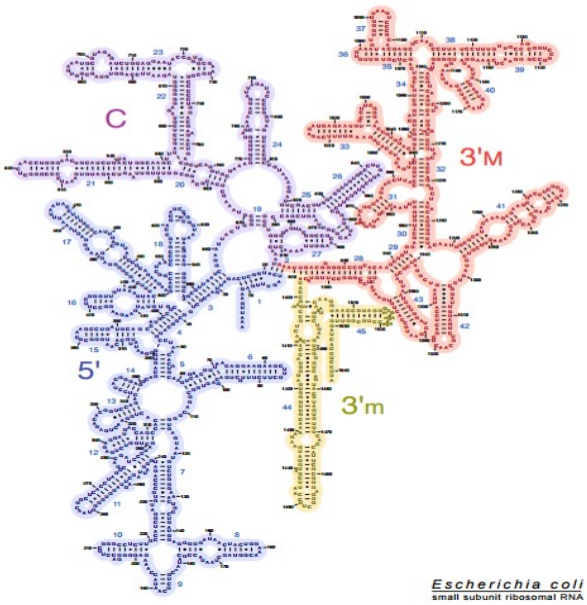

Figure 1.2 The structure of bacterial 16S rRNA. The secondary structure of 16S rRNA can be distinguished into the 5' domain (in blue), the central domain (in purple), the 3'major domain (in red) and the 3' minor domain (in yellow). The four domains of 16S rRNA correspond to the 30S ribosomal subunit domains and are important in maintaining the structure and function of the ribosome (10,11). Figure from *Noller et al 1989.*

1.2.2 Transfer RNA (tRNA)

tRNAs act as flexible adaptors between the codon and the amino acid they specify. *Escherichia coli* has 41 different tRNAs each charged with a specific amino acid that matches with the anticodon triplet and in turn matches with an mRNA codon. tRNAs are between 75-95 nucleotides long (12). The tRNA cloverleaf secondary structure represented in Figure 1.3A consists of the anticodon stem loop (ASL), acceptor stem, D-stem loop, and T-arm. The ASL contains the anticodon complementary to the mRNA codon. The ASL residues 34-37 contain the highest frequency of post transcriptional modifications and are essential for binding tRNA to the ribosome and maintaining fidelity (12). The acceptor stem has the 3' terminal CCA (cytosine-cytosine-adenine) tail on which the amino acid is loaded

(13). The tertiary structure as shown in Figure 1.3B is represented in an L-shaped configuration with acceptor and T-arm on one extreme and D-stem and ASL on the distal part. The anticodon reads the mRNA at one end while the acceptor arm carries the cognate amino acid at the other end (14).

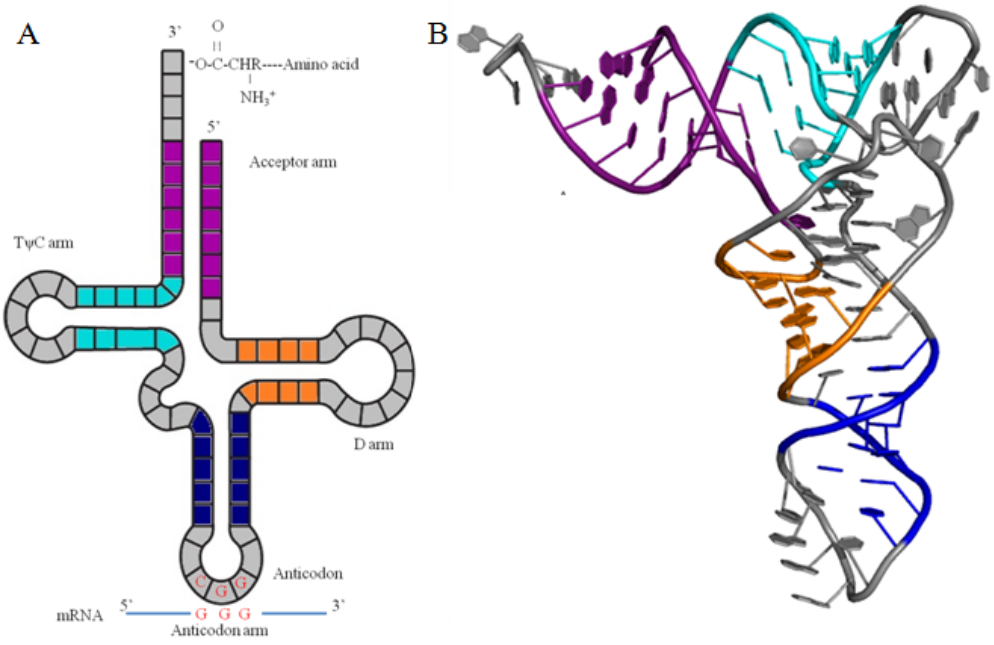

Figure 1.3 The structure of bacterial tRNA. A) The secondary structure of tRNA is represented in the cloverleaf form. B) The tertiary structure of tRNA in an L-shaped configuration. The acceptor arm (purple), T-arm (teal), D-arm (orange) and the anticodon loop (blue) are shown in the figure. The anticodon loop contains the 3 base anticodon that interacts with the mRNA codon (15). Figure from *Sussman et al. 1978.*

1.2.3 Elongation Factors (EF)

Of the three elongation factors in *E.coli*, EF-Tu (temperature unstable) and EF-G (translocase) belong to the G-protein family. EF-Tu binds to aminoacylated tRNA molecule and delivers it to the A site of the ribosome. When cognate correctly charged aa-tRNA binds to the A site, in response to ribosome signaling, EF-Tu undergoes a conformation change, hydrolyzes GTP and ultimately dissociates from the ribosome. EF-Ts acts as a guanine nucleotide exchange factor for EF-Tu, releasing GDP after GTP hydrolysis (16-18). EF-G catalyzes translocation of the tRNA and mRNA using GTP hydrolysis, after the peptide bond is formed (19). During the process of elongation, both EF-Tu and EF-G undergo large conformational changes while interacting with the sarcin-ricin loop (SRL) of the 23S rRNA and GTPase-associated center (GAC) to hydrolyze GTP (18). EF-G domain IV shown in Figure 1.4 is conserved and interacts with A site tRNA before translocation and peptidyl-tRNA after translocation (19).

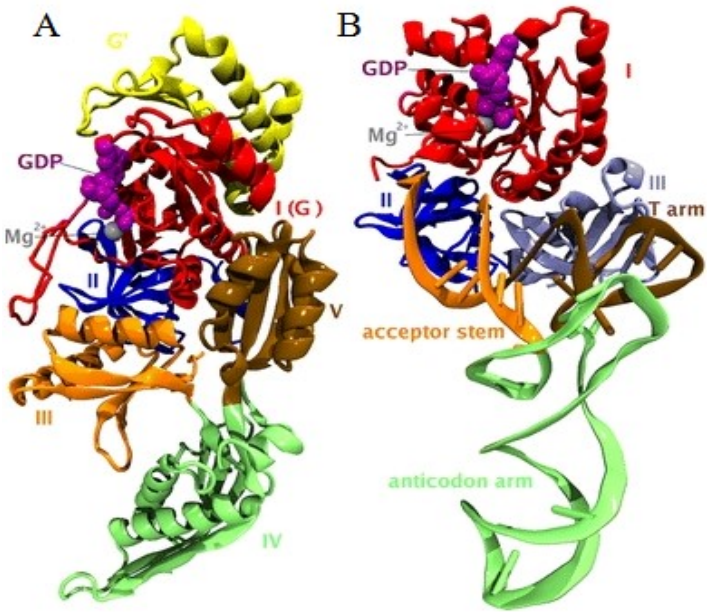

Figure 1.4 The secondary structure of bacterial elongation factors. A) EF-G in complex with GDP B) EF-Tu in complex with aa-tRNA and GDP. In both the figures domain 1 is represented in red, domain II in dark blue, domain III is shown in orange for EF-G and light blue for EF-Tu; EF-G domain IV in brown. Domains I and II of EF-Tu and EF-G are homologous and common for GTPases (18). Figure from *Trylska et al. 2011.*

1.2.4 Bacterial ribosomes

The ribosome has three tRNA binding sites, one mRNA entry and exit channel, one peptide channel, and multiple binding pockets for translation regulating proteins (20).

The bacterial ribosome is a 210Å particle that roughly consists of 2/3 RNA and 1/3 protein. The 2.5 MDa ribosome has a sedimentation rate of the 70S and is made of 30S small subunit (0.8 MDa) and 50S large subunit (1.5MDa) (21). The 30S subunit is assembled on 16S rRNA (1542 nucleotides) with 20 ribosomal proteins and can be structurally divided into the head, shoulder, and body as shown in Figure 1.5A. The head and the body are connected by the neck region. Below the head to the right is a platform in

which anti-SD sequence is located. A deep cleft located at the upper part of the body and lower part of the head houses the decoding center. The mRNA enters through an upstream tunnel formed by portions of the head, platform and neck of the 30S subunit and exits through the downstream tunnel formed by portions of the head, body, and neck. The 30S subunit is involved in mRNA binding, tRNA selection, and codon-anticodon interactions. The 50S subunit consists of 23S rRNA (2904 nucleotides), 5S (120 nucleotides) and 36 ribosomal proteins. The 50S subunit has a central protuberance made of 5S rRNA and its associated proteins, and two flanking arms formed by L1 on one side and L7/L12 multimers on the other side as shown in Figure 1.5B. The 50S subunit also contains a 100 Å long and 25 Å wide polypeptide tunnel that can accommodate a 40 amino acid peptide. The 50S subunit is responsible for catalyzing the peptide bond formation and interactions with the universally conserved amino acid ends of the tRNAs. The two subunits associate to form the 70S ribosomal subunit as shown in Figure 1.5C through a network of molecular interactions along the interface termed intersubunit bridges (22-25).

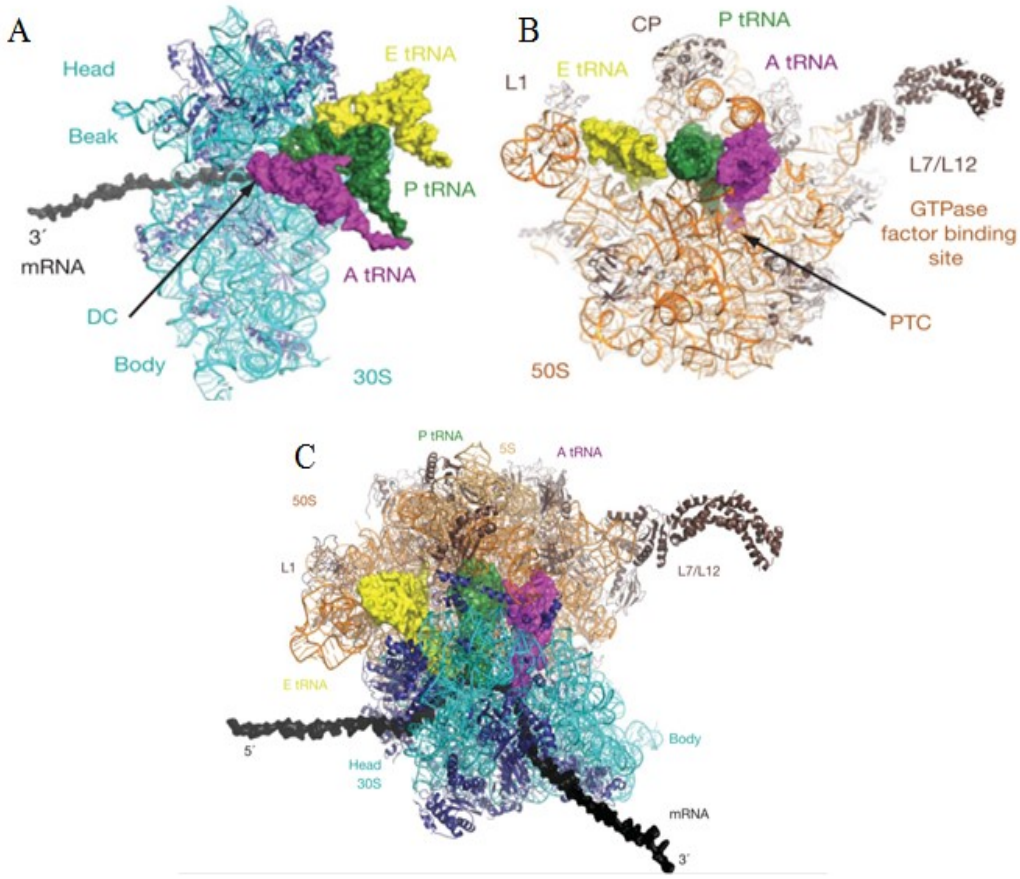

Figure 1.5 The structure of the bacterial ribosome. A) View of the 30S subunit. The figure shows the head and the body region of the 30S subunit. The mRNA is aligned to the A, P, and E site of the decoding center. B) View of the 50S subunit. The peptidyl transferase center of the 50S subunit and the flanking L1 arm on the left and the L7/L12 flanking arm on the right are shown in the figure. C) View of the 70S ribosome. 50S subunit is shown on the top and the 30S subunit is shown at the bottom. The mRNA entry and exit sites are also visible along with the A, P and E site on the 70S ribosome (26). Figure from *Ramakrishnan et al. 2009.*

Assembly of the ribosomal subunits: Ribosome assembly involves coordinated steps of (i) transcription, processing, and modification of rRNA transcripts ii) translation and modification of r-proteins iii) assembly of the ribosome by folding of rRNA and ribosomal proteins (r-proteins) and binding of ribosomal proteins and iv) binding and release of assembly factors. *In vivo* ribosome assembly in *E.coli* occurs in about two minutes at 37˚C (23).

i) rRNA transcription, processing, and modifications: The three ribosomal RNA 5S, 16S and 23S are transcribed from any of the 7 ribosomal RNA (*rrn*) operons (A, B, C, D, E, G, H) into a single transcript. The *rrn* operons contain two promoters P1 and P2 arranged in tandem and separated by ~120bp. *rrnH* and *rrnC* have tRNA genes located downstream of 5S and *rrnD* has two 5S genes separated by a tRNA gene. The primary transcript contains 16S, 23S and 5S in that order with tRNA present in the spacers separating the three RNAs. The nascent transcript undergoes a series of cleavages by RNAse to form mature transcripts as shown in Figure 1.6. Both 16S and 23S rRNA have modifications clustered in the decoding and peptidyl transfer regions respectively and are implied to influence structure and function of the ribosome. 16S rRNA modifications include 10 methylations and 1 pseudouridinylation, whereas 23S rRNA modifications include 14 methylations, 9 pseudouridinylation and 1 methylated pseudouridinylation (23, 27).

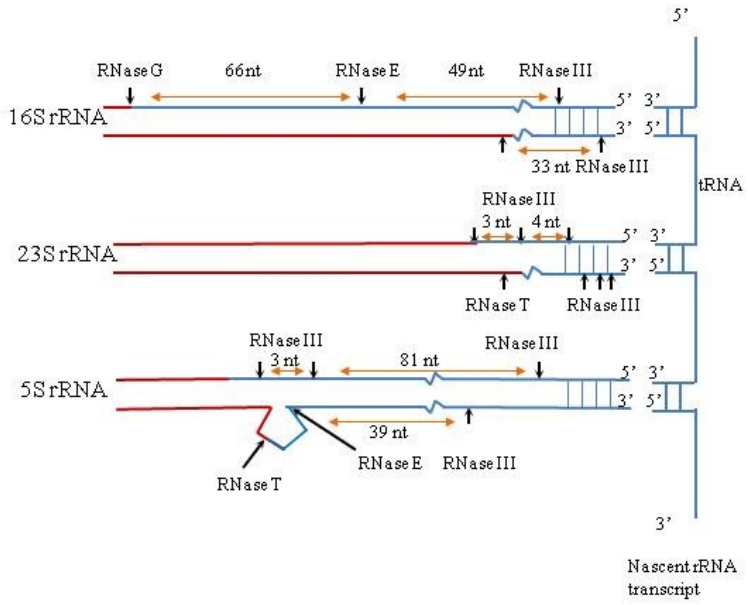

Figure 1.6 Maturation of ribosomal RNAs in bacteria. 16S, 23S, and 5S are transcribed from one of the *rrn* operons into a single transcript with tRNAs in the region between the three rRNAs. The nascent rRNA transcript is cleaved by various RNAses to generate the final mature RNA product. Black arrows represent the point of cleavage on the precursor rRNA whereas the mature products produced after cleavage are shown in red (23). Figure adapted from *Williamson et al. 2011.*

ii) Translation and modification of r-proteins: The *E.coli* ribosome contains 20 proteins in the small subunit and 36 in the large subunit. The ribosomal proteins are transcribed from the 19 protein operons grouped together with other r-proteins or with proteins involved in translation. Ribosomal proteins are regulated by autogenous feedback where one of the r-protein in the operon binds to the operator site, located upstream of the first gene or in between genes, on its own mRNA to stall translation. Some ribosomal proteins are posttranslationally modified by methylation or acetylation. Six proteins (S11,

L3, L11, L7/L12, L16, and L33) are methylated, three proteins (S5, S18, and L7), are acetylated and S12 protein is methylthiolated (23).

iii) Assembly of the ribosome by folding of the rRNA and r-proteins and binding of ribosomal proteins: Assembly of 30S subunit occurs by binding of the r-proteins to 16S rRNA co-transcriptionally, though multiple parallel pathways. The assembly occurs in the 5' to 3' direction. Small subunit (SSU) proteins can be divided in primary, secondary and tertiary proteins based on the hierarchy of binding, with early binding events setting the stage for late binding proteins. The primary binding proteins (S4, S7, S8, S15, S17, and S20) bind directly to the 16S rRNA. The secondary proteins (S6, S9, S11, S13, S16, S18, and S19) interact with the rRNA and the primary binding proteins. The tertiary proteins (S2, S3, S5, S10, S12, S14, and S21) interact with both the primary and secondary protein for correct association (Figure 1.7A) (25). The structure of SSU is divided into head, shoulder and body domains largely conferred by the secondary structure of 16SrRNA (Figure 1.7B, 1.7C). The 5' 16S rRNA domain (helices 1 to 18) and its associated proteins S4, S5, S12, S16, S17, and S20 make up the body of the SSU. The central domain of 16S rRNA (helices 19 to 27) along with five r-proteins, S6, S8, S11, S15, S18, and S21, forms the shoulder region of the 30S ribosomal subunit. The head of the 30S subunit consists of the 3′ major domain of 16S rRNA (helices 2 and 28 to 43) and its associated proteins, S2, S3, S7, S9, S10, S13, S14, and S19. The 3′ minor domain consists of helices 44 and 45 (28). Assembly of large subunit (LSU) follows similar steps as SSU assembly but is more complex due to the size of 23S rRNA, 36 r-proteins, and 5S rRNA. The LSU is not divided into structural domains corresponding to the 6 regions of 23S rRNA.

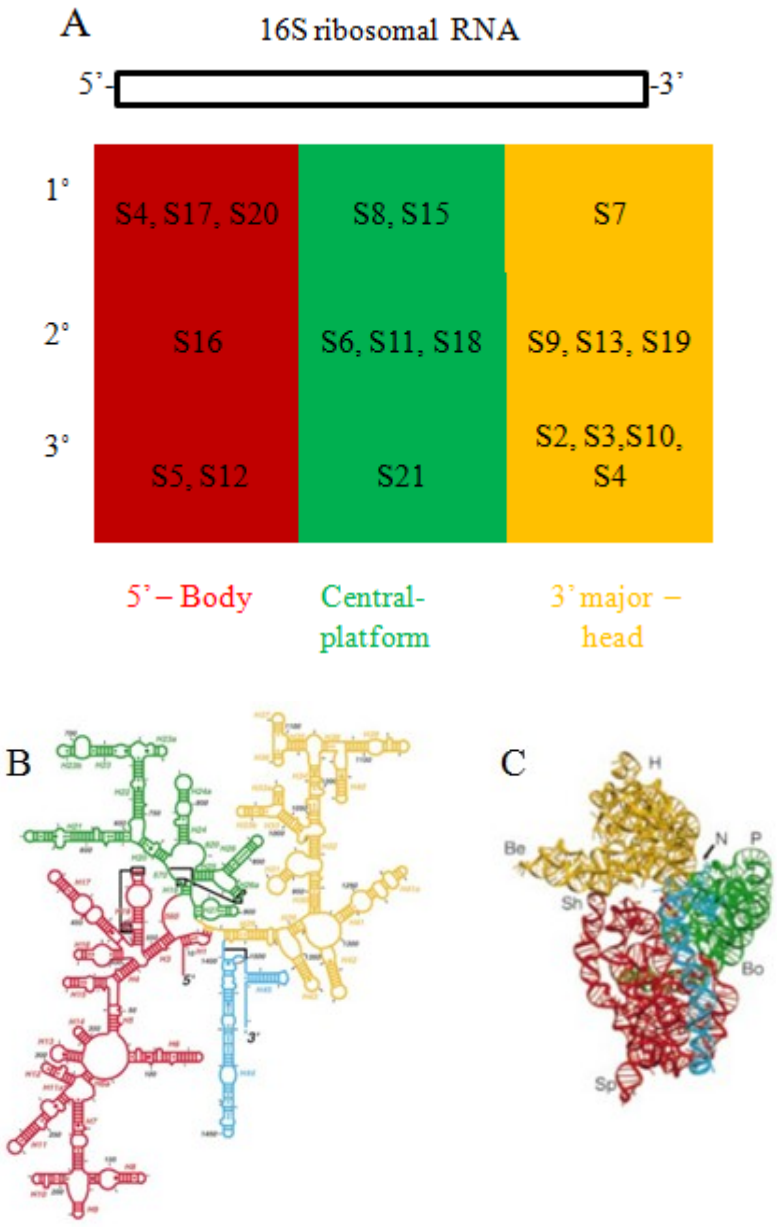

Figure 1.7 Assembly map of SSU r-proteins on 16S rRNA. A) The primary (1˚), secondary (2˚), and tertiary (3˚) binding proteins associate with different regions of the 16S rRNA to form the distinct region of 30S subunit. B) and C) represent the secondary and tertiary structure of 16S rRNA. The red color in all the figures represent the 5' region of 16S rRNA and its associated proteins that form the body of the 30S subunit, green is for the central domain and it's associated proteins that form the platform and yellow is for the 3' major domain corresponding to the head of the 30S subunit. The 3' minor domain of 16S rRNA is shown in blue color (9, 27). Figure from *Ramakrishnan et al. 2000; Culver 2003.*

iv) Binding and release of assembly factors: *E.coli* ribosome assembly *in vivo* involves around 30 assembly factors including chaperones, GTPases and maturation factors that support proper folding, and assembly, and act as checkpoints during the assembly process (29).

The two subunits are held together by a series of non-covalent interactions also called the intersubunit bridges. These bridges serve as a mode of communication between the two subunits and also help regulate translocation (30). The three intersubunit binding sites for tRNA-binding named A, P, and E sites are critical in the elongation process (18).

The A site is the point of entry for the aminoacyl-tRNA (aa-tRNA) ternary complex during elongation. It houses the decoding center which encompasses nucleotides from helix 44 (1400-1500), helix 43 (1050 -1200) and helix 18 (530 loops) of the 16S rRNA as shown in Figure 1.8 (31). The decoding center monitors the correctness of the codon-anticodon interaction. In the 30S A site, four nucleotides of the 16S rRNA contact the anticodon stem loop (ASL) of the tRNA, three of which fit precisely into the minor groove of the codon-anticodon helix (32). The minimal interaction at the third position explains the tolerance of wobble and other codon-anticodon pairs in the genetic code. In the 50S A site, 23S rRNA interacts with the universally conserved 3'CCA end of the tRNA and aids in positioning the aminoacyl group at the 3' end of the incoming aa-tRNA for peptidyl transfer (33,34).

The P site consists of the peptidyl transfer center (PTC) where the peptidyl-tRNA is formed and held tightly during elongation, to prevent loss of the nascent chain after translocation (35). In the 30S P site, the codon–anticodon helix interacts with the major groove on the top part of helix 44 of 16S rRNA as shown in Figure 1.8 (36). In the 50S P site, the minor groove of the P-tRNA D-stems rests on the minor groove of helix 69 of 23S

rRNA. During initiation, the charged $tRNA^{fMet}$ recognizes and base-pairs with the AUG start codon at the P site.

The E or the exit site can only bind tRNAs bearing a free ribose at its acceptor end. The E site thus binds to uncharged deacylated tRNA translocated from the P site after it donates its amino acid to the growing peptide chain (37). The deacylated tRNA is then released from the ribosome (38). In the 30S E site, the ASL interacts with 16S rRNA via backbone-interactions. In the 50S subunit, the elbow of E site tRNA contacts both protein L1 and the head of the L1 stalk (helices 76-78) of 23S rRNA as shown in Figure 1.8 (39).

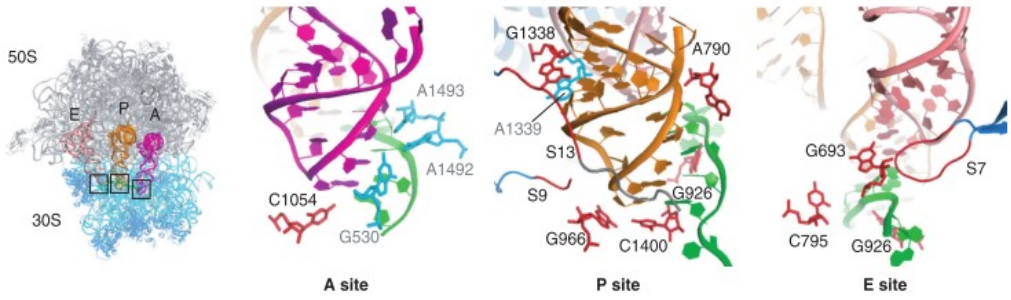

Figure 1.8 Interactions of the ribosomal contacts to tRNA and mRNA in the A, P, and E site. The small subunit is represented in blue, large subunit is shown in gray and the 16S rRNA is green. Residues in the A site are shown in purple, P site in orange and pink for E site. The interactions between the residues of 30S subunit and 16S rRNA are shown for each site (34, 40). Figure from *Fredrick et al. 2009.*

Formation of the 70S ribosome formation occurs during the initiation step of translation. The 30S subunit associates with IF2, mRNA, and fMet-tRNA^{fMet} to form the 30S initiation complex. The Shine-Dalgarno (SD) sequence of the mRNAs interacts with the anti-SD sequence of the 16S rRNA such that the initiation codon is adjusted in the P site of the ribosome. This is followed by association of the 50S subunit to the 30S initiation complex, GTP hydrolysis, and dissociation of the IF2. The newly formed 70S initiation complex with fMet-tRNA^{fMet} at the P site is ready to enter the elongation phase of translation (41).

1.3 The Elongation Cycle

The elongation cycle is highly conserved across all kingdoms of life. Each cycle of elongation adds one amino acid to the C-terminus of the newly synthesized peptide (20). Figure 1.9 describes the steps involved in the elongation cycle.

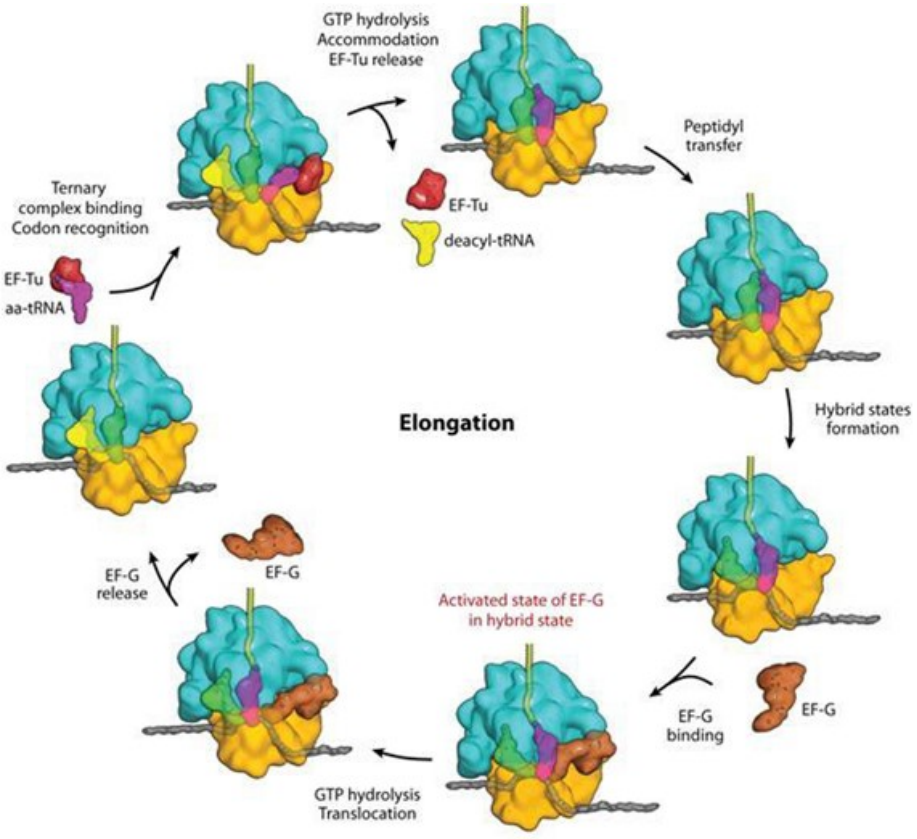

Figure 1.9 The bacterial elongation cycle. The elongation cycle involves sequential addition of amino acid to the growing peptide chain. Aminoacylated tRNA in complex with EF-Tu and GTP interacts with the A site of the decoding center where the correctness of the codon-anticodon is determined. On accommodation, aa-tRNA moves into the PTC after which the ribosome forms the hybrid A/P and P/E state in preparation of translocation. After, GTP hydrolysis, dissociation of EF-Tu-GDP and translocation, new aa-tRNA ternary complex reads the codon on the mRNA and continues this cycle (42). Figure from *Ramakrishnan et al. 2013.*

1.3.1 Aminoacylation and delivery of aa-tRNA to the A site

E.coli has 20 amino acids, 20 aminoacyl-tRNA synthetases (aaRS) and 41 tRNAs with different anticodons (43). The tRNAs are charged with specific amino acids based on their anticodon triplet by the aminoacyltRNA synthetase (aaRS). In an ATP-dependent reaction, the amino acid is transferred to the 2' or 3' hydroxyl group of terminal adenine (A76) at the 3'CCA terminus as shown in Figure 1.10. This process employs dual discrimination based on the rate of reaction and substrate binding affinity (5). After aminoacylation, the charged tRNA forms a ternary complex with EF-Tu and GTP and is ready to be delivered to the A site of the ribosome (44).

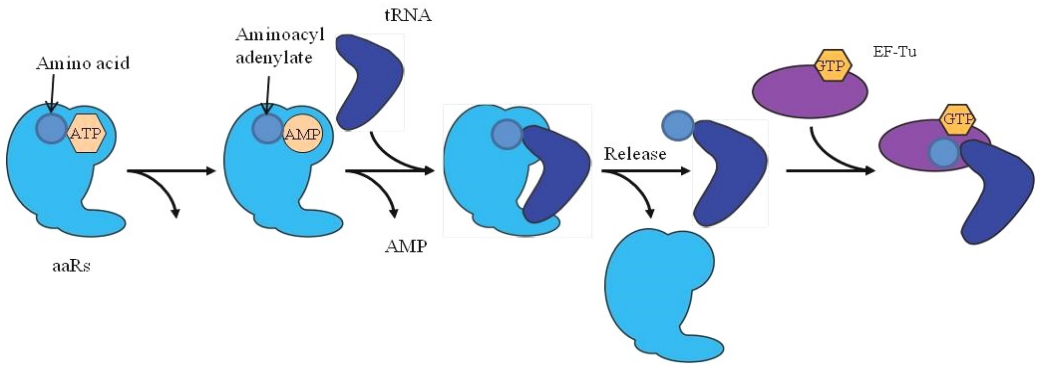

Figure 1.10 Formation of an aminoacylated-tRNA molecule. Aminoacyl-tRNA synthetase (aaRS) activates an amino acid in presence of an ATP molecule to form aminoacyl-adenylate and releases PPi. When a tRNA binds to the aaRS, the activated amino acid is transferred to the 3' end of the tRNA molecule forming aminoacyl-tRNA with the release of adenosine monophosphate (AMP). The aa-tRNA is released from aaRS and can associate with EF-Tu to participate in the elongation cycle (44). Figure adapted from *Ibba et al. 2015.*

1.3.2 Decoding

The ribosome selects aa-tRNA ternary complex based on the ability of its anticodon to base-pair with the mRNA codon. A cognate tRNA anticodon matches all the three base-pairs of the codon on the mRNA. Near-cognate tRNA has one mismatch and non-cognate tRNAs have more than one mismatch. This selection occurs at a rate of 20 amino acids per second and requires EF-Tu and GTP as part of the ternary complex. Decoding can be divided into multiple steps based on kinetic studies as shown in Figure 1.11.

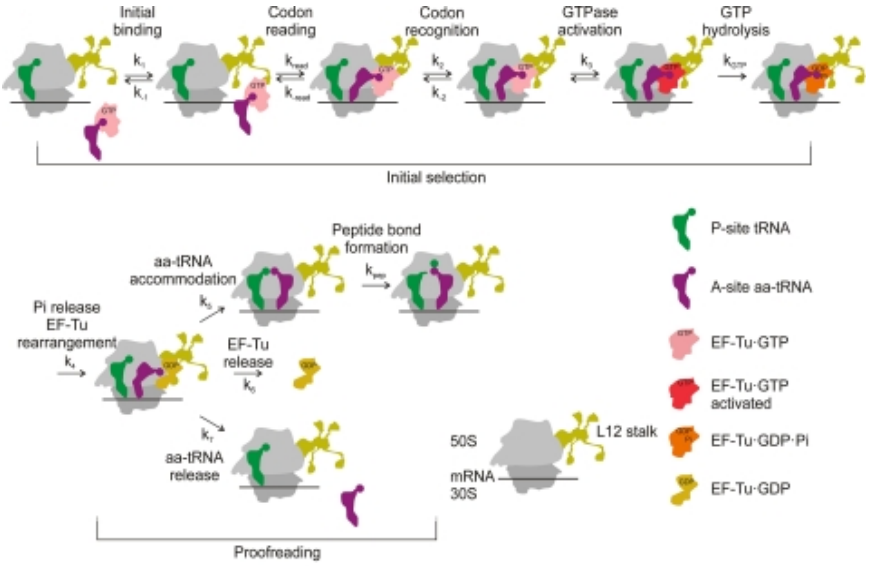

Figure 1.11 Kinetic scheme of decoding. The initial selection step is inclusive of the initial binding, codon reading, codon recognition, GTPase activation and GTP hydrolysis. During initial selection, non-cognate and near-cognate aa-tRNA is rejected while only cognate aa-tRNA is selected. The proofreading step involves EF-Tu rearrangement and accommodation of cognate aa-tRNA finally leading to peptide bond formation. Proofreading step rejects and releases any near-cognate aa-tRNA that may have escaped the initial selection (45). Figure from *Rodnina et al. 2011.*

a) Initial binding and mRNA sampling

The initial binding of the aa-tRNA ternary complex is rapid and independent of mRNA. In this step, the multimeric large ribosomal subunit protein L7/L12 (L7 differs from L12 by an acetylated N-terminus) interacts with helix D of EF-Tu, using its flexible C-terminal domain and delivers the ternary complex to the A site of the ribosome, as shown in Figure 1.12. The stalk is made of two L7/L12 dimers. The N-terminal domain aids in the formation of the dimer and anchoring the protein to the ribosomes whereas the C-terminal domain binds to EF-Tu in the ternary complex (46).

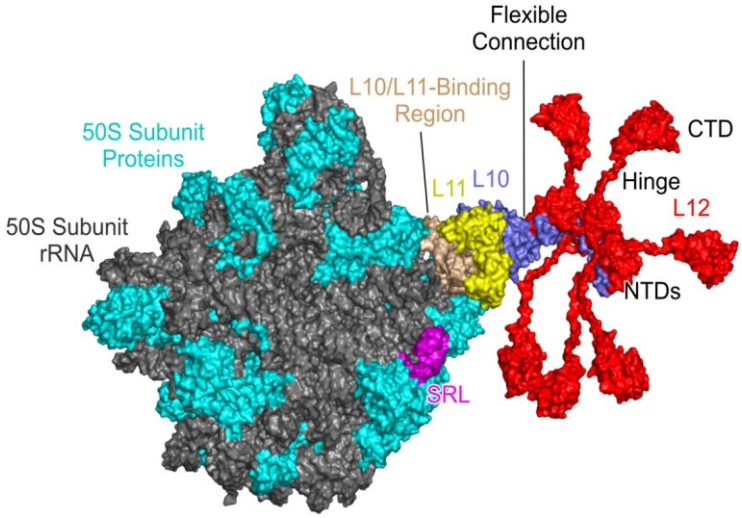

Figure 1.12 Large subunit structure showing L7/L12 stalk. The structure of 50S subunit with rRNA (in gray) and r-proteins (in cyan) is shown. The L12 dimer (red) has a C-terminal domain (CTD), N-terminal domain (NTD) and the hinge region. The L10 that provides flexibility is shown in blue while the L11 acting as an anchor is shown in yellow. The L7/L12 dimer stalk aids in the delivery of the aa-tRNA ternary complex to the A site of the ribosome (47). Figure from *Wahl et al. 2005.*

b) Codon recognition and selection

Base-pairing between the mRNA codon and tRNA anticodon results in the formation of a short double helix called codon-anticodon helix. The decoding center of the ribosome (A site) needs to distinguish between cognate aa-tRNA complex (no mismatch between codon-anticodon base-pairs), near-cognate (one base-pair mismatch) and non-cognate (more than one base-pair mismatch).

The selection of cognate tRNA is believed to occur in two stages, an initial recognition step followed by a proofreading step, separated by the irreversible hydrolysis of GTP by EF-Tu. This approach allows multiple chances to reject the incorrect tRNA species. In both stages, the difference in the binding energy between cognate and near-cognate interactions is used for discrimination. In the initiation recognition step (an induced fit reaction) universally conserved residues A1492, A1493 (H44-16SrRNA) and G530 (shoulder domain) interact with the minor groove of the first and second codon-anticodon base-pairs to sense the geometry and correctness of base-pairing as shown in Figure 1.13. Binding of cognate tRNA will result in codon-anticodon helix displaying geometry characteristics of Watson-Crick base-pairing with enhanced stability and high binding energy. Base-pairing at the third position does not depend on the shape of the minor groove and hence allows wobble base-pairing without affecting binding affinity. Near-cognate interactions such as U-G mismatches, at either of the first two positions, displaces U into the minor groove preventing its interaction with 16S rRNA residues and reducing binding affinity. This difference in binding energy may not be enough to discriminate between cognate and near-cognate tRNA, resulting in few near-cognate tRNA complex escaping this screening process. These near-cognate complexes are removed during the proofreading step

following GTP hydrolysis. Non-cognate tRNAs have reduced binding affinity and are rejected during the initial phase of selection (31).

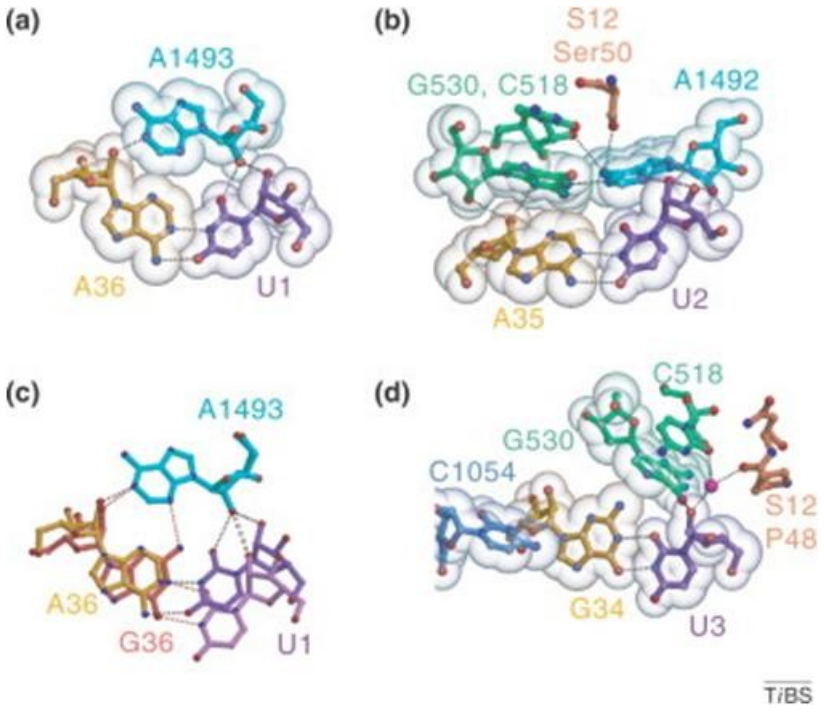

Figure 1.13 Recognition of minor groove geometry by 16S rRNA. A) Interaction of A1493 of 16S rRNA (cyan) with the first codon (purple)-anticodon (gold) base pair. B) Interaction of A1492 (cyan), G530 (turquoise) part of 16S rRNA with the second codon-anticodon base pair. C) The presence of near-cognate anticodon G36 displaces codon uridine (violet) into the minor groove, away from A1493 and leads to disruption of interactions D) Base pair interaction at the third (wobble) position is not as stringently monitored (48). Figure from *Ramakrishnan et al. 2005.*

c) Conformational changes

Conformational changes in the ribosome, tRNA and EF-Tu are used to activate GTP hydrolysis in the GTPase Activating Center (GAC), located 80 Å away from the decoding center.

(i) Conformational changes in the 30S subunit: Energy from the binding of cognate tRNA can induce a transition from an open to closed conformation in 30S subunit, called domain closure. This movement involves rotation of the 30S head domain towards the shoulder domain and subunit interface. Domain closure occurs by disruption of the interface between the S4 and S5 and forms new contacts between H18/530-loop/S12 and H27 and H44 as shown in Figure 1.14 (32).

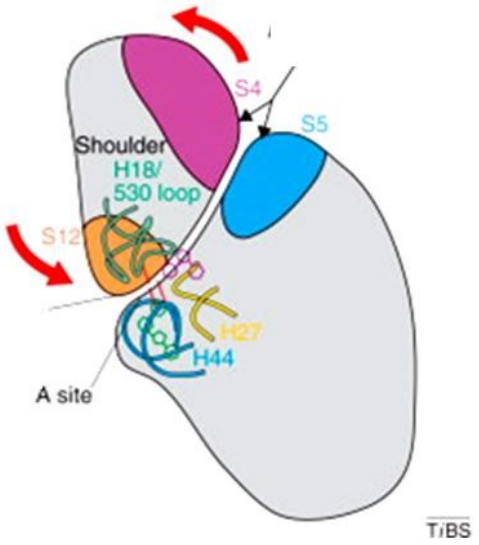

Figure 1.14 Cross-section of 30S subunit in the region of the decoding center. S4 (purple), S5 (blue) and S12 (orange) are the ribosomal proteins critical for domain closure. H44, H27, and H18 with G530 loop are parts of the 16S rRNA. The red arrows show the direction and rotation of the shoulder domain during the transition of the 30S subunit from an open to closed conformation. It involves disruption of interface residues between S4 and S5 and formation of new contacts between H18/G530 loop/S12 with H27 and H44 (49). Figure from *Ramakrishnan et al. 2003.*

(ii) Conformational changes in tRNA: tRNA participates in two simultaneous interactions in the ribosome. The first is the interaction of the tRNA anticodon arm with the 30S A site and the second is binding of the tRNA acceptor stem to EF-Tu. In this A/T state, the tRNA undergoes a ~30 degree bend at the ASL. Upon dissociation of EF-Tu from the ribosome, the tRNA untwists and the acceptor stem swings by 45 Å into the peptidyl transferase center achieving the A/A state (17).

(iii) Conformational changes in EF-Tu: Binding of aa-tRNA to the ribosome and codon recognition results in conformational changes in the GTPase domain of EF-Tu allowing it to position itself for interaction with the highly conserved sarcin-ricin loop (SRL) of 23S rRNA. (19).

d) GTPase activation and GTP hydrolysis

The SRL acts a GTPase activation factor. EF-Tu contacts the A2662 in the SRL and is reoriented towards the γ-phosphate of GTP. A highly conserved His84 in domain I of EF-Tu coordinates a water molecule for an in-line attack on the γ-phosphate of GTP. His84 acts as a general base and deprotonates the water molecule for GTP hydrolysis releasing Pi. On release of the Pi, EF-Tu transitions to its GDP form and dissociates from the ribosome as shown in Figure 1.15. The rate of GTP hydrolysis depends on the presence or absence of cognate aa-tRNA binding to the ribosome (48, 50).

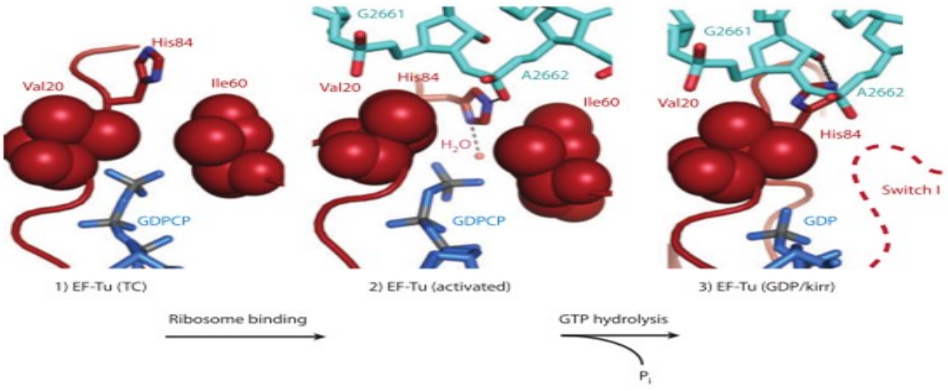

Figure 1.15 Role of His84 of EF-Tu during GTPase activation and GTP hydrolysis. When the GTPase is not activated His84 in domain I of EF-Tu (in red) is rotated away from GTP (in blue). On activation of GTPase by binding of the cognate correctly charged aa-tRNA to the ribosome phosphate of A2662 of SRL positions His84 into the active site to active as a general base. Following GTP hydrolysis and Pi release His84 returns to its inactive conformation (42). Figure from *Ramakrishnan et al. 2013.*

e) Accommodation and proofreading

On dissociation of EF-Tu, the aa-tRNA is bound to the ribosome by its interaction with the decoding center alone. This interaction is comparatively stronger for cognate aa-tRNA than the near or noncognate aa-tRNA. The cognate aa-tRNA proceeds into the peptidyl transfer center (PTC) completing one round of decoding, whereas the near or non-cognate aa-tRNA may dissociate from the ribosome (42).

1.3.3 Peptide Bond Formation

After one round of decoding, the peptidyl-tRNA will be at the P site and aa-tRNA will be at the A site of the ribosome. The α-amino group of the aa-tRNA will initiate a nucleophilic attack on the aminoacyl ester of the peptidyl-tRNA leading to the formation of a peptide bond.

1.3.4 Translocation

During peptide bond formation the nascent polypeptide is transferred to the A-site leaving an empty deacylated P site tRNA. As aa-tRNA ternary complex binds only to the A site during decoding, both the tRNAs need to move through the ribosome to the P and E site respectively, such that the next codon can be read at the empty A site. This movement of the ribosome along the mRNA is a complex multistep process termed as translocation and is catalyzed by the binding of elongation factor G (EF-G) driven by GTP hydrolysis. Translocation occurs within milliseconds and involves large-scale conformational changes (1, 51).

Translocation occurs by formation of 2 intermediate hybrid states as a result of the independent movement of the two tRNA arms (3'CCA-acceptor arm and anticodon arm) as shown in Figure 1.16. In the pre-translocation or PRE complex, a P/E hybrid state is achieved where the anticodon end of the deacylated tRNA is attached to the mRNA codon on the P site of the 30S ribosomal subunit and their 3' ends are present in the 50S E site. Concomitantly the anticodon of the peptidyl-tRNA resides on mRNA codon on the 30S A site, with its 3'end in the 50S P site forming an A/P hybrid state. Formation of both ribosomal hybrid states is coupled with an anticlockwise rotation of the two subunits relative to one another. This transition of the subunits from the classical non-rotated to the rotated

state is also termed as ratcheting. The ratcheted state of the 30S subunit results from the movement of two hinges (hinge I and hinge II) lying within conserved 16S rRNA elements. Following EF-G recruitment and GTP hydrolysis, the anticodon ends of the tRNA along with their associated mRNA move into the P and E site of the 30S subunit to restore the canonical (E/E, P/P) state. This movement results in dissociation of EF-G and E site deacylated tRNA, resets the ratchet restoring the classical non-rotated state of the ribosome and leaves an empty A site ready to accept the next aa-tRNA (1, 3).

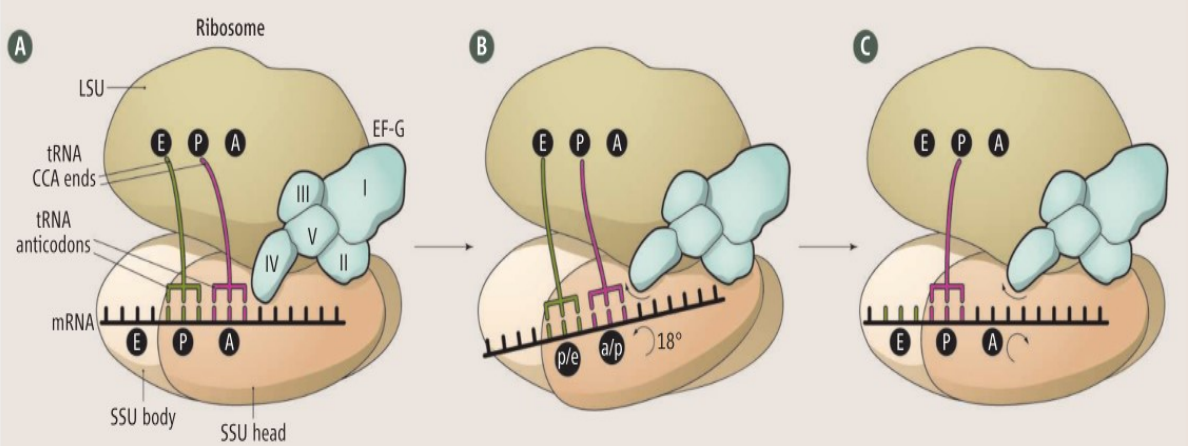

Figure 1.16 Dynamics of translocation. The 30S (SSU) head is shown in orange and SSU body is in peach, the 50S subunit is shown in brown color and the EF-G is blue in color. A) Pretranslocation state: The tRNA anticodons are located in the A and the P site on the SSU whiles the tRNA CCA ends oscillate between A and P or P and E site on the 50S subunit. B) Hybrid state: Racheting of SSU head brings tRNA anticodons and mRNA codons into a hybrid state between A and P (A/P) or P and E (P/E) on SSU. C) Posttranslocation: One tRNA is bound to the ribosome in the P site and one is bound to the E site. The SSU head is rotated backward and normal position is restored (52). Figure from *Rodnina 2013.*

When all the codons on mRNA are read and the ribosome encounters a stop codon, the termination phase of protein synthesis is reached. Stop codons are recognized by RF1 or RF2 that position the universally conserved GGQ motif into the peptidyl transferase center and catalyze the hydrolysis of peptidyl-tRNA (3).

1.4 Genetic Studies on Translational Accuracy

The speed and accuracy of protein synthesis determine cell growth and fitness of cells. High accuracy is critical as misfolded protein can be detrimental and energetically costly to the cell. Too much accuracy at the cost of speed can also be detrimental to the growth of the organism. As decoding is the key to dictating the sequence of newly synthesized proteins (53), the tRNA selection pathway during translation needs to maintain the balance between rate and accuracy (31).

As efficient protein synthesis is essential to cell growth, translational accuracy is one of the important targets of antibiotics. Many antibiotics are directed against bacterial ribosomes and affect decoding and proofreading processes. Mutations within both the rRNA and r-proteins can render the antibiotics ineffective, making antibiotic resistance a predominant problem (54). Genetic, biochemical and structural analyses of antibiotics binding to the ribosome as well as ribosomes that developed resistant to the antibiotic has helped in identifying how different ribosomal components modulate fidelity.

Alterations to the components of the decoding center or the 30S subunit can affect the tRNA selection pathway and result in either error-prone (ram) mutants that lower accuracy or error-restrictive (hyper accurate) mutants that increase accuracy. Recognition and binding of cognate aa-tRNA to the A site of the ribosome results in a transition from an open to a closed conformational in the 30S subunit. This 30S conformational change (domain closure) leads to activation of GAC in the large subunit of the ribosome, GTP hydrolysis of EF-Tu.GTP, accommodation and peptide bond formation. During domain closure, the salt bridges between interface residues of protein S4 and S5 are disrupted, moving the two proteins slightly apart. The breaking of bonds at the S4-S5 interface

contributes to the energetic cost of domain closure. When the shoulder domain moves to the decoding center, additional contacts are made between S12 and ribosomal RNA in the closed form.

Binding of aminoglycosides to rRNA close to the decoding site modifies the ribosomal conformation resulting in partial domain closure in the 30S subunit. This leads to incorporation of near-cognate tRNAs and increased rate of GTP hydrolysis. Similarly, the mutations that disrupt the interface of S4 or S5 increase the ability of near-cognate tRNA to induce domain closure. As the cost of domain closure in both instances has been reduced, the chances of near-cognate tRNA being selected and accommodated are increased, lowering accuracy (55). Restrictive mutants, on the other hand, lead to the formation of additional contacts in the decoding center stabilizing the open conformation. This increases the energy barrier leading to an increase in accuracy at the expense of speed. Increased proofreading efficiency will result in slower elongation process (48).

Early insights into ribosomal fidelity were provided by Gorini and Kataja using streptomycin (56). Streptomycin binds in a pocket at the interface between S12 and h27 of 16s rRNA (57) and interferes with aa-tRNA selection (58). Gorini and colleagues isolated mutant strains of bacteria that displayed three different phenotypes: streptomycin resistant (SmR), streptomycin dependent (SmD) or streptomycin independent (SmI). Although all the mutants could grow in presence of streptomycin, SmD mutants required the presence of the antibiotic for survival and growth. The presence of streptomycin allowed the mutants (e.g. arg^-) to read through nonsense mutations (e.g. UGA in arg biosynthetic genes) and grow in the absence of metabolite they are unable to synthesize (e.g. arginine). Genetic and biochemical characterization of the streptomycin-resistant *E.coli* mutants showed that the

mutations affected the S12 protein. SmD S12 mutants showed an error-restrictive (hyper accurate) phenotype and hence needed the miscoding properties of streptomycin to compensate for the increased accuracy. Revertants of the SmD mutant strains carried additional mutations which reduced the fidelity of translation to levels at which addition of streptomycin was not required and thereby rendered these mutants streptomycin-independent. These second site mutants on their own conferred an error-prone phenotype and were mapped to *rpsD* and *rpsE* genes (59). Similar studies have resulted in the identification of many mutants in few other ribosomal proteins, 16S rRNA, and EF-Tu (60). A few examples of the ribosomal proteins mentioned in this thesis are described in Table 1.1.

Table 1.1 Accuracy altering mutations in r-proteins. Alteration in r-proteins that affect translation accuracy are mentioned in the table below. The location of the r-proteins, the selection method used to isolate the alteration and the effect of specific alteration are given.

r-prot	Location of r-prot	Alteration	Selection / Phenotype	Ref
S4	Binds directly to 5' end 16S rRNA. Part of body region of the 30S subunit	i) Y51D	i) Suppressor mutant of RF1 temperature sensitivity/ weakly error-prone	(61) (62)
		ii) Δ169-206, Δ181-206*, Δ183-206*	ii) Reversal of SmD in S12 mutant/ error-prone	
S5	Part of body region of the 30S subunit	i) G103R, R111L	i) Reversal of SmD in S12 mutant/ Error-prone	(63) (62)
		ii) G108S	ii) Improved growth of error-restrictive S12 mutant /Error-prone	
S12	Part of body region of the 30S subunit, located at the interface of 30S and 50S subunit	i) R3A+I4A, Δ70-118	i) Engineered mutations/ error-prone	(64) (65)
		ii) 41 mutants from T2K - R13H/K107N	ii) Random mutagenesis/ 13 error-prone; 28 error-restrictive	

r-prot	Location of r-prot	Alteration	Selection / Phenotype	Ref
S17	Binds directly to 5' end 16S rRNA. Part of body region of the 30S subunit	i) H30P	i) Neamine resistance/ Error-restrictive	(66, 67)
L6	Near tRNA binding site at PTC at 30S-50S subunit interface.	Δ158-177: 7 nt insertion- premature termination Δ152-177*: 11 nt deletion- premature termination	Gentamicin resistance / Error- restrictive	(54)
L14	Contacts h8 and h14 of 16S rRNA, part of bridge B5 and B8 along with L19	R71C, R105H, R108S, A119V	Compensates for slow growth in error-restrictive L19 mutants in *Salmonella*	(60)
L19	Contacts h44 of 16S rRNA. part of bridge B5 and B8 along with L14	i) Q40R, Q40L, Q40H ii) Range of mutations from W30C to E111*	i) Reversal of S12 SmD/ Error-prone in salmonella ii) Random mutagenesis/ Error-prone in E.coli	(60) (68)

r-prot	Location of r-prot	Alteration	Selection / Phenotype	Ref
L7/L12	Part of the 50S subunit	G74D, E82K, ΔG43*, ΔV38-A42	Reversal of SmD in S12 mutant, suppression of lethality due to $tRNA^{gly-2}$ deficiency, Increased readthrough and increased misreading	(69)

S4 and S5 are the two major proteins discussed in this thesis. S4 (encoded by *rpsD*) is a 205 amino acid long protein, consisting of two conserved globular domains (70) and a 40-residue N-terminal extension. S4 is also a translation repressor protein, controlling the translation of the α-operon coding S13, S11, S4, RNA polymerase α-subunit and L17 (71). The secondary and tertiary structure of the S4 binding site, especially residues in contact with rRNA is strongly conserved among different bacteria (70). It forms extensive interactions with the helix junction in the 5′ domain of the 16S rRNA (72) and stabilizes a conserved pseudoknot in helix (H) 18 that orients G530 in 16S rRNA for its proper interactions with A site tRNAs in the decoding center of the ribosome (11) It also contacts protein S5 in the 30S small subunit.

S5 encoded by the *rpsE* gene, is a 167 amino acid long protein organized into two distinct α/β domains, which interact with each other via highly conserved hydrophobic residues and are connected at valine 7. The N-terminal region is elongated and contains five

main secondary structures. Loop 2 (residues 19-33) in the N-terminal domain connects the strands 1 and 2 and is highly flexible. The C-terminal region contains six secondary structure elements that contact protein S4. The N-terminal domain interacts non-specifically with helix 34 that encompasses nucleotides 1046 to 1067 and 1211 to 1189 and contains the sites of mutation that confer spectinomycin resistance. S5 is acetylated at the α-amino group of the first alanine residue by RimJ (ribosomal modification). RimJ is also associated with other stages of biogenesis of the small ribosomal subunit (73). In the *E. coli* strain with an S5 G27D mutation, the assembly of ribosomes is disturbed, translation accuracy is reduced, and cold sensitivity is observed. The overexpression of RimJ in this strain completely recovers all the translational defects (51, 74)

Most of S4 and S5 compensatory mutations were isolated based on their ability to reverse the error-restrictive phenotype of S12 alterations. These selections resulted in the isolation of mutants located at or near the S4-S5 interface. Most of these mutants showed an error-prone phenotype supporting the domain closure model.

In an effort to gain a better understanding of the range of S4 and S5 residues that could be involved in the modulation of decoding fidelity, we targeted *rpsD* and *rpsE* genes for mutagenesis. Using recombineering techniques we mutagenized *rpsD* and *rpsE* to isolate mutations conferring either increased or decreased accuracy phenotype. We found that, as discussed in chapter 2, a large number of mutations away from the interface can also affect tRNA selection and give rise to error-prone or error-restrictive phenotypes.

As mutations of residues in the S4-S5 interface as well as in residues remote from the interface affect translational fidelity, we explored specific regions of both the S4 and S5 protein known to contribute to accuracy phenotype to gain a better understanding. We also

looked to delineate other sites on the genome that could be important for S4-S5 interaction and accuracy.

Culver *et. al* (75) isolated a G27D mutation in S5 located away from the S4-S5 interface. This mutant on analysis displayed spectinomycin resistance, had an error-prone phenotype, was cold sensitive and accumulated of unprocessed 16S rRNA precursor molecules and was assembly defective. They proposed an alternative model stating the error-prone phenotype of the G27D S5 mutation was due to defective rRNA processing (76, 77). We wanted to further explore if there is any correlation between assembly, processing, accuracy and spectinomycin resistance. We targeted the loop 2 regions of S5, away from the interface, to isolate and analyzed 21 different mutations described in detail in chapter 3.

The C-terminal region of S4 makes extensive contacts with S5. Truncation of the C-terminal region has been shown to result in an error-prone phenotype, temperature sensitivity, ribosome assembly and 16S rRNA processing defects. In chapter 4 we show the effects on the phenotype when the C-terminal region is restored.

To study the interaction between S4/S5 and other sites on the genome we obtained and mapped compensatory mutations in error-prone and error-restrictive mutant strains as discussed in chapter 5.

1.5 References

1. **Caliskan N, Peske F, Rodnina MV.** 2015. Changed in translation: mRNA recoding by -1 programmed ribosomal frameshifting. Trends Biochem Sci **40:**265-274.

2. **J.D. W, Baker TA, Bell SP, Gann A, Levine M, Losick R.** 2009. Molecular Biology of the Gene. Pearson Education, Inc.

3. **Wilson DN.** 2014. Ribosome-targeting antibiotics and mechanisms of bacterial resistance. Nat Rev Microbiol **12:**35-48.

4. **Agirrezabala X, Frank J.** 2010. From DNA to proteins via the ribosome: Structural insights into the workings of the translation machinery. human genomics **4:**226-237.

5. **Reynolds NM, Lazazzera BA, Ibba M.** 2010. Cellular mechanisms that control mistranslation. Nat Rev Microbiol **8:**849-856.

6. **Wohlgemuth I, Pohl C, Mittelstaet J, Konevega AL, Rodnina MV.** 2011. Evolutionary optimization of speed and accuracy of decoding on the ribosome. Philos Trans R Soc Lond B Biol Sci **366:**2979-2986.

7. **Rodnina MV.** 2012. Quality control of mRNA decoding on the bacterial ribosome. Adv Protein Chem Struct Biol **86:**95-128.

8. **Clemons WM, Jr., May JL, Wimberly BT, McCutcheon JP, Capel MS, Ramakrishnan V.** 1999. Structure of a bacterial 30S ribosomal subunit at 5.5 A resolution. Nature **400:**833-840.

9. **Wimberly BT, Brodersen DE, Clemons WM, Jr., Morgan-Warren RJ, Carter AP, Vonrhein C, Hartsch T, Ramakrishnan V.** 2000. Structure of the 30S ribosomal subunit. Nature **407:**327-339.

10. **C.R. Woese, Magrun LJ, Gupta R, Siegel RB, Stahl DA, Kop J, Crawford N, Brosius R, Gutell JJ, Hogan, Noller HF.** 1980. Secondary structure model for bacterial 16S ribosomal RNA: phylogenetic, enzymatic and chemical evidence. Nucleic acids Research **8:**2275-2293.

11. **Stern S, Powers T, Changchien LM, Noller HF.** 1989. RNA-protein interactions in 30S ribosomal subunits: folding and function of 16S rRNA. Science **244:**783-790.

12. **Voorhees RM, Mandal D, Neubauer C, Kohrer C, RajBhandary UL, Ramakrishnan V.** 2013. The structural basis for specific decoding of AUA by isoleucine tRNA on the ribosome. Nat Struct Mol Biol **20:**641-643.

13. **Bouadloun F, Srichaiyo T, Isaksson LA, Bjork GR.** 1986. Influence of modification next to the anticodon in tRNA on codon context sensitivity of translational suppression and accuracy. J Bacteriol **166:**1022-1027.

14. **Agirrezabala X, Valle M.** 2015. Structural insights into tRNA dynamics on the ribosome. Int J Mol Sci **16:**9866-9895.

15. **Sussman JL, Holbrook SR, Warrant RW, Church GM, Kim SH.** 1978. Crystal structure of yeast phenylalanine transfer RNA. I. Crystallographic refinement. J Mol Biol **123:**607-630.

16. **Gao YG, Selmer M, Dunham CM, Weixlbaumer A, Kelley AC, Ramakrishnan V.** 2009. The structure of the ribosome with elongation factor G trapped in the posttranslocational state. Science **326:**694-699.

17. **Schmeing TM, Voorhees RM, Kelley AC, Gao YG, Murphy FVt, Weir JR, Ramakrishnan V.** 2009. The crystal structure of the ribosome bound to EF-Tu and aminoacyl-tRNA. Science **326:**688-694.

18. **Kulczycka K, Dlugosz M, Trylska J.** 2011. Molecular dynamics of ribosomal elongation factors G and Tu. Eur Biophys J **40:**289-303.

19. **Brilot AF, Korostelev AA, Ermolenko DN, Grigorieff N.** 2013. Structure of the ribosome with elongation factor G trapped in the pretranslocation state. Proc Natl Acad Sci U S A **110:**20994-20999.

20. **Yu D, Zhang C, Qin P, Cornish PV, Xu D.** 2014. RNA-protein distance patterns in ribosomes reveal the mechanism of translational attenuation. Sci China Life Sci **57:**1131-1139.

21. **Laursen BS, Sorensen HP, Mortensen KK, Sperling-Petersen HU.** 2005. Initiation of protein synthesis in bacteria. Microbiol Mol Biol Rev **69:**101-123.

22. **Kaczanowska M, Ryden-Aulin M.** 2007. Ribosome biogenesis and the translation process in Escherichia coli. Microbiol Mol Biol Rev **71:**477-494.

23. **Shajani Z, Sykes MT, Williamson JR.** 2011. Assembly of bacterial ribosomes. Annu Rev Biochem **80:**501-526.

24. **Culver GM.** 2001. Meanderings of the mRNA through the ribosome. Structure **9:**751-758.

25. **Bunner AE, Beck AH, Williamson JR.** 2010. Kinetic cooperativity in Escherichia coli 30S ribosomal subunit reconstitution reveals additional complexity in the assembly landscape. Proc Natl Acad Sci U S A **107:**5417-5422.

26. **Schmeing TM, Ramakrishnan V.** 2009. What recent ribosome structures have revealed about the mechanism of translation. Nature **461:**1234-1242.

27. **Culver GM.** 2003. Assembly of the 30S ribosomal subunit. Biopolymers **68:**234-249.

28. **Culver GM, Kirthi N.** 2008. Assembly of the 30S ribosomal subunit. EcoSal Plus **3:**1-12.

29. **Connolly K, Culver G.** 2009. Deconstructing ribosome construction. Trends Biochem Sci **34:**256-263.

30. **Sun Q, Vila-Sanjurjo A, O'Connor M.** 2011. Mutations in the intersubunit bridge regions of 16S rRNA affect decoding and subunit-subunit interactions on the 70S ribosome. Nucleic Acids Res **39:**3321-3330.

31. **Zaher HS, Green R.** 2009. Fidelity at the molecular level: lessons from protein synthesis. Cell **136:**746-762.

32. **Ogle JM, Brodersen DE, Clemons WM, Jr., Tarry MJ, Carter AP, Ramakrishnan V.** 2001. Recognition of cognate transfer RNA by the 30S ribosomal subunit. Science **292:**897-902.

33. **Demeshkina N, Jenner L, Westhof E, Yusupov M, Yusupova G.** 2013. New structural insights into the decoding mechanism: translation infidelity via a G.U pair with Watson-Crick geometry. FEBS Lett **587:**1848-1857.

34. **Shoji S, Walker SE, Fredrick K.** 2009. Ribosomal translocation: one step closer to the molecular mechanism. ACS Chem Biol **4:**93-107.

35. **Selmer M, Dunham CM, Murphy FVt, Weixlbaumer A, Petry S, Kelley AC, Weir JR, Ramakrishnan V.** 2006. Structure of the 70S ribosome complexed with mRNA and tRNA. Science **313:**1935-1942.

36. **Kimura S, Suzuki T.** 2010. Fine-tuning of the ribosomal decoding center by conserved methyl-modifications in the Escherichia coli 16S rRNA. Nucleic Acids Res **38:**1341-1352.

37. **Ramakrishnan V.** 2009. The ribosome: some hard facts about its structure and hot air about its evolution. Cold Spring Harb Symp Quant Biol **74:**25-33.

38. **Kietrys AM.** 2009. Structure and function of intersubunit bridges in procaryotic ribosome. Biotechnogia.**1**:48-58.

39. **Korostelev A, Trakhanov S, Laurberg M, Noller HF.** 2006. Crystal structure of a 70S ribosome-tRNA complex reveals functional interactions and rearrangements. Cell **126:**1065-1077.

40. **Shoji S, Abdi NM, Bundschuh R, Fredrick K.** 2009. Contribution of ribosomal residues to P-site tRNA binding. Nucleic Acids Res **37:**4033-4042.

41. **Milon P, Konevega AL, Gualerzi CO, Rodnina MV.** 2008. Kinetic checkpoint at a late step in translation initiation. Mol Cell **30:**712-720.

42. **Voorhees RM, Ramakrishnan V.** 2013. Structural basis of the translational elongation cycle. Annu Rev Biochem **82:**203-236.

43. **Berman HM, Westbrook J, Feng Z, Gilliland G, Bhat TN, Weissig H, Shindyalov IN, Bourne PE.** 2000. The Protein Data Bank. nucleic acids research **29:**335-342.

44. **Shepherd J, Ibba M.** 2015. Bacterial transfer RNAs. FEMS Microbiol Rev **39:**280-300.

45. **Mittelstaet J, Konevega AL, Rodnina MV.** 2011. Distortion of tRNA upon near-cognate codon recognition on the ribosome. J Biol Chem **286:**8158-8164.

46. **Savelsbergh A, Mohr D, Wilden B, Wintermeyer W, Rodnina MV.** 2000. Stimulation of the GTPase activity of translation elongation factor G by ribosomal protein L7/12. J Biol Chem **275:**890-894.

47. **Diaconu M, Kothe U, Schlunzen F, Fischer N, Harms JM, Tonevitsky AG, Stark H, Rodnina MV, Wahl MC.** 2005. Structural basis for the function of the ribosomal L7/12 stalk in factor binding and GTPase activation. Cell **121:**991-1004.

48. **Ogle JM, Ramakrishnan V.** 2005. Structural insights into translational fidelity. Annu Rev Biochem **74:**129-177.

49. **Ogle JM, Carter AP, Ramakrishnan V.** 2003. Insights into the decoding mechanism from recent ribosome structures. Trends in Biochemical Sciences **28:**259-266.

50. **Maracci C, Peske F, Dannies E, Pohl C, Rodnina MV.** 2014. Ribosome-induced tuning of GTP hydrolysis by a translational GTPase. Proc Natl Acad Sci U S A **111:**14418-14423.

51. **Matassova AB, Rodnina MV, Wintermeyer W.** 2001. Elongation factor G-induced structural change in helix 34 of 16S rRNA related to translocation on the ribosome. RNA **7:**1879-1885.

52. **Rodnina MV.** 2013. Biochemistry. Translocation in action. Science **340:**1534-1535.

53. **Alksne LE, Anthony RA, Liebman SW, Warner JR.** 1993. An accuracy center in the ribosome conserved over 2 billion years. Proc Natl Acad Sci U S A **90:**9538-9541.

54. **Davies C, Bussiere DE, Golden BL, Porter SJ, Ramakrishnan V, White SW.** 1998. Ribosomal proteins S5 and L6: high-resolution crystal structures and roles in protein synthesis and antibiotic resistance. J Mol Biol **279:**873-888.

55. **Pape T, Wintermeyer W, Rodnina MV.** 2000. Conformational switch in the decoding region of 16S rRNA during aminoacyl-tRNA selection on the ribosome. Nat Struct Biol **7:**104-107.

56. **Gorini L, Kataja E.** 1964. Phenotypic repair by streptomycin of defective genotypes in E. Coli. Proc Natl Acad Sci U S A **51:**487-493.

57. **Carter AP, Clemons WM, Brodersen DE, Morgan-Warren RJ, Wimberly BT, Ramakrishnan V.** 2000. Functional insights from the structure of the 30S ribosomal subunit and its interactions with antibiotics. Nature **407:**340-348.

58. **Rodnina MV, Daviter T, Gromadski K, Wintermeyer W.** 2002. Structural dynamics of ribosomal RNA during decoding on the ribosome. Biochimie **84:**745-754.

59. **Gorini L.** 1969. The contrasting role of strA and ram gene products in ribosomal functioning. Cold Spring Harb Symp Quant Biol **34:**101-109.

60. **Maisnier-Patin S, Paulander W, Pennhag A, Andersson DI.** 2007. Compensatory evolution reveals functional interactions between ribosomal proteins S12, L14 and L19. J Mol Biol **366:**207-215.

61. **Dahlgren A, Ryden-Aulin M.** 2000. A novel mutation in ribosomal protein S4 that affects the function of a mutated RF1. Biochimie **82:**683-691.

62. **Bjorkman J, Samuelsson P, Andersson DI, Hughes D.** 1999. Novel ribosomal mutations affecting translational accuracy, antibiotic resistance and virulence of Salmonella typhimurium. Mol Microbiol **31:**53-58.

63. **Wittmann-Liebold B, Greuer B.** 1978. The primary structure of protein S5 from the small subunit of the Escherichia coli ribosome. FEBS Lett **95:**91-98.

64. **Cukras AR, Southworth DR, Brunelle JL, Culver GM, Green R.** 2003. Ribosomal proteins S12 and S13 function as control elements for translocation of the mRNA : tRNA complex. Molecular Cell **12:**321-328.

65. **Agarwal D, Gregory ST, O'Connor M.** 2011. Error-prone and error-restrictive mutations affecting ribosomal protein S12. J Mol Biol **410:**1-9.

66. **Yaguchi M, Wittmann HG, Cabezon T, De Wilde M, Villarroel R, Herzog A, Bollen A.** 1975. Cooperative control of translational fidelity by ribosomal proteins in Escherichia coli. II. Localization of amino acid replacements in proteins S5 and S12 altered in double mutants resistant to neamine. Mol Gen Genet **142:**35-43.

67. **Haft RJ, Keating DH, Schwaegler T, Schwalbach MS, Vinokur J, Tremaine M, Peters JM, Kotlajich MV, Pohlmann EL, Ong IM, Grass JA, Kiley PJ, Landick R.** 2014. Correcting direct effects of ethanol on translation and transcription machinery confers ethanol tolerance in bacteria. Proc Natl Acad Sci U S A **111:**E2576-2585.

68. **VanNice J, Gregory ST, Kamath D, O'Connor M.** 2016. Alterations in ribosomal protein L19 that decrease the fidelity of translation. Biochimie **128-129:**122-126.

69. **Kirsebom LA, Amons' R, Isaksson L.** 1986. Primary structures of mutationally altered ribosomal protein L7/L12 and their effects on cellular growth and translational accuracy. european Journal of Biochemistry **156:**669-675.

70. **Davies C, Gerstner RB, Draper DE, Ramakrishnan V, White SW.** 1998. The crystal structure of ribosomal protein S4 reveals a two-domain molecule with an extensive RNA-binding surface: one domain shows structural homology to the ETS DNA-binding motif. EMBO J **17:**4545-4558.

71. **Mayerle M, Woodson SA.** 2013. Specific contacts between protein S4 and ribosomal RNA are required at multiple stages of ribosome assembly. RNA **19:**574-585.

72. **Brodersen DE, Clemons WM, Jr., Carter AP, Wimberly BT, Ramakrishnan V.** 2002. Crystal structure of the 30 S ribosomal subunit from Thermus thermophilus: structure of the proteins and their interactions with 16 S RNA. J Mol Biol **316:**725-768.

73. **Nesterchuk MV, Sergiev PV, Dontsova OA.** 2011. Posttranslational modifications of ribosomal proteins in Escherichia coli. Acta Naturae **3:**22-33.

74. **Napper N, Culver GM.** 2015. Analysis of r-protein and RNA conformation of 30S subunit intermediates in bacteria. RNA **21:**1323-1334.

75. **Gupta N, Culver GM.** 2014. Multiple in vivo pathways for Escherichia coli small ribosomal subunit assembly occur on one pre-rRNA. Nat Struct Mol Biol **21:**937-943.

76. **Roy-Chaudhuri B, Kirthi N, Culver GM.** 2010. Appropriate maturation and folding of 16S rRNA during 30S subunit biogenesis are critical for translational fidelity. Proc Natl Acad Sci U S A **107:**4567-4572.

CHAPTER 2

MODULATION OF DECODING FIDELITY BY RIBOSOMAL PROTEINS S4 AND S5

2.1 Abstract

Ribosomal proteins S4 and S5 participate in the decoding and assembly processes on the ribosome and the interaction with specific antibiotic inhibitors of translation. Many of the characterized mutations affecting these proteins decrease the accuracy of translation, leading to a ribosomal ambiguity (*ram*) phenotype. Structural analyses of ribosomal complexes indicate that the tRNA selection pathway involves a transition between closed and open conformations of the 30S ribosomal subunit and requires disruption of the interface between S4 and S5 proteins. In agreement with this observation, several of the *ram* mutations alter residues located at the S4-S5 interface. Here, the *Escherichia coli rpsD* and *rpsE* genes encoding S4 and S5 proteins have been targeted for mutagenesis and screened for accuracy-altering mutations. While a majority of the 38 recovered mutants decrease the accuracy of translation, error-restrictive mutations were also recovered; only a minority of the mutant proteins affected rRNA processing, ribosome assembly or interactions with antibiotics. Several of the mutants affect residues at the S4-S5 interface. These include 5 nonsense mutations that generate C-terminal truncations of S4. These truncations are predicted to destabilize the S4-S5 interface and, consistent with the domain closure model, all have *ram* phenotypes. A substantial number of the mutants alter distant locations and conceivably affect tRNA selection through indirect effects on the S4-S5 interface or by

altering interactions with adjacent ribosomal proteins and 16S rRNA.

2.2 Introduction

Cellular protein synthesis systems translate mRNAs quickly and with high accuracy. The accuracy of the decoding process can, however, be altered by agents such as the antibiotic streptomycin that promote miscoding, and by mutations in rRNA, ribosomal proteins or translation factors (1). Among the first such accuracy mutants to be characterized were some of the streptomycin-resistant *E. coli* strains carrying alterations in ribosomal protein S12 (2). Subsequently, *E. coli* mutants carrying altered ribosomal proteins S4 or S5 were isolated that supported increased levels of miscoding (3-5). Since these early studies, many other mutants have been isolated that affect the accuracy of decoding and carry alterations in different components of the translation machinery (1, 4).

The determination of high resolution structures of ribosomes has offered structural interpretations of the effects of some accuracy-altering ribosomal mutations (6). X-ray crystallography of ribosomal complexes has shown that conserved RNA elements of the decoding center use a shape-sensing mechanism to monitor base pairing between the A site codon and the anticodon of incoming aminoacyl-tRNA. Successful interaction of a ternary complex of EF-Tu•GTP•aminoacyl-tRNA with mRNA in the decoding center triggers a series of conformational rearrangements of the head and shoulder domains of the 30S subunit, ultimately resulting in the formation of a 'closed' 30S subunit conformation (7). Comparison of vacant and tRNA-bound 30S subunits showed that transition to the closed conformation involved formation of new S12-rRNA interactions and disruption of some S4-S5 contacts. For instance, in the closed conformation, R53 and K42 of S12 contact h44 and h27, respectively, and mutations in these S12 residues, which are predicted to inhibit domain

closure, have error-restrictive phenotypes. Similarly, transition to the closed conformation requires disruption of contacts along the interface between proteins S4 and S5 and many of the previously-described error-promoting, ribosomal ambiguity (*ram*) mutations in these proteins map to interface residues. Thus, disruption of the S4-S5 contacts at their interface by mutation is predicted to facilitate transition to a closed 30S subunit conformation, neatly explaining the phenotypes and location of the classic S4 and S5 accuracy-altering mutations (7).

Despite its appealing ability to integrate structural, genetic and biochemical data, some observations do not support the notion that accuracy-altering mutations must necessarily affect the S4-S5 interface. In the early genetic studies, it was found that combinations of error-restrictive S12 mutations and error-prone *ram* S4 (or S5) proteins generated a quasi-wild-type error phenotype (3, 5). In terms of the open/closed model, these combinations could be explained by a simple compensation mechanism. However, Bjorkmann *et al.* (8) reported on some novel mutations in S4 that were error-restrictive, but which nonetheless also reversed the restrictiveness of classic S12 mutations, seemingly in conflict with the predictions of the open/closed model. Work from the Culver lab showed that a G27D substitution in S5 (*E. coli* numbering is used throughout and omits the N-terminal Met) in a region remote from the interface with S4, increased miscoding through effects on rRNA processing and subunit assembly (9). This offers an alternative explanation for the effects on decoding, for at least some mutant proteins. The S4-S5 interaction and the effects of accuracy-altering interface mutations have been tested in the context of a yeast two-hybrid system (10). In this, albeit artificial context, proteins S4 and S5 did interact with one another and some accuracy-altering mutations affected their interactions. However, the

effects of the mutations on S4-S5 interactions did not reflect their ribosomal error phenotypes, or predicted effects on S4-S5 interface destabilization. More recently, two 16S rRNA mutations that promote miscoding, G299A and G347U, have been analyzed by X-ray crystallography of the mutant 70S ribosomes (11). Both mutations were found to disrupt bridge B8, one of the intersubunit bridges connecting 30S and 50S subunits in the 70S ribosome. This was not unexpected in the G347U mutant, since this region of 16S rRNA forms part of bridge B8. However, G299 is some 80Å away from bridge B8. Moreover, G299 is close to the S4-S5 interface, raising the possibility that the effects of alterations in proteins S4 and S5 on decoding might also be propagated through bridge B8 (11, 12). The position of bridge B8 relative to S4 and S5 is shown in Figure. S2.1.

In an effort to gain a better understanding of the range of S4 and S5 residues involved in modulating decoding fidelity, we have targeted the *rpsD* and *rpsE* genes encoding these proteins for mutagenesis. In previous genetic studies, S4 and S5 mutants were typically isolated based on their ability to reverse the decreased growth, dependence on streptomycin or error-restrictive effects of S12 alterations (3, 5). In addition, some S5 mutants were also recovered in selections for resistance to spectinomycin or neamine (13, 14). With some exceptions, these selections mostly succeeded in isolating a limited number of error-prone S4 and S5 mutants. We have previously shown that when recombineering approaches are applied to the *rpsL* gene encoding S12, novel mutant proteins, with diverse effects on decoding can be recovered (15). Here, recombineering has allowed us to recover a wide array of alterations in S4 and S5 with diverse effects on decoding fidelity. Many of the substitutions are in residues distant from the S4-S5 interface and few have pronounced effects on rRNA processing or ribosome assembly.

2.3 Materials and Methods

2.3.1 Bacterial Strains and Plasmids.

MC323 (F^-, λ^-, *lacZ521* (Tn*10* linked), *rph-1*) was the host strain used for recombineering and screening for accuracy-altering mutations. MC361 (F^-, *ara*$^-$ Δ(*gpt-lac*)*5 thi*$^-$ *prfB* [*E. coli* B]) carries the fully active A246 RF2 allele (16) and was used for reconstruction of the selected mutants. Plasmids pKD46, pKD4 and pCP20 were used in recombineering (17).

The *lacZ* plasmid, pLG3/4 UGA, carrying a UGA stop codon in the 5' region of the coding sequence was used to monitor stop codon readthrough (18). The ampicillin resistant, dual luciferase plasmids pEK4, pEK5, pEK7 and pEK24, were a gift of Dr. Philip Farabaugh, University of Maryland and were used to monitor missense decoding. These plasmids encode a single polypeptide consisting of the firefly luciferase (F-luc) fused in frame to the Renilla luciferase (R-luc). Lysine 529 of F-luc is an essential, active site residue and plasmid pEK4 carries the wild type lysine 529 codon. In plasmids pEK7 and pEK24, the AAA lysine codon at position 529 has been replaced by AAU (Asn) and AGG (Arg), respectively. In strains carrying pEK7 or pEK24, near-cognate decoding of AGG or AAU by the AAA/G-decoding $tRNA^{Lys}$ is required for the synthesis of proteins with F-luc activity. Plasmid pEK5 carries a UUU codon at position 529 and serves as a negative control.

2.3.2 Random Mutagenesis of *rpsD* and *rpsE*

The *rpsD* gene encoding S4 protein and the *rpsE* gene encoding S5 protein were each targeted for random mutagenesis. To facilitate subsequent genetic manipulations, a kanamycin cassette was first linked to each of the genes, using recombineering techniques. The intergenic spacers between *rpsD* and *rpoA* and *rpsE* and *rpmD* are 24 and 3 nt,

respectively, so the kanamycin cassette was inserted immediately after the stop codon in both the *rpsD* and *rpsE* genes. MC323 carries a premature UGA mutation in the *lacZ* gene (*lacZ521*). Due to near-cognate decoding of UGA by $tRNA^{Trp}$, this *lacZ* allele supports a low level of β-galactosidase activity and MC323 colonies appear pale blue on 5-bromo-4-chloro-3-indolyl-β-D-galactopyranoside (X-gal) plates, facilitating detection of increased and decreased UGA readthrough, by error-prone and error-restrictive ribosomes, respectively.

For random mutagenesis, a 1.2 kb segment of DNA encoding S4 or S5 linked to the Kan cassette was amplified using the error-prone polymerase Mutazyme (Agilent Technologies, Santa Clara, CA) as recommended by the manufacturers. The template concentrations and amplification conditions were adjusted to allow the incorporation of 1-2 errors per amplified molecule. Electrocompetent MC323 cells expressing lambda red recombinase were electroporated with this randomly mutagenized DNA and plated on LB medium containing kanamycin, IPTG and X-gal. Kanamycin resistant colonies that were either bluer or whiter than the wild type were identified, purified and sequenced. Selected *rpsD* or *rpsE* alleles that showed altered *lac* phenotypes on X-gal plates were transferred into MC361 by P1-mediated transduction. The Kan cassettes were removed by transient expression of the Flp recombinase and the *rpsD* or *rpsE* genes from each kanamycin sensitive strain were re-sequenced to confirm the presence of the desired mutation and the absence of any additional, unanticipated base changes.

2.3.3 Growth Rate and Antibiotic Sensitivity Determinations, Enzyme Assays, rRNA Processing and Ribosome Analyses

Growth rate determination was carried out in LB medium at 37˚C. Temperature sensitivity was analyzed by plating 10 fold serial dilutions of overnight cultures on LB agar plates and incubated at 20˚C, 37˚C and 42˚C for 24-48 hrs. Antibiotic resistances were determined using two-fold serial dilution of each antibiotic (streptomycin for S4 and S5; spectinomycin for S5) in 96 well microtiter dishes.

Detergent lysates of logarithmically growing cells were prepared as described previously. 30S and 50S subunits were separated from 70S ribosomes and polysomes by centrifugation through linear 10 to 40% sucrose gradients in a Beckman SW28 rotor for 18 h at 38,191 *x* g. The gradients were analyzed on an ISCO gradient fractionator connected to an ISCO UV5 detector.

Isolation of total RNA from logarithmically-growing cells and analysis of rRNAs on 0.7% agarose/0.9% synergel gels was carried out as described by Wachi and Nagai (19). In addition, RNAs were also isolated from wild type strains treated with chloramphenicol (final concentration of 60 mg/l) for 30 min. Chloramphenicol is known to inhibit rRNA processing and leads to the accumulation of 17S precusors of 16S rRNA (20, 21).

Firefly (F-luc) and Renilla (R-luc) luciferase activities were assayed using the Dual-Luciferase Reporter Assay System (Promega; Madison WI). Cell lysates were prepared and assayed, following the manufacturer's instructions and luminescence was measured using a Glomax 20/20 luminometer. R-luc activity served as an internal standard to control for variations in mRNA and protein levels between cultures. Each plasmid-containing strain was assayed at least in triplicate and F-luc/R-luc ratios were calculated. The frequency of

misreading in strains expressing the K529N or K529R firefly luciferases was expressed (in arbitrary, relative light units (RLU)) as the F-luc/R-luc ratio normalized to the F-luc/R-luc ratio from isogenic strains expressing the wild type, K529 firefly luciferase (22). β-galactosidase assays were performed as described previously and expressed in Miller units (23).

2.4 Results

2.4.1 Random Mutagenesis of the *rpsD* and *rpsE* Genes Encoding Ribosomal Proteins S4 and S5

The *rpsD* and *rpsE* genes and their respective, linked kanamycin resistance cassettes were each amplified in an error-prone PCR and the mutagenized fragments were electroporated into strain MC323. The leaky *lacZ521* UGA mutation in MC323 was used to identify mutants with increased or decreased decoding fidelity (15). From 20 electroporations with mutated *rpsD* fragments, 1,221 transformants were recovered on X-gal, IPTG, kanamycin plates. Of these, 38 displayed a dark blue, *ram* phenotype, while 3 had an error-restrictive phenotype. Several of the putative *ram* mutants were unstable and were not pursued. Previous work in *Salmonella* has shown that certain error-restrictive S4 mutants confer resistance to low levels of streptomycin (8). However, replica-printing of all of the transformants onto LB plates supplemented with 10 mg/l of streptomycin did not yield any streptomycin-resistant colonies. Sequencing of 26 *ram* mutants showed that 17 carried unique mutations while the 3 restrictive mutants each contained different *rpsD* sequences (Table 2.1). Similarly, 21 electroporations with mutated *rpsE* fragments generated 2,270 transformants that yielded 24 *ram* and 7 restrictive mutants. Sequencing of 15 of the *ram* mutants showed that 14 carried unique changes, while 5 unique alterations were found among the 6 sequenced, restrictive *rpsE* mutants (Table 2.1). A majority of the mutants produced S4 or S5 proteins with single amino acid substitutions. However, among the 3 restrictive S4 mutants, 2 carried single amino acid substitutions (G86C and L202F) while the remaining mutant carried the G86C substitution along with a Q151P alteration (Table 2.1). Only the mutant carrying the G86C single amino acid substitution was pursued further.

Among the collection of S5 mutants, 5 mutants (2 *ram*, 3 restrictive) carried more than one substitution at non-adjacent codons in *rpsE*. Attempts to separate the mutations and correlate accuracy phenotypes with single amino acid substitutions were unsuccessful and these S5 double mutants were not studied further. S4 is a primary binding protein and a surprising feature of the collection of S4 *ram* mutants is the occurrence (5/20) of truncated S4 proteins. This is nonetheless consistent with previous work which has shown that accuracy-altering *rpsD* mutations can generate shortened S4 proteins (24). A single mutant had an S4 protein with a two amino acid (+ tyr val) C-terminal extension.

Table 2.1 Effects of altered S4 and S5 ribosomal proteins on growth and antibiotic sensitivity

Mutated residue(s)[a]	Accuracy Phenotype[b]	Doubling time (min)	Streptomycin MIC (μg/ml)
S4 WT	WT	28 ± 1	12.5
D49Y	*ram*	33 ± 2	12.5
Q53H	*ram*	40 ± 2	6.25
Q53P	*ram*	37 ± 2	12.5
E68D	*ram*	29 ± 1	12.5
R69P	*ram*	37 ± 2	12.5
G86C	restrictive	30 ± 2	25
G86C; Q151P	restrictive	ND	ND
E165*	*ram*	50 ± 2	12.5
W169*	*ram*	30 ± 1	12.5
E196D	*ram*	30 ± 1	12.5
E196*	*ram*	32 ± 2	12.5
I199N	*ram*	30 + 2	6.25
E201G	*ram*	33 ± 1	12.5
E201*	*ram*	30± 2	12.5
L202F	restrictive	33 ± 1	12.5
S204T	*ram*	30 ± 2	12.5
K205*	*ram*	31 ± 1	12.5
K205E	*ram*	31 ± 2	12.5

Mutated residue(s)[a]	Accuracy Phenotype[b]	Doubling time (min)	Streptomycin MIC (μg/ml)
K205T	*ram*	31 ± 1	12.5
+Tyr-Val	*ram*	32 ± 2	6.25

Mutated residue(s)	Accuracy Phenotype[b]	Doubling time (min)	Streptomycin MIC (μg/ml)	Spectinomycin MIC (μg/ml)
S5 WT	WT	28 ± 2	12.5	50
K13M; S91Y	*ram*	ND	ND	ND
F30V	restrictive	31 ± 1	25	25
E54D; I104T; I140I	*ram*	ND	ND	ND
L75R	*ram*	30 ± 2	6.25	25
L80Q	*ram*	56 ± 1	25	50
G86C	*ram*	31 ± 1	12.5	50
T89S; G86C	*ram*	ND	ND	ND
Q96E	*ram*	30 ± 2	12.5	25
T102I	*ram*	27 ± 2	12.5	25
I104L	restrictive	29 ± 1	12.5	25
A109V	*ram*	31 ± 1	12.5	25
E115Q	restrictive	29 ± 2	12.5	50
N121H	*ram*	30 ± 1	25	25

Mutated residue(s)	Accuracy Phenotype[b]	Doubling time (min)	Streptomycin MIC (μg/ml)	Spectinomycin MIC (μg/ml)
L123Q	*ram*	34 ± 1	12.5	25
A126D	*ram*	31 ± 2	12.5	25
N134Y	*ram*	56 ± 2	3.125	25
V135L; E162D	restrictive	ND	ND	ND
P149Q	*ram*	30 ± 1	12.5	50

[a]Mutations that generate in-frame stop codons are indicated with an asterisk (*); a + indicates a C-terminal extension of the protein. [b]Accuracy phenotypes reflect alterations in readthrough of the *lacZ521* (UGA) allele in MC323, used in the initial screening of mutants. Strains carrying multiple changes were not pursued beyond the initial screening and sequencing. The S5 mutant carrying E54D and I104T substitutions also carries silent I140I alterations. All strains carry, in addition to the changes indicated, an 85-bp 'scar' sequence produced by flippase-mediated recombination of the kanamycin resistant cassettes downstream of the S4 and S5 coding region. [c]DT, doubling time,
[d]WT, wild type,
[e]ND, not determined

A mutant S4 protein, truncated at residue E201 has also been described in *Salmonella* (8). However, in contrast to the analogous *E. coli* mutant described here that has a strong *ram* phenotype (based on readthrough of the *lacZ* (UGA) allele in MC323), the *Salmonella* mutant restricts UGA readthrough, has a decreased rate of polypeptide synthesis and a substantially increased resistance to streptomycin (8). To explore this unexpected discrepancy between these two closely-related bacteria, the *E. coli rpsD* fragment carrying the E201* alteration and the downstream kanamycin cassette was amplified and electroporated into MC323 cells expressing λ Red recombinase. Transformants were plated on X-gal and kanamycin plates. A total of 281 transformants were recovered from 9

independent electroporations and these colonies had either a dark blue (*ram*) phenotype (191 colonies) or the pale blue color characteristic of cells with wild type ribosomes (90 colonies). Importantly, no white colonies with an error-restrictive phenotype were recovered. Reconstruction of the E201* mutant in MC361 by transduction also yielded a *ram* strain (see below). This suggests that either the S4 protein truncated at E201 has divergent effects on decoding in *S. enterica* and *E. coli*, or that additional, suppressor mutations are present in the *S. enterica* strain that alter its decoding properties.

Most of the collection of 19 S4 and 14 S5 mutants characterized here grew well in liquid medium at 37°C (Table 1). Only the S5 mutants carrying L80Q, L123Q and N134Y substitutions and the S4 mutants carrying Q53H, Q53P and R69P alterations or truncated at E165 had substantially longer doubling times (>1.2X that of wild type; Table 1). Similarly, most mutants grew well on solid media at 20°C, 37°C and 42°C (Figure. 2.1). Cold sensitivity is a classic phenotype of ribosome assembly-defective mutants. Among the collection, the N134Y and L80Q S5 mutants failed to grow at 20°C while several S4 and S5 mutants, including the R69P and Q53P alterations in S4 showed decreased growth at this temperature (Figure.2.1). Growth at 42°C was decreased in the R69P S4 mutant and, to a lesser extent, in the N134Y and L80Q S5 mutants (Figure. 2.1). Nonetheless, the ribosomes in a majority of the mutants assemble and function at levels that can support robust bacterial growth.

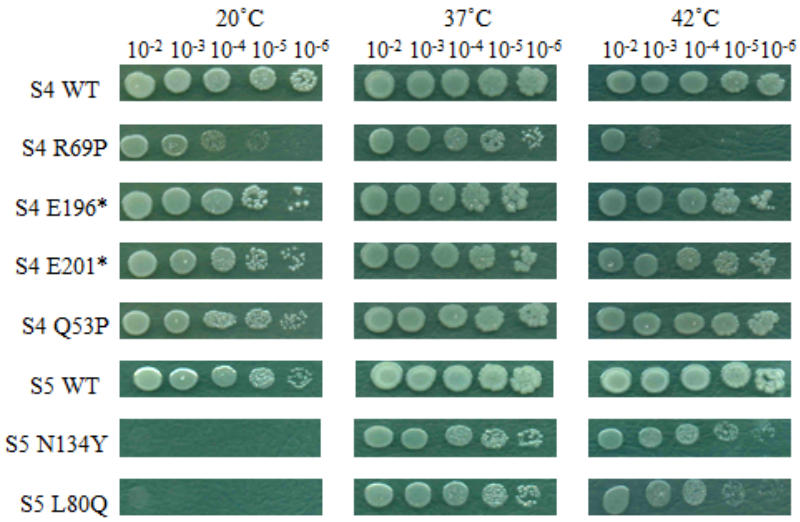

Figure 2.1 Effects of selected mutations in ribosomal proteins S5 and S4 on growth on solid media at 20ºC, 37ºC and 42ºC. 3 µl aliquots of serially diluted (10^{-2} -10^{-6}) overnight cultures of the indicated mutants were spotted onto antibiotic-free LB plates and incubated for 24-48 hrs.

Several of the previously characterized S4 and S5 mutants display altered sensitivity to the error-inducing antibiotic, streptomycin (3, 25). The responses of the mutants isolated here to streptomycin were quantitated in a minimum inhibitory concentration (MIC) assay. While 8 mutants show two-fold differences from the wild type MIC, only the N134Y S5 mutant shows a substantial, four-fold decrease in MIC. Resistance to the aminocyclitol antibiotic spectinomycin can be achieved by alterations in ribosomal protein S5 (26). However, while 10 out of the 14 S5 mutants studied here showed a two-fold decrease in their spectinomycin MICs, relative to wild type, none showed an increased MIC (Table 2.1).

2.4.2 Miscoding Properties of S4 and S5 Mutants.

Many of the reporter genes used to measure the fidelity of decoding, including the one used here to screen for accuracy-altering mutations, rely on decoding of a stop codon by a wild-type tRNA. In principle, such readthrough events can reflect defects either in the decoding or termination processes. In contrast, missense errors uniquely reflect decoding of a sense codon by a near-cognate tRNA. Here, both luciferase-based miscoding and β–galactosidase-based UGA readthrough assays were used to characterize the S4 and S5 mutants and the results of these assays are presented in Figure. 2.2. The missense decoding values in Figure. 2.2 reflect near-cognate decoding of AAU by the AAA/G-decoding $tRNA^{Lys}$. Similar patterns of miscoding were obtained with pEK24-transformed cells, encoding a K529R luciferase and requiring near-cognate decoding of AGG by $tRNA^{Lys}$ (data not shown). By and large, both data sets are consistent with one another; mutants that promote miscoding also promote readthrough. Conversely, the four restrictive mutants analyzed here (G86C and L202F in S4, I104L and E115Q in S5) show reduced UGA readthrough in *lacZ* (25-79% of the assay values of the corresponding wild-type strains) as well as decreased miscoding in the F-luc (K529N) construct used (36-64% of the activities measured in the corresponding wild-type strains). All of the *ram* mutants stimulated both miscoding and readthrough. However, the extent of these effects differed. Relative to wild-type strains, increases in miscoding ranged from 1.4-34.3 fold, while readthrough levels ranged from 1.3-5.2 fold. Clearly, mutants such as the S4 Q53P and the S5 A109V stimulate miscoding to a far greater extent (34.3- and 16.3-fold, respectively) than they increase readthrough (3.0- and 4.0-fold, respectively). Other mutants such as the S5 L123Q and the S4 R69P promote similar levels of miscoding (2.2- and 3.0-fold, respectively) and

readthrough (1.5- and 2.3-fold, respectively). The altered decoding properties of the mutants also reflect the screen for readthrough of UGA codons used to isolate them. Had we screened initially for mutants showing altered miscoding (using a missense decoding assay, for instance (27)), it is highly likely that a different spectrum of mutants with a distinct bias for miscoding *vs.* readthrough would have been recovered. Nonetheless, for the S4 and S5 mutants isolated here, while the magnitude of effects on miscoding and readthrough differs among individuals, all of the ribosomal mutations affect both processes.

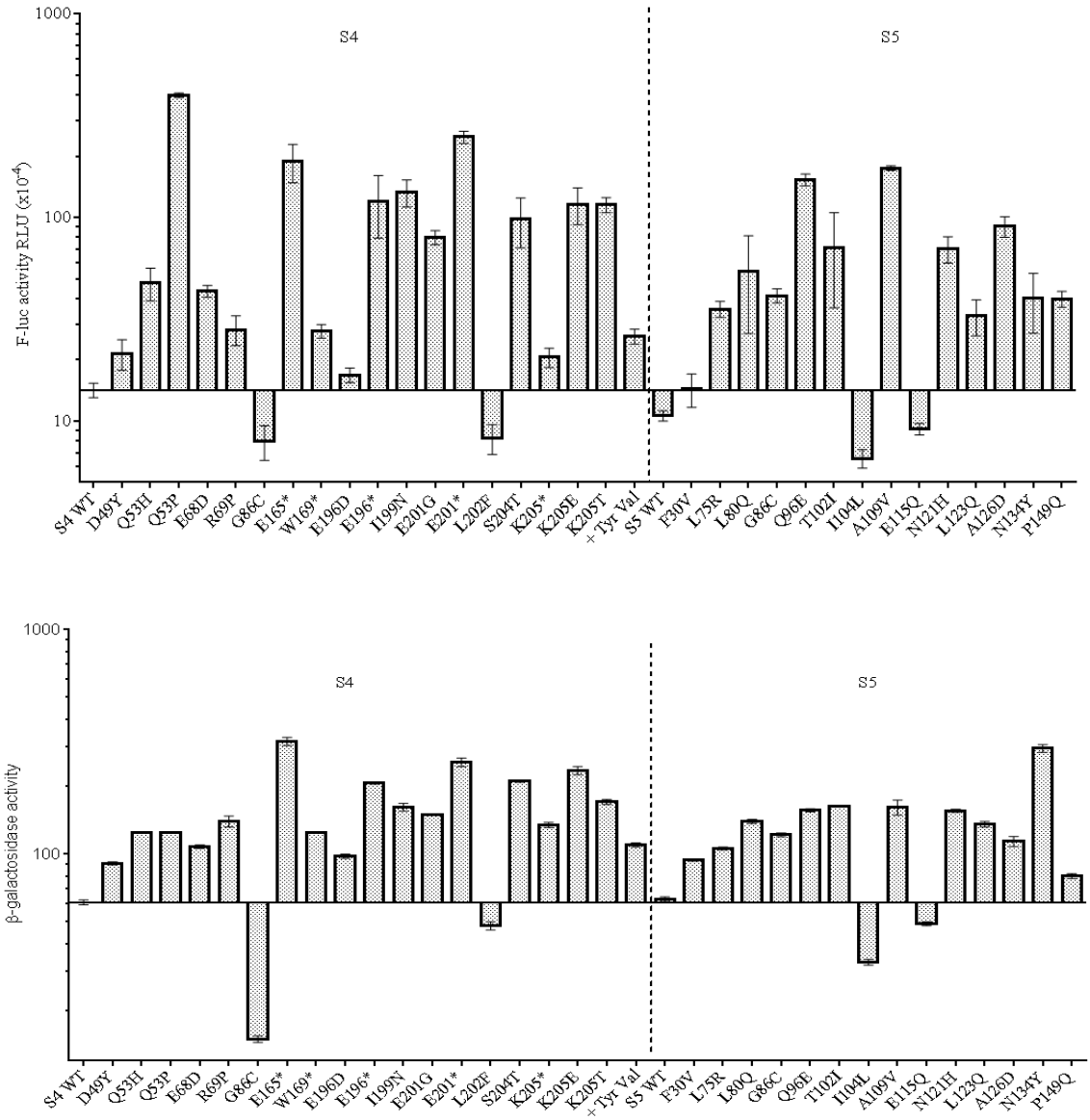

Figure 2.2 Effects of altered ribosomal proteins S4 and S5 on missense decoding (upper panel) and UGA readthrough (lower panel). Missense decoding values were obtained from pEK7-transformed cells and reflect near-cognate decoding of AAU by the AAA/G-decoding $tRNA^{Lys}$. Misreading levels are expressed in relative light units (RLU), as described in the text. Readthrough levels were obtained from strains transformed with the *lacZ* plasmid pSG3/4 UGA, carrying a UGA mutation in the 5' end of the β-galactosidase coding region. Bars represent (Miller) units of β-galactosidase activity (43). +Tyr-Val indicates a C-terminal extension of S4.

2.4.3 A Minority of Altered S4 and S5 Proteins Affect rRNA Processing and 30S Subunit Assembly

Ribosomal protein S4 is a primary binding protein and alterations in this protein, including those that alter decoding have been shown to affect ribosome assembly (28, 29). In addition, recent analysis of ribosomes carrying a G27D alteration in ribosomal protein S5 established a link between defective rRNA processing and translational fidelity (9). These studies raise the possibility that at least some of the phenotypes of ribosomal mutants, including altered decoding, may be due to indirect effects on rRNA processing and ribosomal subunit assembly. To pursue this possibility, cell lysates from each of the 33 mutants studied here were analyzed by sucrose gradient centrifugation. Only 4 mutants (R69P and E165* in S4; L80Q and N134Y in S5) displayed ribosome profiles that differed from the wild-type strain (Figure. 2.3). All 4 had high levels of 70S ribosomes and while no additional peaks corresponding to assembly intermediates were observed, gradients of these 4 mutants contained reduced amounts of free 30S particles and increased amounts of 50S particles, relative to gradients of wild-type ribosomes. This suggests that these specific alterations in S4 and S5 affect the assembly and/or stability of the mutant 30S subunits.

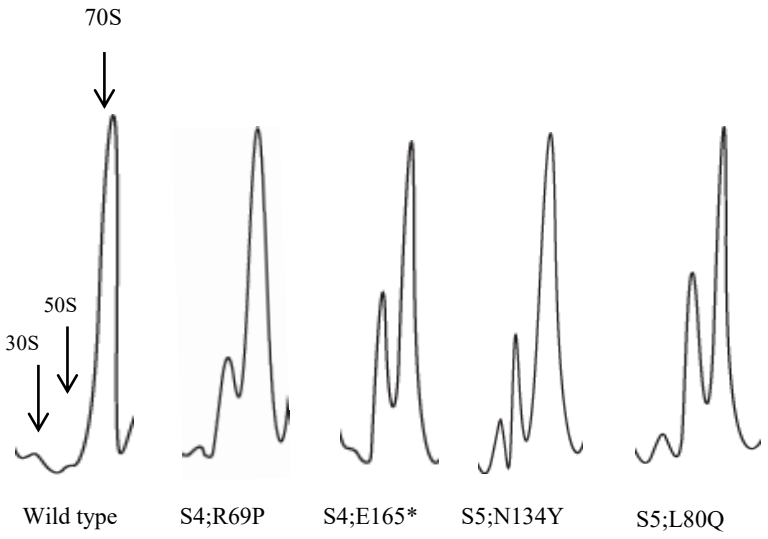

Figure 2.3 Ribosome profiles of a wild-type strain and selected S4 and S5 mutants that displayed altered profiles. The positions of 30S and 50S subunits and 70S ribosomes are indicated on the profile of the wild type strain and the direction of sedimentation is from left to right.

Lysates from each of the 33 ribosomal mutants were also analyzed on agarose/synergel gels. This gel system can resolve 16S rRNA precursors from mature, processed 16S and 23S rRNAs (19). Of the entire mutant collection, only the S5 L80Q and N134Y mutants showed substantial accumulation of precursor 16S rRNA (Figure. 2.4). These precursors migrate at the same position as the 17S precursor species produced by the addition of chloramphenicol to wild type cells (Figure. 2.4, 2nd lane from left; (20, 21)), suggesting that processing step(s) after cleavage of the initial rRNA transcript by RNase III is affected in the mutants (19, 30). These same S5 mutants displayed irregular ribosome profiles and failed to grow at 20°C (Figures 2.1, 2.3). Of the two S4 mutants with altered ribosome profiles (Figure.2.3) only the R69P mutant showed a slight accumulation of precursor 16S rRNA. In repeated rRNA analyses, the S4 E165* mutant that also displayed

an irregular ribosome profile, failed to show any such accumulation of precursor 16S rRNA. The difference in rRNA processing between the S4 and S5 mutants with altered ribosome profiles is noteworthy; while all four mutants have an altered ratio of free 30S *vs.* 50S subunits, the 30S peaks are distinctly larger in the two S5 mutants (Figure. 2.3). This may suggest that while rRNA processing is altered in all four mutants with irregular ribosome profiles, assembling 30S subunits assembled with unprocessed 16S rRNAs are especially unstable in the two S4 mutants. Two additional S4 mutants, carrying Q53H or Q53P substitutions showed slight, variable accumulation of precursor 16S rRNA (Figure.2.4). Overall, these analyses show that only a minority of the accuracy-altering mutations in proteins S4 and S5 affect rRNA processing and ribosomal subunit assembly.

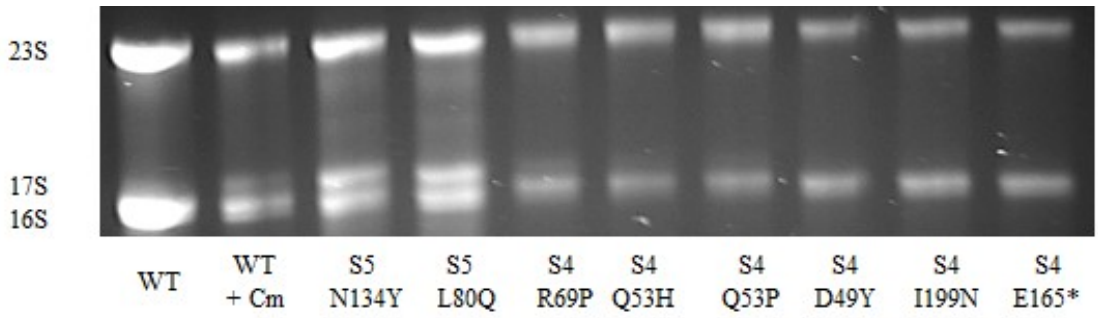

Figure 2.4 rRNA processing in wild type and selected S4 and S5 mutant strains. Total RNAs from logarithmically growing wild type and mutant strains were extracted, electrophoresed on agarose/synergel gels and stained with ethidium bromide. The second lane from the left contains RNAs extracted from wild type cells treated with chloramphenicol for 30 min., leading to the accumulation of unprocessed 17S rRNA precursors (20, 21).

2.5 Discussion

The accuracy screen used here has succeeded in isolating a large collection of S4 and S5 mutants with effects on decoding. This collection includes many of the accuracy-altering mutations isolated previously in *E. coli*, *B. subtilis* and *S. enterica* (summarized in Table S2.1). The well-studied *E. coli rpsD12*, *rpsD14* and *rpsD16* mutations (22, 24, 31, 32) all generate truncated forms of ribosomal protein S4 and *rpsD16* is identical to the W169* mutant isolated here. In *S. enterica*, selections for compensatory mutations that reversed the streptomycin dependence or slow-growth phenotypes conferred by altered S12 proteins allowed the isolation of S4 proteins with changes at residues D49, Y50, Q53, A78, N84, T85, I199, V200, E201, Y203, S204 and K205 (8, 33). The same selections in *B. subtilis* led to the isolation of S4 proteins carrying substitutions at E54 as well as insertions or deletions at residues 74-78 (34, 35). Early work in *E. coli* led to the isolation of S5 *ram* mutants carrying alterations at G103 or R111 (36). Identical mutations affecting decoding were later isolated in *B. subtilis* (35). The selections in *S. enterica* for S12-compensating mutations described above also generated S5 mutants carrying alterations at residues A98, G101, I105, A106, G108, R111, I122 and T130. While the majority of the *S. enterica* mutants were not separated from the S12 mutations(s) and assayed for their specific effects on decoding, the remarkable correspondence between the set of *E. coli* mutants described here and the *S. enterica* mutants, isolated through differing selections, suggest that a limited set of conserved residues in S4 and S5 are involved in modulating decoding activities.

2.5.1 Structural Basis for Mutant Phenotypes

To attempt to assess the structural basis for the phenotypes of mutations described above, we examined the positions of mutated residues in the context of the *E. coli* 70S

ribosome structure (pdb entry 2avy; (37)). Distance measurements are presented in Supplemental Table S2.2, and potential structural effects are summarized in Supplemental Table S2.3. S2.4 and S2.5 are located on the solvent side of the 30S subunit and share an extensive protein-protein interface (Figure. 2.5A). As in previous studies of *ram* mutations, a number of amino acid substitutions were found at the S4-S5 interface (Figure. 2.5B). These include the S4 substitutions D49Y, Q53H, Q53P, E201G, S204T, K205E and K205T, and the S5 substitutions K13M, I104L, E115Q and N121H. Additional substitutions occur not at the interface itself, but are buried within the protein and probably affect S4-S5 interaction indirectly (Figure. 2.5C). These include the S4 substitutions R69P, G86C, E196D, I199N and L202F and the S5 substitutions L75R, L80Q, T102I and A109V. The nonsense mutations in S4, including those at E165, W169, E196, E201 and K205, cause loss of the C-terminal α-helix that is a major component of the S4-S5 interface. Consistent with the domain closure model, all 5 truncation mutants have a *ram* phenotype.

Both S4 and S5 make direct contact with 16S rRNA, including at the S4-S5 interface, and several amino acid substitutions could potentially perturb these interactions. Q96 of S5 is in position to hydrogen bond with A7 of 16S rRNA (Figure. 2.5D); this base stacks on A298, consistent with the reported *ram* phenotype of both A7G and G299A base substitutions (27). Several protein-RNA interactions are distant from the S4-S5 interface. Q151 of S4 is less than 4 Å from U437 at the base of 16S rRNA helix 17 (Figure 2.5E), near the site of previously identified *ram* mutations at positions G423 and G424 (27). However, as the Q151P mutation was found only in combination with G86C, which alone produces a *ram* phenotype, the influence of the Q151P mutation is not clear. E68 of S4 is within hydrogen bonding distance of both the phosphate oxygen of C545 at the base of 16S rRNA

helix 18 and the hydroxyl group of Y203 of S4. The E68D mutation could thus perturb both an rRNA contact and destabilize the local structure of S4. The adjacent R69 does not make any direct contacts, although introduction of a rigidifying proline at this position could disrupt the local conformation of the α-helix and indirectly have the same effects as the E68D mutation.

S5 also makes contacts with 16S rRNA distant from the S4-S5 interface (Figure.2.5F). Two of the S5 mutations, N134Y and L80Q, cause defects in 16S rRNA processing. These observations are consistent with processing of 17S rRNA precursor occurring subsequent to assembly of S5 into the 30S subunit (38). The phosphate oxygen of A19 is within hydrogen bonding distance of both S5-N134 and S5-S129, while the O4' of G15 is within hydrogen bonding distance of the amino group of R28 of S5. 16S rRNA helix 1 residues A7 and G15 interact with S5 via contacts with R28 and Q96, respectively. In contrast, L80 of S5 is some 11 Å from 16S rRNA helix 1. However, it is buried within the S5 structure, and replacement of a hydrophobic side chain with a polar one could disrupt the structure to prevent stable interaction of the aforementioned residues with 16S rRNA. These observations suggest an important role for S5 in organizing the 5' end of the 17S rRNA precursor for processing.

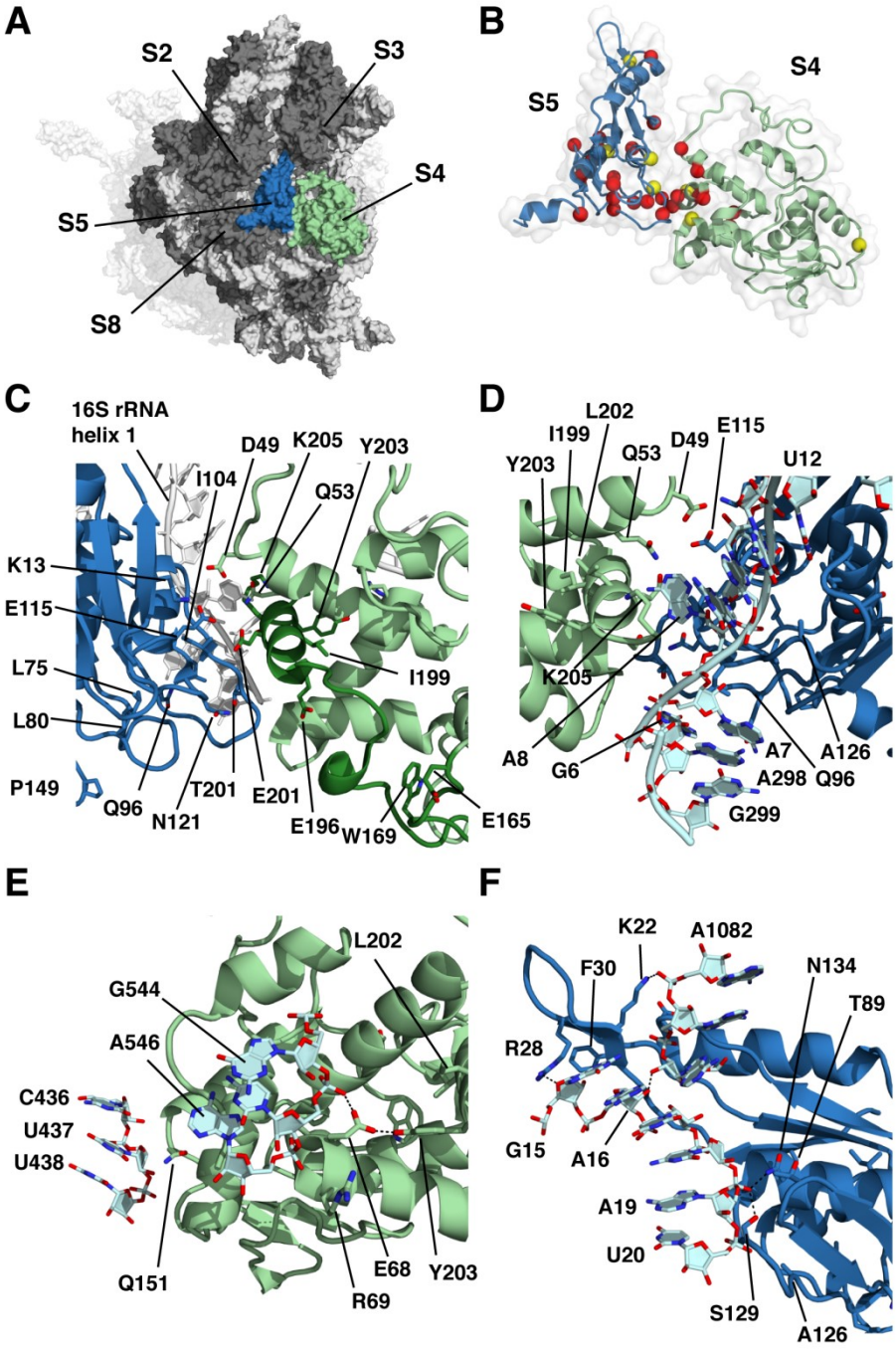

Figure 2.5 Prediction of structural effects of amino acid substitutions and termination mutants, based on the wild-type *E. coli* 70S ribosome crystal structure (36); pdb entries 2AVY and 2AW4). In all panels, S4 in colored blue, S5 is colored red, other ribosomal proteins are colored dark gray and 16S rRNA is colored light gray. (A) Surface representation of the solvent side of the 30S subunit showing the relative locations of ribosomal proteins S4 (pale green) and S5 (light blue). For orientation, the 50S subunit is shown as a transparent surface behind the 30S subunit. (B) Sites of amino acid substitutions

in S4 and S5 identified in this study. The α-carbons of residues mutated in restrictive and *ram* mutants are shown as yellow and red spheres, respectively. (C) Sites of substitutions potentially affecting the S4-S5 interface either directly by changing residues involved at the interface or indirectly by affecting local S4 or S5 conformation. Positions in S4 from E165 to the C-terminus are colored dark green including the C-terminal α-helix at the S4-S5 interface. Mutated residues are shown as sticks. 16S rRNA is colored white. (D) Proximity of 16S rRNA residues to the S4-S5 interface. (E) Sites of mutations potentially affecting S4-16S rRNA interactions distant from the S4-S5 interface. (F) Sites of mutations potentially affecting S5-16S rRNA interactions distant from the S4-S5 interface. The N134Y substitution affects processing of 16S rRNA

Several amino acid substitutions occur at sites interacting with other ribosomal proteins. For instance, G86 of S5 is on the protein surface, near sites of contact with protein S8, while E54 of S5 contacts K134 of S3. These substitutions suggest that the proper organization of S4 and S5 are essential for accurate decoding, and is stabilized by a number of interactions with other components of the ribosome. While all deletion mutations and most substitutions produce a *ram* phenotype, the S4-L202F substitution produces a restrictive phenotype. L202 is not in a position to contact S5, but is adjacent to two tyrosine residues, Y201 and Y50. In the context of the domain closure model, we would predict that this substitution would enhance S4-S5 interaction. Similarly, a restrictive phenotype is associated with the G86C substitution and would favor the closed conformation according to the domain closure model. Structure determination of these two mutants are needed to test this hypothesis.

The application of pre-steady state kinetics and single molecule FRET techniques have advanced our understanding of the individual steps of tRNA selection (39-41). Using fast kinetic approaches, Zaher and Green (31) showed that, contrary to earlier studies, ribosomes carrying an error-restrictive K42N substitution in S12 are altered in the

proofreading step of selection, while *ram* ribosomes carrying a C-terminal deletion in S4 are impaired in the initial selection step. One interpretation of the authors is that disruption of the S4-S5 interface occurs during the initial selection step and S12's interaction with h27 and h44 of 16S rRNA occurs subsequently, during proofreading. This would mean that two structural rearrangements occur at distinct points on the selection pathway. However, at least some 16S rRNA mutations that promote miscoding, including G299A which is close to S4 and S5, affect both the initial selection and proofreading steps of tRNA selection (42). Thus, it remains unclear whether the effects of altered S4 and S12 proteins on initial selection and proofreading, respectively, reflect distinct functional roles of these individual ribosomal proteins, or unique properties of the characterized mutants. The many *ram* and restrictive S4, S5, S12 and rRNA alterations described here and in earlier studies (1, 15, 42, 43) provide some of the tools needed to test these and related models for tRNA selection.

2.6 Acknowledgement

We are indebted to Dr. Philip Farabaugh for supplying the luciferase plasmids, to Dr. Sullivan Read for use of a luminometer, to Somanon Bhattacharya for assistance with figures and to Dr. Jennifer Carr for her comments on the manuscript. This work was supported by grants # MCB0745025 from the National Science Foundation (to MOC) and GM094157 from the National Institutes of Health (to SG).

2.7 References

1. **Dinman JD, OC, M.** 2010. Mutants that affect recoding, p. 321-344. *In* Atkins JFaG, R.F. (ed.), Recoding: expansion of decoding rules enriches gene expression. Springer, New York, Dordrecht, Heidelberg, London.

2. **Gorini L, Jacoby GA, Breckenridge L.** 1966. Ribosomal ambiguity. Cold Spring Harb Symp Quant Biol **31:**657-664.

3. **Rosset R, Gorini L.** 1969. A ribosomal ambiguity mutation. J Mol Biol **39:**95-112.

4. **Parker J.** 1989. Errors and alternatives in reading the universal genetic code. Microbiol Rev **53:**273-298.

5. **Piepersberg W, Bock A, Wittmann HG.** 1975. Effect of different mutations in ribosomal protein S5 of Escherichia coli on translational fidelity. Mol Gen Genet **140:**91-100.

6. **Ogle JM, Ramakrishnan V.** 2005. Structural insights into translational fidelity. Annu Rev Biochem **74:**129-177.

7. **Ogle JM, Murphy FV, Tarry MJ, Ramakrishnan V.** 2002. Selection of tRNA by the ribosome requires a transition from an open to a closed form. Cell **111:**721-732.

8. **Bjorkman J, Samuelsson P, Andersson DI, Hughes D.** 1999. Novel ribosomal mutations affecting translational accuracy, antibiotic resistance and virulence of Salmonella typhimurium. Mol Microbiol **31:**53-58.

9. **Roy-Chaudhuri B, Kirthi N, Culver GM.** 2010. Appropriate maturation and folding of 16S rRNA during 30S subunit biogenesis are critical for translational fidelity. Proc Natl Acad Sci U S A **107:**4567-4572.

10. **Vallabhaneni H, Farabaugh PJ.** 2009. Accuracy modulating mutations of the ribosomal protein S4-S5 interface do not necessarily destabilize the rps4-rps5 protein-protein interaction. RNA **15:**1100-1109.

11. **Fagan CE, Dunkle JA, Maehigashi T, Dang MN, Devaraj A, Miles SJ, Qin D, Fredrick K, Dunham CM.** 2013. Reorganization of an intersubunit bridge induced by disparate 16S ribosomal ambiguity mutations mimics an EF-Tu-bound state. Proc Natl Acad Sci U S A **110:**9716-9721.

12. **Moore PB.** 2013. Ribosomal ambiguity made less ambiguous. Proc Natl Acad Sci U S A **110:**9627-9628.

13. **DeWilde M, Wittmann-Liebold B.** 1973. Localization of the amino-acid exchange in protein S5 from an Escherichia coli mutant resistant to spectinomycin. Mol Gen Genet **127:**273-276.

14. **Yaguchi M, Wittmann HG, Cabezon T, De Wilde M, Villarroel R, Herzog A, Bollen A.** 1975. Cooperative control of translational fidelity by ribosomal proteins in Escherichia coli. II. Localization of amino acid replacements in proteins S5 and S12 altered in double mutants resistant to neamine. Mol Gen Genet **142:**35-43.

15. **Agarwal D, Gregory ST, O'Connor M.** 2011. Error-prone and error-restrictive mutations affecting ribosomal protein S12. J Mol Biol **410:**1-9.

16. **O'Connor M, Gregory ST.** 2011. Inactivation of the RluD pseudouridine synthase has minimal effects on growth and ribosome function in wild-type Escherichia coli and Salmonella enterica. J Bacteriol **193:**154-162.

17. **Datsenko KA, Wanner BL.** 2000. One-step inactivation of chromosomal genes in Escherichia coli K-12 using PCR products. Proc Natl Acad Sci U S A **97:**6640-6645.

18. **Sun Q, Vila-Sanjurjo A, O'Connor M.** 2011. Mutations in the intersubunit bridge regions of 16S rRNA affect decoding and subunit-subunit interactions on the 70S ribosome. Nucleic Acids Res **39:**3321-3330.

19. **Wachi M, Umitsuki G, Shimizu M, Takada A, Nagai K.** 1999. Escherichia coli cafA gene encodes a novel RNase, designated as RNase G, involved in processing of the 5' end of 16S rRNA. Biochem Biophys Res Commun **259:**483-488.

20. **Hayes F, Vasseur M.** 1976. Processing of the 17-S Escherichia coli precursor RNA in the 27-S pre-ribosomal particle. Eur J Biochem **61:**433-442.

21. **Harvey RJ, Koch AL.** 1980. How partially inhibitory concentrations of chloramphenicol affect the growth of Escherichia coli. Antimicrob Agents Chemother **18:**323-337.

22. **Kramer EB, Farabaugh PJ.** 2007. The frequency of translational misreading errors in E. coli is largely determined by tRNA competition. RNA **13:**87-96.

23. **O'Connor M, Thomas CL, Zimmermann RA, Dahlberg AE.** 1997. Decoding fidelity at the ribosomal A and P sites: influence of mutations in three different regions of the decoding domain in 16S rRNA. Nucleic Acids Res **25:**1185-1193.

24. **Dahlgren A, Ryden-Aulin M.** 2000. A novel mutation in ribosomal protein S4 that affects the function of a mutated RF1. Biochimie **82:**683-691.

25. **Cabezon T, Herzog A, De Wilde M, Villarroel R, Bollen A.** 1976. Cooperative control of translational fidelity by ribosomal proteins in Escherichia coli. III. A ram mutation in the structural gene for protein S5 (rpx E). Mol Gen Genet **144:**59-62.

26. **Bollen A, Davies J, Ozaki M, Mizushima S.** 1969. Ribosomal protein conferring sensitivity to the antibiotic spectinomycin in Escherichia coli. Science **165:**85-86.

27. **McClory SP, Leisring JM, Qin D, Fredrick K.** 2010. Missense suppressor mutations in 16S rRNA reveal the importance of helices h8 and h14 in aminoacyl-tRNA selection. RNA **16:**1925-1934.

28. **Olsson M, Isaksson L, Kurland CG.** 1974. Pleiotropic effects of ribosomal protein s4 studied in Escherichia coli mutants. Mol Gen Genet **135:**191-202.

29. **Mayerle M, Woodson SA.** 2013. Specific contacts between protein S4 and ribosomal RNA are required at multiple stages of ribosome assembly. RNA **19:**574-585.

30. **Li Z, Pandit S, Deutscher MP.** 1999. RNase G (CafA protein) and RNase E are both required for the 5' maturation of 16S ribosomal RNA. EMBO J **18:**2878-2885.

31. **Zaher HS, Green R.** 2010. Hyperaccurate and error-prone ribosomes exploit distinct mechanisms during tRNA selection. Mol Cell **39:**110-120.

32. **Andersson DI, Kurland CG.** 1983. Ram ribosomes are defective proofreaders. Mol Gen Genet **191:**378-381.

33. **Maisnier-Patin S, Berg OG, Liljas L, Andersson DI.** 2002. Compensatory adaptation to the deleterious effect of antibiotic resistance in Salmonella typhimurium. Mol Microbiol **46:**355-366.

34. **Henkin TM, Chambliss GH, Grundy FJ.** 1990. Bacillus subtilis mutants with alterations in ribosomal protein S4. J Bacteriol **172:**6380-6385.

35. **Inaoka T, Kasai K, Ochi K.** 2001. Construction of an in vivo nonsense readthrough assay system and functional analysis of ribosomal proteins S12, S4, and S5 in Bacillus subtilis. J Bacteriol **183:**4958-4963.

36. **Wittmann-Liebold B, Greuer B.** 1978. The primary structure of protein S5 from the small subunit of the Escherichia coli ribosome. FEBS Lett **95:**91-98.

37. **Schuwirth BS, Borovinskaya MA, Hau CW, Zhang W, Vila-Sanjurjo A, Holton JM, Cate JH.** 2005. Structures of the bacterial ribosome at 3.5 A resolution. Science **310:**827-834.

38. **Yang Z, Guo Q, Goto S, Chen Y, Li N, Yan K, Zhang Y, Muto A, Deng H, Himeno H, Lei J, Gao N.** 2014. Structural insights into the assembly of the 30S ribosomal subunit in vivo: functional role of S5 and location of the 17S rRNA precursor sequence. Protein Cell **5:**394-407.

39. **Zaher HS, Green R.** 2009. Fidelity at the molecular level: lessons from protein synthesis. Cell **136:**746-762.

40. **Rodnina MV, Gromadski KB, Kothe U, Wieden HJ.** 2005. Recognition and selection of tRNA in translation. FEBS Lett **579:**938-942.

41. **Johansson M, Lovmar M, Ehrenberg M.** 2008. Rate and accuracy of bacterial protein synthesis revisited. Curr Opin Microbiol **11:**141-147.

42. **McClory SP, Devaraj A, Fredrick K.** 2014. Distinct functional classes of ram mutations in 16S rRNA. RNA **20:**496-504.

43. **Agarwal D, O'Connor M.** 2014. Diverse effects of residues 74-78 in ribosomal protein S12 on decoding and antibiotic sensitivity. Biochem Biophys Res Commun **445:**475-479.

2.8 Supplemental Information

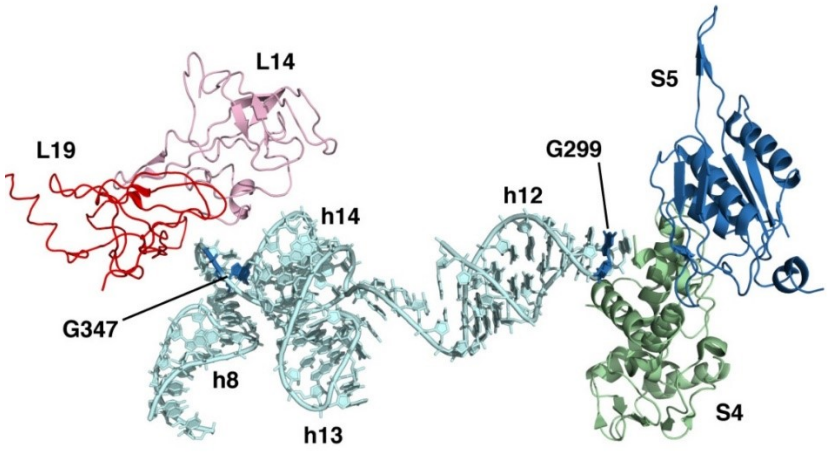

Supplemental Figure S2.1. Intersubunit bridge B8. This bridge is formed by elements of 16S rRNA and a contact with 50S ribosomal subunit proteins L14 and L19. Mutations G299A and G347U have been found by others as *ram* mutations. B8 is connected to 30S proteins S4 and S5 via 16S rRNA helix 12.

Table S2.1. Previously reported alterations affecting ribosomal proteins S4 and S5

r-prot	*rpsD* Allele/S4 Alteration	Selection Used	Accuracy Phenotype	Ref
S4				
	E. coli mutants			
	rpsD12 = Δaa 180-205#	reversal of *rpsL*-associated streptomycin dependence	*ram*	(1)
	rpsD14 = Δaa 182-205#	reversal of *rpsL*-associated streptomycin dependence	*ram*	(1)
	rpsD16 = W169Stop	reversal of *rpsL*-associated streptomycin dependence	*ram*	(1)
	rpsD101 = Y50D	suppression of a temperature sensitive *prfA* (RF1) allele	*ram*	(1)
	Q53K	reversal of *rpsL*-associated streptomycin dependence	ND	(2)
	N84Y	reversal of *rpsL*-associated streptomycin dependence	ND	(2)
	Y203	reversal of *rpsL*-associated streptomycin dependence	ND	(2)
	Δaa 198-205#	reversal of *rpsL*-associated streptomycin dependence	ND	(2)

r-prot	*rpsD* Allele/S4 Alteration	Selection Used	Accuracy Phenotype	Ref
	S. enterica mutants			(3)
	D49Y	amelioration of slow growth of *rpsL* allele	ND	(3)
	Y50C	amelioration of slow growth of *rpsL* allele	ND	(3)
	Q53L	reversal of *rpsL*-associated streptomycin dependence and amelioration of slow growth of *rpsL* allele	restrictive	(3, 4)
	Q53P	reversal of *rpsL*-associated streptomycin dependence and amelioration of slow growth of *rpsL* allele	*ram*	(3, 4)
	Q53R	amelioration of slow growth of *rpsL* allele	ND	(3)
	A78V	amelioration of slow growth of *rpsL* allele	ND	(3)
	N84D	amelioration of slow growth of *rpsL* allele	ND	(3)
	N84S	amelioration of slow growth of *rpsL*	ND	(3)

r-prot	*rpsD* Alteration	Allele/S4	Selection Used	Accuracy Phenotype	Ref
	T85I		amelioration of slow growth of *rpsL* allele	ND	(3)
	I199N		reversal of *rpsL*-associated streptomycin dependence	*ram*	(4)
	ΔV200		reversal of *rpsL*-associated streptomycin dependence	restrictive	(4)
	E201G		amelioration of slow growth of *rpsL* allele	ND	(3)
	E201V		amelioration of slow growth of *rpsL* allele	ND	(3)
	E201stop		reversal of *rpsL*-associated streptomycin dependence	restrictive	(4)
	Y203C		amelioration of slow growth of *rpsL* allele	ND	(3)
	S204F		amelioration of slow growth of *rpsL* allele	ND	(3)
	S204T		amelioration of slow growth of *rpsL* allele	ND	(3)
	S204P		amelioration of slow growth of *rpsL* allele	ND	(3)

r-prot	*rpsD* Allele/S4 Alteration	Selection Used	Accuracy Phenotype	Ref
	K205N	amelioration of slow growth of *rpsL* allele	*ram*	(3, 4)
	K205T	reversal of *rpsL*-associated streptomycin dependence	*ram*	(4)
	+5 aa C-terminal extension	amelioration of slow growth of *rpsL* allele	ND	(3)
	B. subtilis mutants			
	E74K	amelioration of slow growth of *rpsL* allele		(5)
	Duplication of aa 74-77	amelioration of slow growth of *rpsL* allele	*ram*	(5, 6)
	ΔA74-L77	amelioration of slow growth of *rpsL* allele	*ram*	(5, 6)
	E45K	amelioration of slow growth of *rpsL* allele		(5)
S5				
	E. coli mutants			
	R19L	Spectinomycin resistance	ND	(7)
	V20E	Spectinomycin resistance	ND	(7)

r-prot	*rpsE* Allele/S5 Alteration	Selection Used	Accuracy Phenotype	Ref
	S21P	Spectinomycin resistance	Unaffected	(7, 8)
	G27D	Spectinomycin resistance, cold sensitivity	*ram*	(9)
	G103R	reversal of *rpsL*-associated streptomycin dependence	ND	(7)
	R111G	neamine resistance	ND	(7)
	R111L	neamine resistance and reversal of *rpsL*-associated streptomycin dependence	*ram*	(7)
	R111S	neamine resistance	ND	(7)
	E161Stop	Suppression of temperature sensitivity of an alanyl-tRNA synthetase mutant	Unaffected	(7, 8)
	S. enterica mutants			
	A98V	amelioration of slow growth of *rpsL* allele	ND	(3)
	G101A	amelioration of slow growth of *rpsL* allele	ND	(3)
	T102A	amelioration of slow growth of *rpsL* allele	ND	(3)
	T102I	amelioration of slow growth of *rpsL* allele	ND	(3)

r-prot	*rpsE* Alteration	Allele/S5	Selection Used	Accuracy Phenotype	Ref
	I105S		amelioration of slow growth of *rpsL* allele	ND	(3)
	I105V		amelioration of slow growth of *rpsL* allele	ND	(3)
	A106S		amelioration of slow growth of *rpsL* allele	ND	(3)
	G108A		amelioration of slow growth of *rpsL* allele	ND	(3)
	G108D		amelioration of slow growth of *rpsL* allele	ND	(3)
	G108S		amelioration of slow growth of *rpsL* allele	ND	(3)
	A109V		amelioration of slow growth of *rpsL* allele	ND	(3)
	V122A		amelioration of slow growth of *rpsL* allele	ND	(3)
	T130I		amelioration of slow growth of *rpsL* allele	ND	(3)
B. subtilis mutants					
	G27V		Spectinomycin resisance	unaffected	(5)

r-prot	*rpsE* Allele/S5 Alteration	Selection Used	Accuracy Phenotype	Ref
	R111C	amelioration of slow growth of *rpsL* allele	ND	(5)
	R111H	amelioration of slow growth of *rpsL* allele	*ram*	(5)
	G103R	amelioration of slow growth of *rpsL* allele	ND	(5)
	Neisseria gonorrhoeae mutants			
	T23P	Spectinomycin resisance	ND	(10)
	ΔV24/K25E	Spectinomycin resisance	ND	(11)
	Pasteurella multocida mutants			
	ΔK22	Spectinomycin resisance	ND	(12)
	S31I/ΔF32	Spectinomycin resisance	ND	(12)

ND; not determined; # The C-termini of these proteins also differs from the wild type

Table S2.2 Distance measurements of residues involved in protein-protein and protein-rRNA contacts. All measurements performed using PyMol and the *E. coli* 70S ribosome structure, pdb entry 2AVY (13).

Atom pairs	Distance (Å)
S4-Q53(Nε2)/S5-Q115(Oε2)	5.4
S4-Q53(Nε2)/S4-E201(Oε2)	3.4
S4-E68(Oε1)/S4-Y203(OH)	2.6
S4-E68(Oε2)/16S-C545(OP1)	3.0
S4-Q151(Nε2)/16S-U437(O3')	3.4
S4-Q151(Nε2)/16S-U438(OP1)	4.0
S5-D134(Nδ2)/16S-A19(OP1)	2.5
S5-S129(Oγ)/16S-A19(OP1)	2.8
S5-R28(NH1)/16S-G15(O4')	2.7
S5-K22(Nζ)/16S-A1082(OP1)	2.8
S5-E54(Oε1)/S3-Y167(OH)	4.0
S5-E54(Oε2)/S3-K134(Nζ)	2.9
S5-Q96(Nε2)/16S-A7(N7)	3.1
S5-L123(Cδ2)/16S-G6(N7)	4.3
S5-L123(Cδ1)/16S-A7(N7)	4.3
S5-K125(Nζ)/16S-A8(OP1)	3.3
S5-A126(Cβ)/16S-A9(OP1)	3.6
S5-N134(Nδ2)/16S-A19(OP1)	2.5

Table S2.3 Summary of probable structural effects of amino acid substitutions.

Amino acid substitution	putative interaction(s) affected
S4-D49Y	S4-S5 interface
S4-Q53H or Q53PP	S4-S5 interface
S4-E68D	S4 conformation, S4-rRNA interaction
S4-R69P	S4-S5 interface (indirect)
S4-G86C	S4-S5 interface (indirect)
S4-G86C, Q151P	S4-S5 interface (indirect)
S4-E165-term	S4-S5 interface
S5-W169-term	S4-S5 interface
S4-E196D	S4-S5 interface (indirect)
S4-E196-term	S4-S5 interface
S4-I199N	S4-S5 interface (indirect)
S4-E201G	S4-S5 interface
S4-E201-term	S4-S5 interface
S4-L202F	S4-S5 interface (indirect)
S4-S204T	S4-S5 interface, S4-rRNA interaction
S4-E205-term	S4-S5 interface
S4-K205E or K205T	S4-S5 interface, S4-rRNA interaction
S5-K13M, S91Y	S4-S5 interface
S5-F30V	S5-rRNA interaction (indirect)
S5-E54D, I104T	S4-S5 interface, S5-S3 interaction

Amino acid substitution	putative interaction(s) affected
S5-L75R	S4-S5 interface (indirect), S5-rRNA interaction (indirect)
S5-L80Q	S4-S5 interface (indirect), S5-rRNA interaction (indirect)
S5-G86C	S5 protein conformation
S5-G86C, T89S	S5 protein conformation
S5-Q96E	S5-rRNA interaction
S5-T102I	S4-S5 interface (indirect)
S5-I104L	S4-S5 interface
S5-A109V	S4-S5 interface (indirect)
S5-E115Q	S4-S5 interface
S5-N121H	S4-S5 interface
S5-L123Q	S5-rRNA interaction
S5-A126D	S5-rRNA interaction
S5-N134Y	S5-rRNA interaction
S5-V135L, E162D	S5-rRNA interaction
S5-P149Q	S5-S8 interaction

Table S2.4 Oligoneucleotide used in chapter 2

Oligo name	Oligo sequence (5` - 3`)	Application
rpsEnewup	AGTCGTCCGCACCAAAGAGG	To sequence S5 gene
rpsEnewdown	ACCACCCTCGAAACCGCGAC	To sequence S5 gene
rpsEdrug3’	CTGTGGGTAAAGCTGTCGCT	To amplify S5 gene
rpsEdrug 5’	GTGACCAATACGACGCAGAC	To amplify S5 gene
rpsDamp 5’	CAGGGTAACGCGTTGGGTTG	To amplify S4 gene
rpsDamp 3’	CATCTTTGCCCTGAACTCTC	To amplify S4 gene
rpsD-drug 5’	GTCCAGGCCGCGAATCTACT	To sequence S4 gene
rpsD-drug 3’	ACGCTCTAAAGGCTCAAGGG	To sequence S4 gene

2.9 References for Supplemental Information

1. **Dahlgren A, Ryden-Aulin M.** 2000. A novel mutation in ribosomal protein S4 that affects the function of a mutated RF1. Biochimie **82:**683-691.

2. **Holberger LE, Hayes CS.** 2009. Ribosomal protein S12 and aminoglycoside antibiotics modulate A-site mRNA cleavage and transfer-messenger RNA activity in Escherichia coli. J Biol Chem **284:**32188-32200.

3. **Maisnier-Patin S, Berg OG, Liljas L, Andersson DI.** 2002. Compensatory adaptation to the deleterious effect of antibiotic resistance in Salmonella typhimurium. Mol Microbiol **46:**355-366.

4. **Bjorkman J, Samuelsson P, Andersson DI, Hughes D.** 1999. Novel ribosomal mutations affecting translational accuracy, antibiotic resistance and virulence of Salmonella typhimurium. Mol Microbiol **31:**53-58.

5. **Inaoka T, Kasai K, Ochi K.** 2001. Construction of an in vivo nonsense readthrough assay system and functional analysis of ribosomal proteins S12, S4, and S5 in Bacillus subtilis. J Bacteriol **183:**4958-4963.

6. **Henkin TM, Chambliss GH, Grundy FJ.** 1990. Bacillus subtilis mutants with alterations in ribosomal protein S4. J Bacteriol **172:**6380-6385.

7. **Wittmann-Liebold B, Greuer B.** 1978. The primary structure of protein S5 from the small subunit of the Escherichia coli ribosome. FEBS Lett **95:**91-98.

8. **Piepersberg W, Bock A, Wittmann HG.** 1975. Effect of different mutations in ribosomal protein S5 of Escherichia coli on translational fidelity. Mol Gen Genet **140:**91-100.

9. **Kirthi N, Roy-Chaudhuri B, Kelley T, Culver GM.** 2006. A novel single amino acid change in small subunit ribosomal protein S5 has profound effects on translational fidelity. RNA **12:**2080-2091.

10. **Ilina EN, Malakhova MV, Bodoev IN, Oparina NY, Filimonova AV, Govorun VM.** 2013. Mutation in ribosomal protein S5 leads to spectinomycin resistance in Neisseria gonorrhoeae. Front Microbiol **4:**186.

11. **Unemo M, Golparian D, Skogen V, Olsen AO, Moi H, Syversen G, Hjelmevoll SO.** 2013. Neisseria gonorrhoeae strain with high-level resistance to spectinomycin due to a novel resistance mechanism (mutated ribosomal protein S5) verified in Norway. Antimicrob Agents Chemother **57:**1057-1061.

12. **Kehrenberg C, Schwarz S.** 2007. Mutations in 16S rRNA and ribosomal protein S5 associated with high-level spectinomycin resistance in Pasteurella multocida. Antimicrob Agents Chemother **51:**2244-2246.

13. **Schuwirth BS, Borovinskaya MA, Hau CW, Zhang W, Vila-Sanjurjo A, Holton JM, Cate JH.** 2005. Structures of the bacterial ribosome at 3.5 A resolution. Science **310:**827-834.

CHAPTER 3

THE LOOP 2 REGION OF RIBOSOMAL PROTEIN uS5 INFLUENCES SPECTINOMYCIN SENSITIVITY, TRANSLATIONAL FIDELITY AND RIBOSOME BIOGENESIS

3.1 Abstract

Ribosomal protein uS5 is an essential component of the small ribosomal subunit that is involved in subunit assembly, maintenance of translational fidelity and the ribosome's response to the antibiotic spectinomycin. While many of the characterized uS5 mutations that affect decoding map to its interface with uS4, more recent work has shown that residues distant from the uS4-uS5 interface can also affect the decoding process. We have targeted one such interface-remote area, the loop 2 region (residues 20-31) for mutagenesis in *E. coli* and have generated 21 unique mutants. A majority of the loop 2 alterations confer resistance to spectinomycin and affect the fidelity of translation. However, only a minority show altered rRNA processing or ribosome biogenesis defects.

3.2 Introduction

An essential function of the ribosome is to discriminate between cognate and near-cognate aminoacyl tRNAs at the ribosomal A site. Multiple genetic screens for mutants that display increased or decreased miscoding have identified specific ribosomal protein residues and rRNA nucleotides that are involved in this discrimination (1). Structural and biochemical investigations have provided a mechanistic framework that helps explain the effects of at least some of these ribosomal mutations on decoding fidelity (2-5).

Among the first-isolated mutants displaying an increased miscoding, or ribosomal ambiguity (*ram*) phenotype were those carrying alterations in ribosomal protein uS5 (6). Other mutations affecting uS5 have been isolated that confer resistance to the aminocyclitol antibiotic spectinomycin (7). This antibiotic impedes protein synthesis by inhibiting elongation factor G (EF-G)-catalyzed translocation, but does not affect decoding fidelity (8, 9). X-ray crystallography of ribosome-tRNA complexes suggests that ribosomal proteins uS4 and uS5 affect tRNA selection by controlling the transition between 'open' and 'closed' conformations of the 30S ribosomal subunit during tRNA selection (10). This transition involves disruption of an interface between uS4 and uS5, located on the solvent side of the 30S subunit (Figure. 3.1A). Amino acid substitutions potentially destabilizing this interface are predicted to alter tRNA selection pathways by favoring the transition to the closed conformation. In keeping with this interpretation, many of the classical, and some of the newly-isolated uS4 and uS5 miscoding mutants affect residues at this interface (11, 12). However, the affected residues in some other uS4 and uS5 accuracy-altering mutants are distant from the interface and it is unclear how they disrupt decoding.

The best-studied uS5 mutant distant from the uS4-uS5 interface carries a glycine to aspartate substitution at residue 27 (13) (numbering throughout does not include the N-terminal methionine, which is removed *in vivo* (14)). This G27D mutant has cold-sensitive, spectinomycin-resistance and increased miscoding phenotypes. Analysis of the aberrant 16S rRNA processing in this mutant led to the proposal that altered 5' processing of 16S rRNA precursors disrupts fidelity by affecting the conformation of 16S rRNA in the assembled ribosomes (15). To explore the connections between spectinomycin resistance, translational fidelity and rRNA processing, we have targeted the *E. coli rpsE* gene in the vicinity of the G27 region of uS5 for mutagenesis and have characterized 21 distinct mutants with alterations in this region of the protein. These mutants display a range of spectinomycin-resistance phenotypes and the collection includes both *ram* and error-restrictive mutants. However, at least under routine growth conditions at 37˚C (where miscoding phenotypes are evident) only a minority of the mutants display rRNA processing or ribosome biogenesis defects and we do not find a strict correlation between decreased decoding accuracy and defective rRNA processing phenotypes.

3.3 Materials and Methods

3.3.1 Bacterial Strains and Plasmids

E. coli MC323 (F^- λ^- *lacZ521* [Tn10 linked] *rph-1)* was used to screen for accuracy-altering mutations. This strain carries a UGA nonsense mutation in the *lacZ* gene (*lacZ521*) and supports a low level of β-galactosidase activity, due to near-cognate decoding of UGA. MC323 colonies appear pale blue on 5-bromo-4-chloro-3-indolyl-β-D-galactopyranoside (X-gal) plates, facilitating the detection of increased and decreased miscoding, by error-prone and error-restrictive ribosomes, respectively. MC361 (F^- *ara* Δ(*gpt-lac*) *5 thi prfB* [from *E.coli* B]) carries a fully active A246 RF2 allele (16) and was used to isolate spectinomycin-resistance mutations. MC361, or a derivative containing *ΔcysG776::kan* (closely linked to *rpsE*) was used for reconstruction of the selected mutants. Plasmid pCP20 was used in recombineering procedures (17).

Stop codon readthrough was measured using the ampicillin-resistant plasmids p34-11 and p12-6 that carry a UGA or UAG stop codon, respectively, in the 5' region of the *lacZ* coding sequence (18, 19). Missense decoding was measured using the ampicillin-resistant, dual-luciferase plasmids pEK4, pEK5, pEK7 and pEK24 (20). These plasmids encode a single polypeptide consisting of the firefly luciferase (F-luc) fused in frame to the Renilla luciferase (R-luc). Lysine 529 of F-luc is an essential, active site residue. Plasmid pEK4 encodes the wild type lysine 529 codon, whereas in plasmids pEK7 and pEK24, the AAA Lys529 codon is replaced with AAU (Asn) and AGG (Arg) codons, respectively. Near-cognate decoding of this AAU or AGG codon by the AAA/AAG-decoding $tRNA^{Lys}$ is required for the synthesis of catalytically active F-luc-R-luc fusion proteins. The negative control plasmid pEK5, carries a UUU triplet at the Lys529 codon.

3.3.2 PCR Mutagenesis of *rpsE*

Mutagenesis of the *rpsE* gene was facilitated by the use of a strain carrying a kanamycin-resistance cassette downstream of the *rpsE* coding region, as described previously (11). The GGT glycine codon corresponding to Gly27 in protein uS5 was targeted for mutagenesis in two separate experiments with two different oligonucleotides. The initial mutagenesis experiment was designed to reconstruct the spectinomycin-resistant, error-prone G27D mutant previously described by Kirthi *et al.* (13). To this end, the *rpsE* gene and the downstream kanamycin-resistance cassette were first amplified using a 22-mer oligonucleotide carrying GAY (Y=T/C) substitutions at codon 27. The mutagenized *rpsE* fragment was electroporated into MC323 and MC361 expressing the λ Red recombinase, to identify accuracy-altering and spectinomycin-resistance mutations, respectively. MC323 colonies that were paler or darker blue compared to the wild type were selected for further analysis. Kanamycin-resistant MC361 colonies obtained after electroporation were screened for spectinomycin-resistance by replica printing onto LB-spectinomycin (60 μg/ml). The mutations in the *rpsE* genes of selected colonies were identified by sequencing. Selected *rpsE* mutants emerging from these screens were reconstructed in MC361 by P1-mediated transduction. The kanamycin-resistance cassettes were removed by transient expression of the Flp recombinase from pCP20 (17) and the *rpsE* genes from each kanamycin-sensitive strain were re-sequenced to confirm the presence of the desired mutation and the absence of any additional, unanticipated base changes.

In the second oligonucleotide-based method, MC361 cells expressing the λ Red recombinase were electroporated directly with a 60-mer *rpsE* oligonucleotide carrying RRY substitutions at codon 27 (where R=A/G; Y=T/C) and transformants were selected on LB-

spectinomycin (60 µg/ml). Selected colonies were sequenced and the mutations were transferred into MC361 *ΔcysG776::kan* by P1-mediated transduction, selecting for *cysG*$^+$ transductants and screening for the spectinomycin-resistance phenotype. The *rpsE* gene was re-sequenced to confirm the presence of the desired mutation(s).

3.3.3 Isolation of Spontaneous Spectinomycin-resistant Mutants

Wild type MC361 cells were grown overnight at 37˚C and 0.1 ml aliquots were plated on LB-spectinomycin (60µg/ml) to select for spontaneously-arising mutants. Selected mutants were sequenced and reconstructed in MC361 *ΔcysG776::kan*, as described above.

3.3.4 Growth Rate and Antibiotic Sensitivity Determination, Enzyme Assays, and rRNA Processing and Ribosome Analyses

Growth rates were determined on at least 3 independent cultures grown at 37˚C in LB medium. Growth on solid medium at various temperatures was analyzed by plating 10-fold serial dilutions of overnight cultures on LB agar plates and incubating them at 20˚C, 37˚C and 42˚C for 24 to 48 hrs. Minimal inhibitory concentrations of various antibiotics were determined (in triplicate) by monitoring growth in 2-fold serial dilutions of each antibiotic in 96-well microtiter dishes.

Detergent lysates of logarithmically growing cells at 37˚C were prepared as described previously (21, 22) in buffers containing 25 mM TrisHCl pH 8.0/60 mM KCl/10 mM $MgCl_2$. Ribosomal subunits and 70S ribosomes were separated by centrifugation through linear 10 to 40% sucrose gradients (in 25 mM TrisHCl, pH 7.8/50 mM KCl/ 10 mM $MgCl_2$/ 3 mM DTT) in a Beckman SW28 rotor for 18 h at 38,191 x g. The gradients were then analyzed on an ISCO gradient fractionator connected to an ISCO UV6 detector. At

least two different lysates from each mutant or wild type strain were analyzed on sucrose gradients.

Total RNA was isolated from logarithmically growing cells and analyzed on 0.7% agarose/0.9% Synergel gels, as described by Wachi *et al.* (23). This gel system is capable of separating 23S rRNA from 16S rRNA, as well as resolving the 17S, 16.5S and 16.3S precursors of 16S rRNA that can accumulate when processing is impeded. RNAs from at least three cultures of each mutant or wild type strain (grown at 37˚C) were analyzed by this means. In addition, RNAs were also isolated from chloramphenicol-treated wild-type cells, added at a final concentration of 60 mg/ liter for 30 min before harvesting. Chloramphenicol inhibits rRNA processing and leads to accumulation of 17S precursors of 16S rRNA (24).

β-galactosidase assays were carried out on permeabilized, logarithmically-growing cells and activity was expressed in Miller units (11, 25). Luciferase assays to test for missense errors were performed using the Dual-Luciferase Reporter Assay System from Promega, and luminescence was measured with a GloMax 20/20 luminometer, according to the manufacturers' instructions. F-luc/R-luc ratios were calculated for each luciferase plasmid-containing strain. The miscoding frequencies (expressed in relative light units (RLUs)), were calculated as the F-luc/R-luc ratios from pEK7- or pEK24-containing strains, normalized to the F-luc/R-luc ratio from isogenic strains expressing the wild-type K529 firefly luciferase from pEK4 (11). All enzyme assays were carried out on at least 3 independent cultures, grown at 37˚C.

3.4 Results

3.4.1 Generation and Growth Characteristics of uS5 Mutants

Using a recombineering approach, the Gly27 codon of *rpsE* encoding S5 was targeted for mutagenesis with two different mutagenic oligonucleotides, followed by screens for accuracy phenotypes or spectinomycin resistance. In addition, spontaneous spectinomycin resistant mutants were selected directly on antibiotic-containing medium. In total, 21 unique mutants were isolated by these means (listed in Table 3.1 and summarized in Table S3.1) and each was reconstructed in a clean genetic background prior to further analyses. Details of the specific selections used are given in the supplemental materials section.

One of our original goals was to reconstruct the G27D mutant described by Kirthi *et al.* (13). From our two oligonucleotide-based mutagenesis experiments targeting the Gly27 codon, we recovered A, C, R, K, W, and V alterations at position 27, but were not able to isolate a G27D (or G27N) alteration alone. However, we did obtain the G27D alteration in combination with a K25N substitution and recovered G27N in combination with K25N, G26D or ΔR28/I29L. The cultivation conditions and screens we used should have yielded the G27D mutant and the failure to recover this mutant is puzzling and unexplained.

The doubling time, for most of the mutants in liquid LB medium at 37˚C was not very different from the wild type strain (28 ± 2 min; Table 3.1). Only the uS5 mutants carrying V20E and G27W substitutions had substantially longer doubling times of 47 ± 1 and 51 ± 1, respectively. While all the mutants grew well on solid medium at 37˚C and 42˚C, a subset of 11 mutants showed variable degrees of reduced growth on solid medium at 20˚C. This includes all the 6 mutants with single base substitution at G27 position and 5

other uS5 mutant strains carrying the mutations V20E, G26D, K25N/G27D, K25N/G27N and G27S/ΔF30/ΔS31 (Figure 3.2).

Table 3.1 Spectinomycin resistance, decoding, cold sensitivity phenotypes and doubling times of uS5 mutants.

Mutation[a]	Decoding and cold sensitivity phenotypes of mutants	Spectinomycin MIC (mg/l)	Doubling time (min)
Wild type		50	28 ± 2
V20E	Error-prone, Cold sensitive	400	47 ± 1
V24F	Error-prone	400	30 ± 1
G26D	Error-restrictive, Cold sensitive	200	31 ± 2
G26V	Error-restrictive	100	39 ± 1
ΔG26	Error-prone	400	34 ± 2
G27A	Error-prone, Cold sensitive	100	37 ± 2
G27C	Error-prone, Cold sensitive	100	41 ± 2
G27K	Error-prone, Cold sensitive	200	33 ± 1
G27R	Error-prone, Cold sensitive	100	31 ± 1
G27V	Error-prone, Cold sensitive	400	34 ± 2
G27W	Error-prone, Cold sensitive	400	51 ± 1
F30L	Error-prone	25	28 ± 1
ΔV24/G27S	Error-prone	400	34 ± 2
K25N/G27D	Cold sensitive	400	42 ± 1

Mutation[a]	Decoding and cold sensitivity phenotypes of mutants	Spectinomycin MIC (mg/l)	Doubling time (min)
K25N/G27N	Error-prone, Cold sensitive	400	33 ± 1
ΔK25/G26S/G27S	Error-prone	400	36 ± 2
G26D/G27N	Error-prone	400	31 ± 2
G26D/G27S	Error-prone	400	34 ± 2
ΔG26/R28S	Error-prone	400	32 ± 2
G27N/ΔR28/I29L	Error-prone	400	30 ± 1
G27S/ΔF30/ΔS31	Error-prone Cold sensitive	400	32 ± 2

[a] Residue numbers do not include the N-terminal methionine.

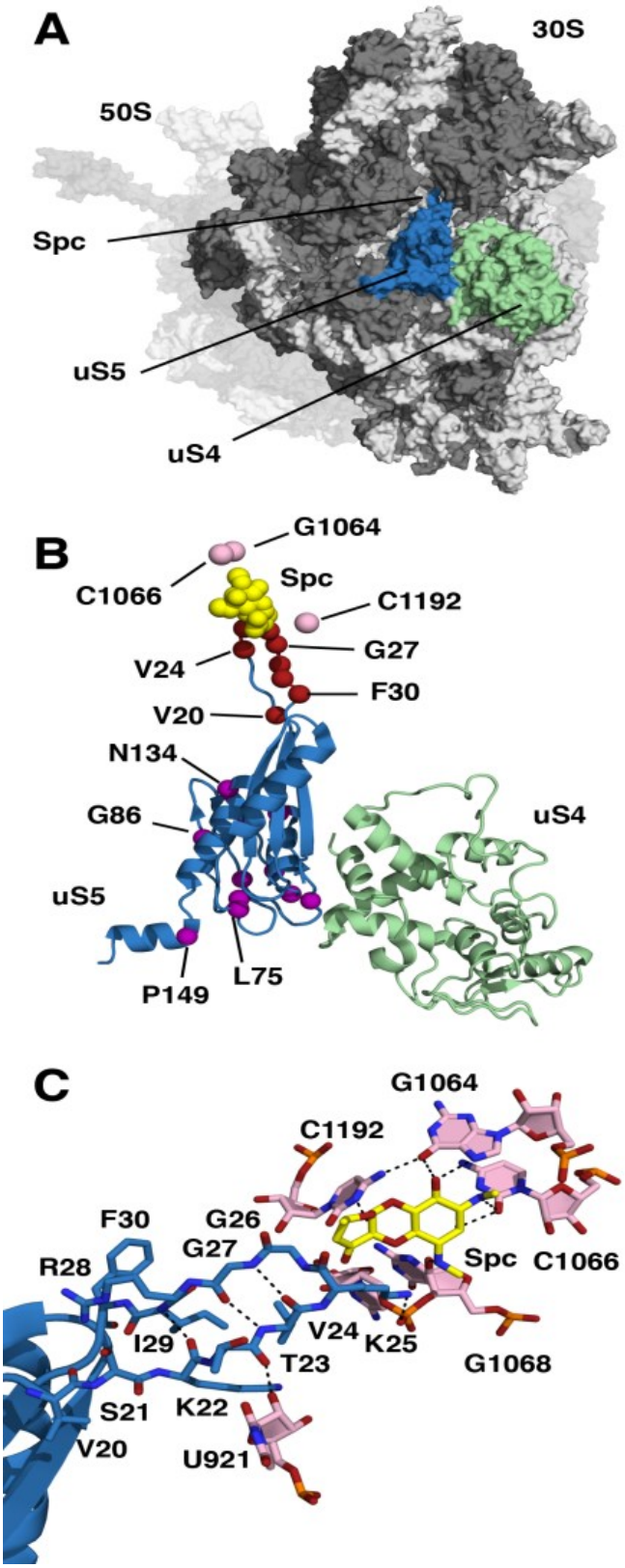
A
30S
50S
Spc
uS5
uS4
B
G1064
C1066
Spc
C1192
G27
V24
F30
V20
N134
G86
uS4
uS5
L75
P149
C
G1064
C1192
F30
G26
G27
R28
Spc
C1066
V24
K25
I29
T23
G1068
S21
K22
V20
U921

Figure 3.1 Location of ribosomal protein S5 amino acid substitutions in the ribosome three-dimensional structure. (A) The *E. coli* 70S ribosome complexed with spectinomycin (pdb entry 4v56; (9)). Ribosomal proteins are colored dark gray, except uS4 and uS5, which are colored pale green and blue, respectively, and rRNAs are colored light gray. 'Spc' indicates the binding site for spectinomycin, which is buried behind 16S rRNA and not visible in this view. The 50S subunit is shown as transparent. (B) Cartoon rendering of ribosomal proteins uS4 (pale green) and uS5 (pale blue), with spectinomycin shown as yellow spheres, the phosphates of 16S rRNA residues involved in spectinomycin sensitivity are shown as pink spheres, the α carbons of uS5 residues previously identified *ram* mutations are indicated by purple spheres, and the α carbons of uS5 residues identified as spectinomycin-resistance and/or *ram* mutations identified in this study are indicated by red spheres. (C) Close-up view of the spectinomycin binding site in the *E. coli* 70S ribosome in complex with spectinomycin (9). Ribosomal protein uS5 is colored blue, 16S rRNA is colored light pink and spectinomycin ('Spc') is shown as yellow sticks. uS5 amino acid residues in the loop containing G27 are shown as sticks. Selected 16S rRNA residues that may contact spectinomycin or the uS5 loop are indicated as sticks. Potential hydrogen bonding interactions are shown as dashes. All other components of the 30S subunit are omitted for clarity. Spectinomycin resistance and/or *ram* phenotypes result from amino acid substitutions in this uS5 loop or at position 1064, 1066 or 1192 of 16S rRNA. Figures were produced with PyMol (46)

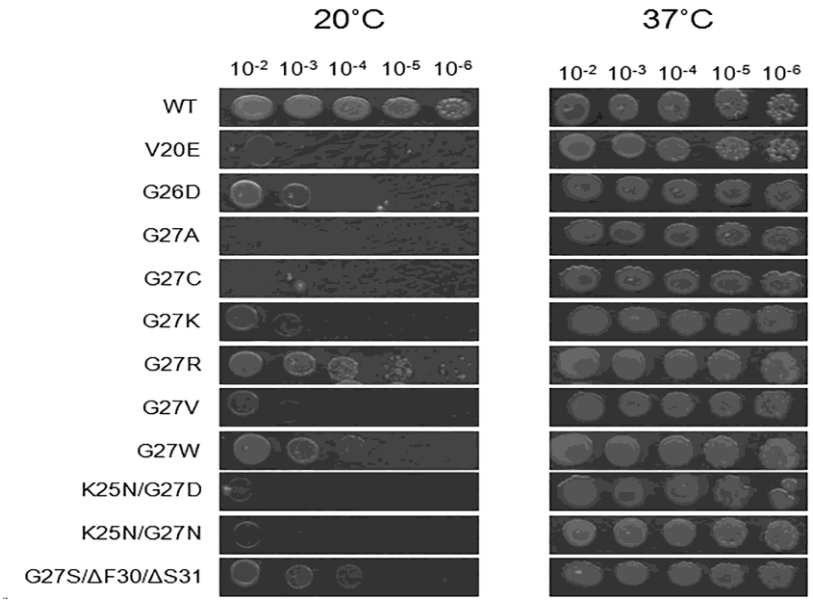

Figure 3.2 Effects of selected ribosomal proteins uS5 mutations on growth at 20°C and 37°C on solid media. Three-microliter aliquots of serially diluted (10^{-2} to 10^{-6}) overnight cultures were spotted onto antibiotic-free LB plates and incubated for 24 to 48 h. WT, wild type.

3.4.2 Effect of Mutations on Antibiotic Resistances

In addition to conferring spectinomycin resistance, distinct ribosomal protein uS5 alterations have also been shown to affect the cell's response to streptomycin (26-28) and to neamine (29, 30). In our collection of 21 mutants, five displayed two-fold differences in their response to streptomycin (four showed decreased and one showed increased resistance). Eight mutants showed two-fold lower resistance to neamine (data not shown). Since the MIC assays use a two-fold dilution series, the significance of these small differences cannot be assessed. A majority of the mutations (16 out of 21) conferred high level resistance to spectinomycin, irrespective of the genetic screens or selections used to isolate them (Tables 3.1 and S3.1).

Spectinomycin-resistance mutations, all of which alter residues in the loop 2 region of uS5 have been isolated in several bacteria. In *E. coli*, in addition to the G27D substitution, R19L, V20E and S21P substitutions have previously been reported (7). The S21P mutant ribosomes have been assayed for their miscoding properties and do not affect the accuracy of translation (6). In *Bacillus subtilis*, G27V, K25I, as well as deletion of Arg30 (equivalent to Ile29 in *E. coli*) all confer spectinomycin-resistance (31-33). In *Neisseria gonorrhoeae*, T23P, and ΔV24/K25E alterations confer resistance (34, 35), while in *Pasteurella multocida*, S31I/ΔF32 and ΔK22 alterations have been identified in resistant strains (36).

3.4.3 Miscoding Properties of uS5 Mutants

A majority of the uS5 mutants (16/21) showed increased readthrough of both UAG (Figure. 3.3) and UGA (Figure. S3.1) codons. Two mutant strains G27R and G27S/ΔF30/ΔS31 did not show significant ($P > 0.05$) changes in UAG readthrough, but displayed increased UGA readthrough. The K25N/G27D mutant did not show significant changes ($P > 0.05$) in either UAG or UGA readthrough. The strongest effects were seen with the F30L, ΔG26/R28S and G27K mutants. Only two mutants, G26D and G26V, showed an error-restrictive phenotype, displaying decreased UGA and UAG readthrough (Figs.3.3 and 3S1). Curiously, while the G26D mutation on its own is error-restrictive, the double mutant combinations G26D/G27N and G26D/G27S, are error prone. A subset of seven uS5 mutants were also tested in the luciferase-based miscoding assays to determine if the pattern of missense decoding mimicked that seen in stop codon readthrough assays (Fig. 3.4). The G27A, G27C, G27R, and F30L mutants all showed an error-prone phenotype while G26D displayed an error-restrictive phenotype, consistent with the *lacZ* readthrough assay. V20E and G26Vwhich showed error-prone and error-restrictive phenotypes, respectively, in the

lacZ assay, did not show statistically significant differences from wild type in the miscoding assay. In summary, with the exception of the K25N/G27D mutant, all the other uS5 mutants affected decoding fidelity in at least one of the assays used; while the majority of the mutants promoted increased errors, 2 mutants were error-restrictive.

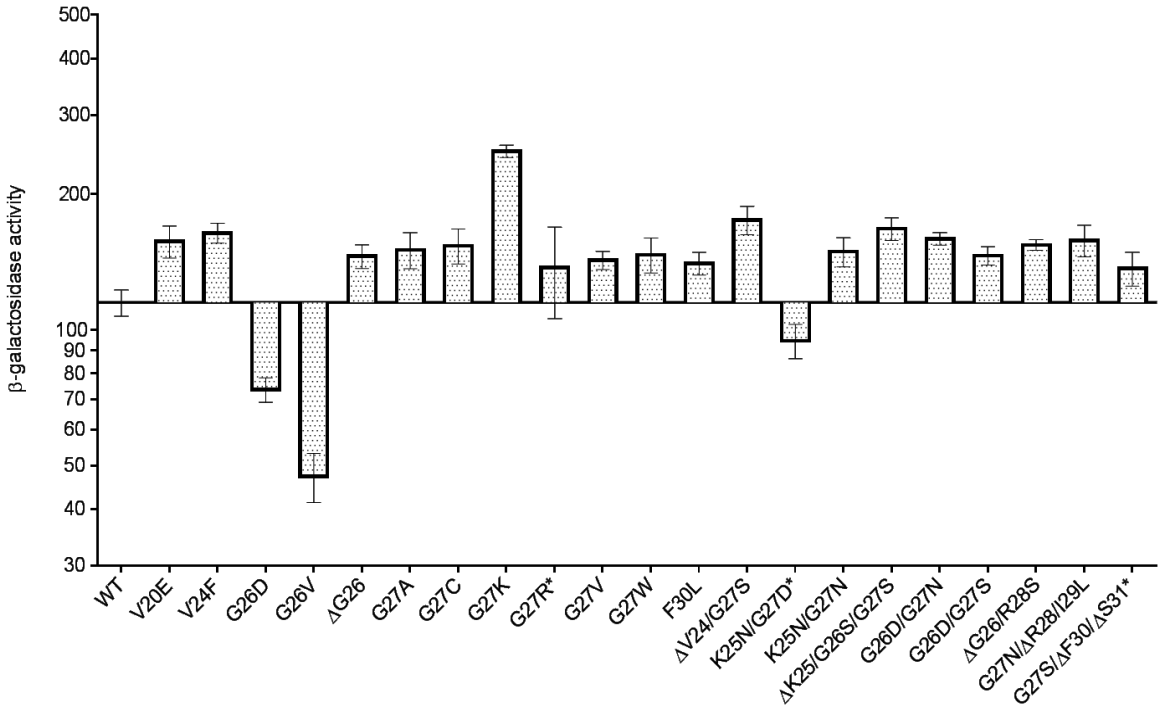

Figure 3.3 Effects of altered ribosomal protein uS5 on UAG readthrough. Readthrough levels were measured in strains transformed with p12-6, a *lacZ* plasmid carrying a UAG mutation in the 5' end of the β-galactosidase coding region. Bars represent (Miller) units of β-galactosidase activity. Each bar represents the average of at least three independent assays ± SE. WT, wild type. An asterisk (*) indicates that the activity measured for the indicated mutant did not differ significantly (P>0.05) from that of the corresponding wild-type strain.

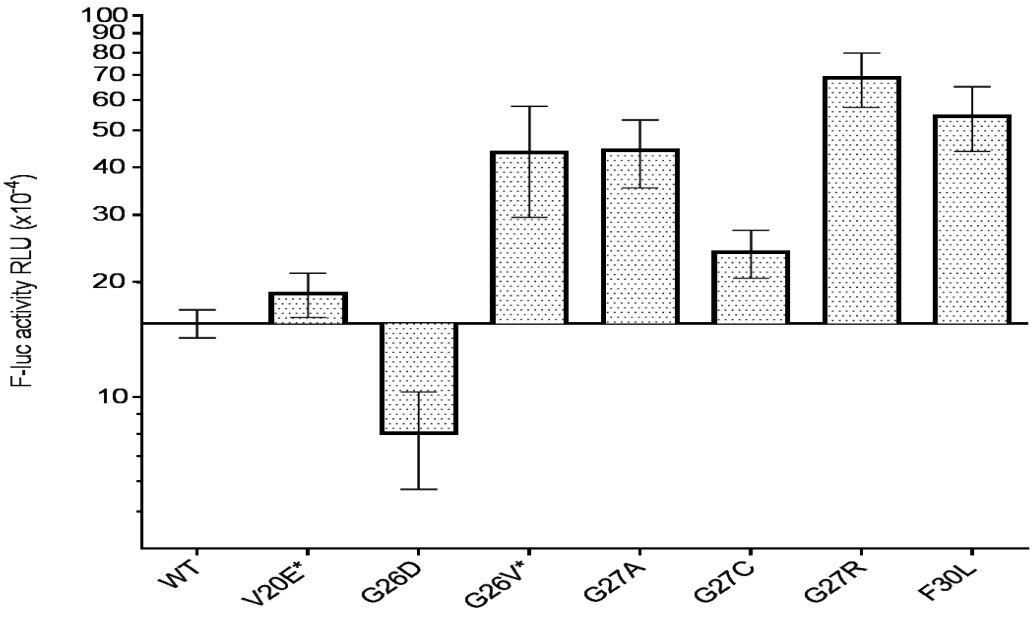

Figure 3.4 Effects of altered uS5 ribosomal proteins on missense decoding. Missense decoding values were obtained from assays of pEK7-transformed cells and reflect near-cognate decoding of AAU by the AAA/G-decoding $tRNA^{Lys}$. Misreading levels are expressed in RLU as described in the text and are the average values of at least 3 independent determinations ± SE. WT, wild type. An asterisk (*) indicates that the activity measured for the indicated mutant did not differ significantly (P>0.05) from that of the corresponding wild-type strain.

3.4.4 Effects of uS5 Alterations on Ribosome Biogenesis and rRNA Processing

The uS5 protein is a tertiary binding protein and is essential for correct assembly of the 30S subunit (37, 38). When lysates from each of the 21 mutants (grown at 37°C) were analyzed by sucrose gradient centrifugation, six mutants (V20E, G27C, G27W, ΔV24/G27S, K25N/G27N, ΔK25/G26S/G27S) showed substantially increased amounts of free 50S and 30S subunits. This defect was most pronounced in the V20E mutant. Five other mutants (G26V, G27A, K25N/G27D, ΔG26/R28S and G27S/ΔF30/ΔS31) showed marginal increases in the amounts of 50S and 30S particles. The remaining 10 mutants had profiles

similar to that of wild type (Fig. 3.5). Cold sensitivity is a phenotype often associated with defective ribosome assembly and 11 of the mutants analyzed here showed reduced growth at 20°C (Fig. 3.2). However, when grown at 37˚C, only some of the 11 cold sensitive mutants showed altered ribosome profiles, while others such as G26D, G27K, G27R and G27V did not. Is is noteworthy that while the previously characterized G27D mutant is cold sensitive, its defects in miscoding and ribosome biogenesis were manifested at 37˚C and altered ribosome profiles were evident under similar buffer conditions (10 mM $MgCl_2$) to those we have used here (39).

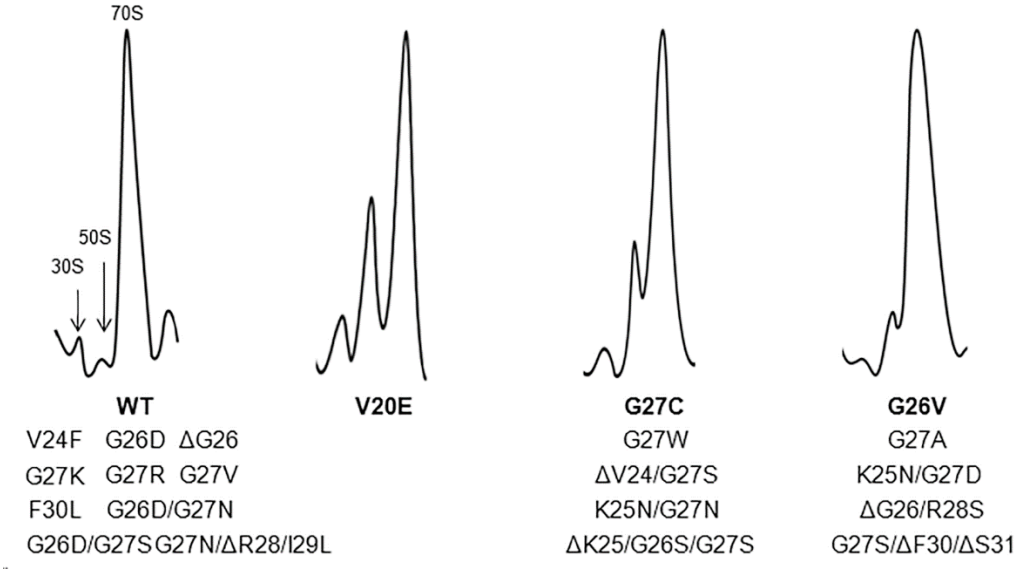

Figure 3.5 Ribosome profiles of a wild-type and uS5 mutant strains grown at 37°C. Mutants were grouped according to the relative abundance of free 30S and 50S subunits *vs.* 70S ribosomes. Representative profiles are presented and the identities of other members of each gradient group are indicated beneath. The positions of 30S and 50S subunits and 70S ribosomes are indicated on the profile of the wild-type strain. A_{260} absorbance readings are indicated on the Y-axis and the direction of sedimentation (on the X-axis) is from left to right.

Processing of the primary transcript of *rrn* operons to generate the mature 16S rRNA occurs in several steps and 16S rRNA precursors accumulate in strains defective in specific nucleases, as well as in some ribosomal mutants (15, 23, 40). Analysis of the *E.coli* uS5 mutant G27D suggests a link between defective rRNA processing and translational fidelity (13, 15). However, when crude extracts of the 21 uS5 mutants were analyzed on agarose/synergel gels, only the V20E and G27S/ΔF30/ΔS31 mutants showed substantial accumulation of 16S rRNA precursors (Fig. 3.6). The V20E mutant also had a substantially altered ribosome profile, while the G27S/ΔF30/ΔS31 profile was only mildly affected (Figure. 3.5). Strains carrying the K25N/G27N, ΔG26/R28S or ΔK25/G26S/G27S alterations in uS5 showed modest accumulation of 16S rRNA precursor and at least some increase in the amounts of free 30S and 50S subunits. All the 6 mutant strains with substitutions at the G27 positions showed some slight accumulation of the 16S rRNA precursor whereas only three of these (G27W, G27A and G27C) showed an altered ribosome profile. Thus, among this collection of mutants at least, there is no strict correlation between defective rRNA processing and defective 30S assembly and 70S ribosome formation. In summary, when grown at 37˚C under the same cultivation conditions where we observe miscoding phenotypes, only a minority of the mutants are grossly defective in processing of 16S rRNA precursors and/or ribosome assembly. The majority of the mutants, including some with cold sensitive phenotypes, contain fully processed rRNAs and wild type levels of 70S ribosomes.

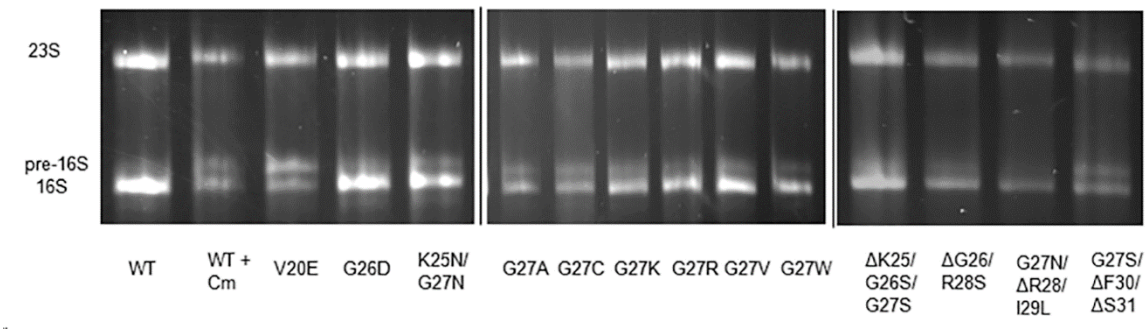

Figure 3.6 rRNA processing in wild-type (WT) and selected uS5 mutant strains. Total RNAs were extracted from logarithmically growing cells grown at 37°C, electrophoresed on agarose-synergel gels and stained with ethidium bromide. The second lane from the left contains RNAs extracted from wild-type cells that were treated with chloramphenicol for 30 min, leading to the accumulation of unprocessed precursors of 16S rRNA

3.5 Discussion

The availability of high resolution structures of ribosome complexes has revolutionized our understanding of the protein synthesis machinery and has also provided critical insights into the structural and functional effects of some mutant ribosomal proteins and rRNAs (41, 42). The multiple ribosomal mutations that affect the accuracy of decoding constitute a diverse class, affecting critical functional centers involved in decoding or factor binding, as well as the conformational changes accompanying decoding. The latter category includes some of the mutants affecting proteins uS4 and uS5.

The G27 region of uS5 is clearly distant from the uS4-uS5 interface, rendering direct effects of alterations at G27 on the uS4-uS5 interface unlikely. An alternative model put forward by Culver and co-workers posits that the effects of the G27D mutation on decoding derive from aberrant processing of 16S rRNA precursors. Other mutations that lead to accumulation of 16S rRNA precursors, including the deletion of the 16S rRNA processing nuclease, RNaseG, or loss of the assembly factors KsgA or RimF also promoted miscoding errors (15). However, at least some of the results presented here are difficult to interpret in terms of this model. While a majority of the mutants we have isolated promote at least some miscoding events, we have isolated two (G26D, G26V) that are error-restrictive, a phenotype that is difficult to reconcile with the defective rRNA processing model. Moreover, at least when grown at 37°C, only a minority of the miscoding mutants we have isolated show obvious defects in 16S rRNA processing, or substantial alterations in ribosome profiles. Thus, in our collection, there are multiple examples of mutations affecting the G27 region of uS5 that miscode, yet have at most, very mild effects on 16S rRNA processing or 30S biogenesis.

The spectinomycin-resistance mutations described here all introduce amino acid substitutions or deletions in the general vicinity of the spectinomycin binding site. Some of the substituted amino acid residues are within several Ångstroms of spectinomycin (Figure. 3.1B, C), while others are more distant in the loop formed by residues 20-30. The native conformation of this loop is stabilized by a number of hydrogen bonds between the two strands of the loop, and substitutions at positions further away from the spectinomycin binding site could act indirectly by disrupting the overall conformation of the loop, thus rearranging residues in position to make contact with spectinomycin. Alternatively, amino acid substitutions in uS5 could be substantial enough to distort the conformation of 16S rRNA residues critical for spectinomycin binding. Base substitutions at several residues, including G1064, C1066 or C1192, confer high-level spectinomycin resistance (43-45). It should be emphasized that these two mechanisms are not mutually exclusive. Elucidation of the precise mechanism will require structure determination of mutant ribosomes.

The sites of spectinomycin-resistance mutations we have identified in this study are distant from sites of previously described *ram* mutations in uS5, with some being as far as 57 Å from the uS4-uS5 interface. However, some of the *ram* mutations we reported previously (11), such as G86C or N134Y, occur not at the uS4-uS5 interface, but at, or near sites of interaction with 16S rRNA. These mutations, together with those in loop 2 (Figure. 3.1, B, C) are distinct from those at the uS4-uS5 interface and would at first glance seem to influence fidelity by a different mechanism.

We suggest the existence of two distinct classes of uS5 *ram* mutants. One class, identified previously, acts by destabilizing the uS4-uS5 interface and favoring 30S domain closure. The second class, exemplified by the amino acid substitutions described here, occur

at the interface between uS5 and 16S rRNA. This class is expected to have a similar effect of favoring 30S domain closure. Thus, uS5 has two functionally important interfaces; one with uS4 and one with 16S rRNA. While the former is normally dynamic and undergoes changes during decoding, the latter is normally stable, but can become more dynamic as a result of amino acid substitutions in uS5.

3.6 Acknowledgements

We thank Somanon Bhattacharya for his assistance with the figures.

3.6 References

1. **Dinman JD, O'Connor M.** 2010. Mutants that affect recoding. Recoding: expansion of decoding rules enriches gene expression **24:**321-344.

2. **Zaher HS, Green R.** 2010. Hyperaccurate and error-prone ribosomes exploit distinct mechanisms during tRNA selection. Mol Cell **39:**110-120.

3. **Bilgin N, Claesens F, Pahverk H, Ehrenberg M.** 1992. Kinetic properties of Escherichia coli ribosomes with altered forms of S12. J Mol Biol **224:**1011-1027.

4. **Bilgin N, Ehrenberg M.** 1994. Mutations in 23 S ribosomal RNA perturb transfer RNA selection and can lead to streptomycin dependence. J Mol Biol **235:**813-824.

5. **Saarma U, Remme J, Ehrenberg M, Bilgin N.** 1997. An A to U transversion at position 1067 of 23 S rRNA from Escherichia coli impairs EF-Tu and EF-G function. J Mol Biol **272:**327-335.

6. **Piepersberg W, Bock A, Wittmann HG.** 1975. Effect of different mutations in ribosomal protein S5 of Escherichia coli on translational fidelity. Mol Gen Genet **140:**91-100.

7. **Wittmann-Liebold B, Greuer B.** 1978. The primary structure of protein S5 from the small subunit of the Escherichia coli ribosome. FEBS Lett **95:**91-98.

8. **Bilgin N, Richter AA, Ehrenberg M, Dahlberg AE, Kurland CG.** 1990. Ribosomal RNA and protein mutants resistant to spectinomycin. EMBO J **9:**735-739.

9. **Borovinskaya MA, Shoji S, Holton JM, Fredrick K, Cate JH.** 2007. A steric block in translation caused by the antibiotic spectinomycin. ACS Chem Biol **2:**545-552.

10. **Ogle JM, Murphy FV, Tarry MJ, Ramakrishnan V.** 2002. Selection of tRNA by the ribosome requires a transition from an open to a closed form. Cell **111:**721-732.

11. **Agarwal D, Kamath D, Gregory ST, O'Connor M.** 2015. Modulation of decoding fidelity by ribosomal proteins S4 and S5. J Bacteriol **197:**1017-1025.

12. **Dahlgren A, Ryden-Aulin M.** 2000. A novel mutation in ribosomal protein S4 that affects the function of a mutated RF1. Biochimie **82:**683-691.

13. **Kirthi N, Roy-Chaudhuri B, Kelley T, Culver GM.** 2006. A novel single amino acid change in small subunit ribosomal protein S5 has profound effects on translational fidelity. RNA **12:**2080-2091.

14. **Nesterchuk MV, Sergiev PV, Dontsova OA.** 2011. Posttranslational modifications of ribosomal proteins in Escherichia coli. Acta Naturae **3:**22-33.

15. **Roy-Chaudhuri B, Kirthi N, Culver GM.** 2010. Appropriate maturation and folding of 16S rRNA during 30S subunit biogenesis are critical for translational fidelity. Proc Natl Acad Sci U S A **107:**4567-4572.

16. **O'Connor M.** 2015. Interactions of release factor RF3 with the translation machinery. Mol Genet Genomics **290:**1335-1344.

17. **Datsenko KA, Wanner BL.** 2000. One-step inactivation of chromosomal genes in Escherichia coli K-12 using PCR products. Proc Natl Acad Sci U S A **97:**6640-6645.

18. **O'Connor M, Thomas CL, Zimmermann RA, Dahlberg AE.** 1997. Decoding fidelity at the ribosomal A and P sites: influence of mutations in three different regions of the decoding domain in 16S rRNA. Nucleic Acids Res **25:**1185-1193.

19. **O'Connor M, Gregory ST, Dahlberg AE.** 2004. Multiple defects in translation associated with altered ribosomal protein L4. Nucleic Acids Res **32:**5750-5756.

20. **Kramer EB, Farabaugh PJ.** 2007. The frequency of translational misreading errors in E. coli is largely determined by tRNA competition. RNA **13:**87-96.

21. **Liiv A, O'Connor M.** 2006. Mutations in the intersubunit bridge regions of 23 S rRNA. J Biol Chem **281:**29850-29862.

22. **Qin D, Fredrick K.** 2013. Analysis of polysomes from bacteria. Methods Enzymol **530:**159-172.

23. **Wachi M, Umitsuki G, Shimizu M, Takada A, Nagai K.** 1999. Escherichia coli cafA gene encodes a novel RNase, designated as RNase G, involved in processing of the 5' end of 16S rRNA. Biochem Biophys Res Commun **259:**483-488.

24. **Harvey RJ, Koch AL.** 1980. How partially inhibitory concentrations of chloramphenicol affect the growth of Escherichia coli. Antimicrob Agents Chemother **18:**323-337.

25. **Miller JH.** 1993. A Short Course in Bacterial Genetics. Cold Spring Harbor Laboratory Press, New York.

26. **Ito T, Wittmann HG.** 1973. Amino acid replacements in proteins S5 and S12 of two Escherichia coli revertants from streptomycin dependence to independence. Mol Gen Genet **127:**19-32.

27. **Carr JF, Lee HJ, Jaspers JB, Dahlberg AE, Jogl G, Gregory ST.** 2015. Phenotypic suppression of streptomycin resistance by mutations in multiple components of the translation apparatus. J Bacteriol **197:**2981-2988.

28. **Maisnier-Patin S, Berg OG, Liljas L, Andersson DI.** 2002. Compensatory adaptation to the deleterious effect of antibiotic resistance in Salmonella typhimurium. Mol Microbiol **46:**355-366.

29. **Yaguchi M, Wittmann HG, Cabezon T, De Wilde M, Villarroel R, Herzog A, Bollen A.** 1975. Cooperative control of translational fidelity by ribosomal proteins in Escherichia coli. II. Localization of amino acid replacements in proteins S5 and S12 altered in double mutants resistant to neamine. Mol Gen Genet **142:**35-43.

30. **De Wilde M, Cabezon T, Villarroel R, Herzog A, Bollen A.** 1975. Cooperative control of translation fidelity by ribosomal proteins in Escherichia coli. I. Properties of ribosomal mutants whose resistance to neamine is the cumulative effect of two distinct mutations. Mol Gen Genet **142:**19-33.

31. **Itoh T.** 1976. Amino acid replacement in the protein S5 from a spectinomycin resistant mutant of Bacillus subtilis. Mol Gen Genet **144:**39-42.

32. **Higo K, Itoh T, Osawa S.** 1982. Alteration of ribosomal protein S5 from two spectinomycin-resistant mutants of Bacillus subtilis: deletion of one amino acid residue. Mol Gen Genet **185:**205-206.

33. **Inaoka T, Kasai K, Ochi K.** 2001. Construction of an in vivo nonsense readthrough assay system and functional analysis of ribosomal proteins S12, S4, and S5 in Bacillus subtilis. J Bacteriol **183:**4958-4963.

34. **Ilina EN, Malakhova MV, Bodoev IN, Oparina NY, Filimonova AV, Govorun VM.** 2013. Mutation in ribosomal protein S5 leads to spectinomycin resistance in Neisseria gonorrhoeae. Front Microbiol **4:**186.

35. **Unemo M, Golparian D, Skogen V, Olsen AO, Moi H, Syversen G, Hjelmevoll SO.** 2013. Neisseria gonorrhoeae strain with high-level resistance to spectinomycin due to a novel resistance mechanism (mutated ribosomal protein S5) verified in Norway. Antimicrob Agents Chemother **57:**1057-1061.

36. **Kehrenberg C, Schwarz S.** 2007. Mutations in 16S rRNA and ribosomal protein S5 associated with high-level spectinomycin resistance in Pasteurella multocida. Antimicrob Agents Chemother **51:**2244-2246.

37. **Clatterbuck Soper SF, Dator RP, Limbach PA, Woodson SA.** 2013. In vivo X-ray footprinting of pre-30S ribosomes reveals chaperone-dependent remodeling of late assembly intermediates. Mol Cell **52:**506-516.

38. **Bunner AE, Beck AH, Williamson JR.** 2010. Kinetic cooperativity in Escherichia coli 30S ribosomal subunit reconstitution reveals additional complexity in the assembly landscape. Proc Natl Acad Sci U S A **107:**5417-5422.

39. **Roy-Chaudhuri B, Kirthi N, Kelley T, Culver GM.** 2008. Suppression of a cold-sensitive mutation in ribosomal protein S5 reveals a role for RimJ in ribosome biogenesis. Mol Microbiol **68:**1547-1559.

40. **Sulthana S, Deutscher MP.** 2013. Multiple exoribonucleases catalyze maturation of the 3' terminus of 16S ribosomal RNA (rRNA). J Biol Chem **288:**12574-12579.

41. **Vila-Sanjurjo A, Ridgeway WK, Seymaner V, Zhang W, Santoso S, Yu K, Cate JH.** 2003. X-ray crystal structures of the WT and a hyper-accurate ribosome from Escherichia coli. Proc Natl Acad Sci U S A **100:**8682-8687.

42. **Demirci H, Wang L, Murphy FVt, Murphy EL, Carr JF, Blanchard SC, Jogl G, Dahlberg AE, Gregory ST.** 2013. The central role of protein S12 in organizing the structure of the decoding site of the ribosome. RNA **19:**1791-1801.

43. **Brink MF, Brink G, Verbeet MP, de Boer HA.** 1994. Spectinomycin interacts specifically with the residues G1064 and C1192 in 16S rRNA, thereby potentially freezing this molecule into an inactive conformation. Nucleic Acids Res **22:**325-331.

44. **Johanson U, Hughes D.** 1995. A new mutation in 16S rRNA of Escherichia coli conferring spectinomycin resistance. Nucleic Acids Res **23:**464-466.

45. **O'Connor M, Dahlberg AE.** 2002. Isolation of spectinomycin resistance mutations in the 16S rRNA of Salmonella enterica serovar Typhimurium and expression in Escherichia coli and Salmonella. Curr Microbiol **45:**429-433.

46. **Schrödinger L.** 2012. The PyMOL molecular graphics system, version 1.5. http://www.pymol.org/.

3.7 Supplemental Information

3.7.1 Generation of Mutations in the *rpsE* Gene Encoding Ribosomal Protein uS5

Targeted mutagenesis of the Gly27 codon of *rpsE* with the GAY mutant oligonucleotide yielded 3,914 MC323 transformants from 9 electroporations. Of these, 2,208 displayed a dark blue, ribosomal-ambiguity phenotype while the remaining 1,706 had a pale blue, wild-type phenotype. Sequencing of 36 *ram* mutants showed that 6 carried unique mutations (Tables 3.1 and S3.1). Using the same mutated *rpsE* fragments, 456 kanamycin-resistant MC361 transformants were recovered from 6 electroporations. Replica printing of the transformants onto spectinomycin plates yielded 251 resistant mutants. Sequencing of 15 spectinomycin-resistant mutants showed that 5 carried unique mutations (Tables 3.1 and S3.1). All the mutants obtained using the amplified mutagenized fragment carried single amino acid substitutions or deletions in uS5. In principle, this mutagenesis experiment should have yielded only glycine to aspartate changes in the protein; however, multiple mutations in codon 27 other than the anticipated G27D, as well as base changes in surrounding codons were recovered. Presumably these base changes occurred as a consequence of errors during oligonucleotide synthesis, as has been encountered by others (1). Reconstruction and resequencing of the *rpsE* genes in new strain backgrounds ensured that no changes in *rpsE* other than those indicated were present in the reconstructed strains used for subsequent characterizations.

Electroporation of MC361 cells with a 60-mer oligonucleotide carrying RRY substitutions at Gly27 yielded 546 spectinomycin-resistant transformants, from 12 independent electroporations. Sequencing of 35 spectinomycin-resistant mutants showed that 14 carried unique mutations (Table 3.1). Again, the direct oligonucleotide

electroporations unexpectedly resulted in the recovery of several mutants containing single or multi-base alterations in the V20-S31 region, in addition to base changes at the targeted codon 27. Nine of the spectinomycin-resistant mutants from this experiment carried changes in two or more codons (Table 3.1) and it is unclear if all of these codon changes are required for the spectinomycin-resistance phenotype. While most of the previously-reported alterations in uS5 conferring resistance to spectinomycin are due to single amino acid changes, spontaneous, multi-site mutations conferring spectinomycin-resistance have also been reported (2, 3).

In a final selection, spontaneous, spectinomycin-resistant mutants were selected directly by plating unmutagenized cultures on LB plates containing 60 μg/ml spectinomycin. From 8 independent overnight cultures, 305 spectinomycin-resistant colonies were obtained. Sequencing of 9 spectinomycin-resistant colonies showed that 4 carried unique mutations (Tables 3.1 and S3.1). From all the approaches mentioned above, a cumulative total of 21 unique mutants were reconstructed and pursued for further characterizations. 6 of these mutations were isolated from more than one screen or selection method (Table S3.1).

We note that three mutations that were originally isolated on the basis of their spectinomycin-resistance phenotypes showed only a two-fold (G26V; G27A), or no measurable difference (G27R) in the MIC for spectinomycin in the reconstructed strains. This may indicate that additional mutations, unlinked to *rpsE*, were present in the original isolates of these strains, that contributed to the spectinomycin-resistance phenotype

Table S3.1 Methods of isolation of uS5 mutants.

Mutation[a]	Mutagenesis[b], screens and selections used for mutant isolation
Wild type	
V20E	Mutagenesis of Gly27 (RRY), spectinomycin resistance
	Spontaneous spectinomycin resistance
V24F	Mutagenesis of Gly27 (RRY), spectinomycin resistance
	Spontaneous spectinomycin resistance
	Mutagenesis of Gly27 (GAY), accuracy screen
G26D	Mutagenesis of Gly27 (RRY), spectinomycin resistance
	Mutagenesis of Gly27 (GAY), spectinomycin resistance
G26V	Mutagenesis of Gly27 (GAY), spectinomycin resistance
ΔG26	Mutagenesis of Gly27 (RRY), spectinomycin resistance
G27A	Mutagenesis of Gly27 (GAY), accuracy screen
	Mutagenesis of Gly27 (GAY), spectinomycin resistance
G27C	Mutagenesis of Gly27 (GAY), accuracy screen
G27K	Mutagenesis of Gly27 (GAY), accuracy screen
G27R	Mutagenesis of Gly27 (GAY), accuracy screen
	Mutagenesis of Gly27 (GAY), spectinomycin resistance
	Spontaneous spectinomycin resistance
G27V	Mutagenesis of Gly27 (RRY), spectinomycin resistance
	Spontaneous spectinomycin resistance
G27W	Mutagenesis of Gly27 (GAY), spectinomycin resistance

Mutation[a]	Mutagenesis[b], screens and selections used for mutant isolation
F30L	Mutagenesis of Gly27 (GAY), accuracy screen
ΔV24/G27S	Mutagenesis of Gly27 (RRY), spectinomycin resistance
K25N/G27D	Mutagenesis of Gly27 (RRY), spectinomycin resistance
K25N/G27N	Mutagenesis of Gly27 (RRY), spectinomycin resistance
ΔK25/G26S/G27S	Mutagenesis of Gly27 (RRY), spectinomycin resistance
G26D/G27N	Mutagenesis of Gly27 (RRY), spectinomycin resistance
G26D/G27S	Mutagenesis of Gly27 (RRY), spectinomycin resistance
ΔG26/R28S	Mutagenesis of Gly27 (RRY), spectinomycin resistance
G27N/ΔR28/I29L	Mutagenesis of Gly27 (RRY), spectinomycin resistance
G27S/ΔF30/ΔS31	Mutagenesis of Gly27 (RRY), spectinomycin resistance

[a] Residue numbers do not include the N-terminal methionine. [b]Mutagenesis of the Gly27 codon with oligonucleotides carrying RRY or GAY substitutions also resulted in the generation of mutations outside the targeted codon

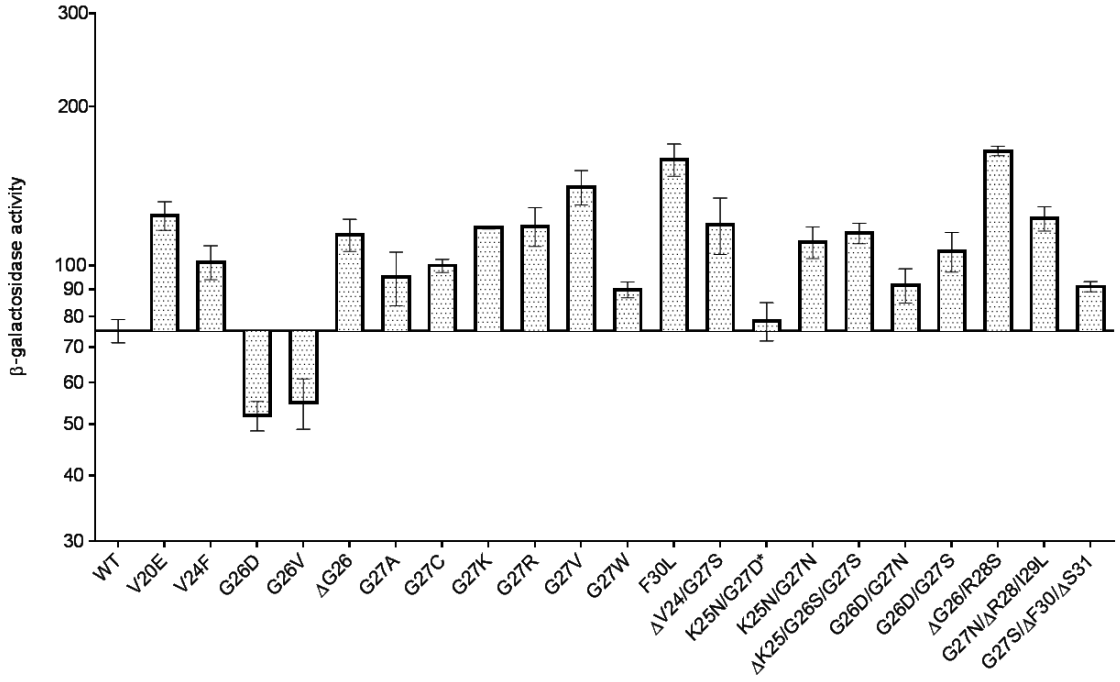

Figure S3.1 Effects of altered ribosomal protein uS5 on UGA readthrough. Readthrough levels were obtained from strains transformed with the *lacZ* plasmid p34-11. This plasmid carries a UGA mutation in the 5' end of the β-galactosidase coding region. Bars represent (Miller) units of β-galactosidase activity and each bar represents the average of at least three independent assays ± SD. WT, wild type. An asterisk (*) indicates that the activity measured for the indicated mutant did not differ significantly (P>0.05) from that of the corresponding wild-type strain.

Table S3.2 Oligonucleotides used in chapter 3

Oligo name	Sequence (5' – 3`)	Application
S55'mut	AGTTCTGGTAGCTGCTTCTA	Used as forward primer during extension overlap PCR
S53'mut	TCATACCGCGAATAGCAGGA	Used as reverse primer during extension overlap PCR
S53'internall	TCCCCAGAATTTCTTCAACG	To determine seq just before kan casette
rpsEG28D	AAAGGTGAYCGTATTTTCTCC	22-mer oligo carrying GAY (Y=T/C)
S5G28N&D	AAACCGCGTATCTAAAACCGTTAAAGGTRGYCGTATTTTCTCCTTCACAGCTCTGACTGT	GGT changed to RGY- oligo directly used for electroporation. Remade similar oligo as we needed RAY change
G28DnN60mer	AAACCGCGTATCTAAAACCGTTAAAGGTRAYCGTATTTTCTCCTTCACAGCTCTGACTGT	GGT- changed to RAY, oligo used for direct electroporation

3.9 Reference for Supplemental Information

1. **Wang H, Bian X, Xia L, Ding X, Muller R, Zhang Y, Fu J, Stewart AF.** 2014. Improved seamless mutagenesis by recombineering using ccdB for counterselection. Nucleic Acids Res **42:**e37.

2. **Unemo M, Golparian D, Skogen V, Olsen AO, Moi H, Syversen G, Hjelmevoll SO.** 2013. Neisseria gonorrhoeae strain with high-level resistance to spectinomycin due to a novel resistance mechanism (mutated ribosomal protein S5) verified in Norway. Antimicrob Agents Chemother **57:**1057-1061.

3. **Kehrenberg C, Schwarz S.** 2007. Mutations in 16S rRNA and ribosomal protein S5 associated with high-level spectinomycin resistance in Pasteurella multocida. Antimicrob Agents Chemother **51:**2244-2246.

CHAPTER 4

THE C-TERMINUS OF r-PROTEIN S4 CONTRIBUTES TO 30S SUBUNIT ASSEMBLY AND FIDELITY OF TRANSLATION

4.1 Abstract

Ribosomal protein S4 is an essential primary ribosomal binding protein that binds to the 16S rRNA and initiates nucleation and subunit assembly. The S4-S5 interaction is crucial in maintaining the open conformation of the 30S ribosomal subunit. Truncations of the C-terminal region in classical mutants D12, D14, and D16 can destabilize the S4-S5 interface resulting in temperature sensitive error-prone mutants. Here, we have obtained temperature insensitive mutants that have restored the C-terminal region. The restoration partially rescues the miscoding phenotype and nearly completely rescues the ribosome assembly defect at 42˚C. We also compared the effect of an unexpected S17 mutation on D12 and a D12 temperature insensitive mutant and found that presence of S17 alteration can aggravate assembly defects at high temperatures. The *de novo* constructed ΔV200 and E201* alterations conferred error-prone phenotype in both *E.coli* and *Salmonella*.

4.2 Introduction

Translational fidelity depends on the selection of correct amino-acyl-tRNA complementary to the mRNA codon. Interaction of a cognate correctly charged aminoacyl-tRNA ternary complex with the mRNA codon triggers conformational changes in the 30S subunit. The conformational rearrangement results in the movement of the 30S shoulder domain towards the decoding center in a process termed domain closure and facilitates GTP hydrolysis and peptide bond formation (1).

Early genetic studies using streptomycin, isolated alterations in *rpsL* (S12) that conferred an error-restrictive phenotype. The error-restrictive accuracy phenotype could be suppressed by mutations that mapped to *rpsD* (S4), *rpsE* (S5) or *rplS* (L19) and these suppressor mutations on their own displayed an error-prone phenotype (2). Structural studies show that domain closure occurs by disruption of few interactions in the S4-S5 interface region and the formation of new contacts between S12 and h44 and h27 of 16S rRNA in the decoding region (3). Mutations of the residues at the S4-S5 interface can reduce the cost of domain closure and alter the tRNA selection process resulting in a ribosomal ambiguity (*ram*) phenotype (4). Many of the classical mutants disrupt the S4-S5 interface leading to an error-prone phenotype (4). Three classical C-terminal truncated mutants D12, D14, and D16 show an error-prone phenotypes, temperature sensitivity, and ribosome assembly defects. The C-terminal region of S4 protein makes extensive contacts with S5 and any of these truncations would be expected to destabilize the S4-S5 interface (5). To explore the role of the C-terminal region we obtained derivatives of an S4 truncation mutant and characterized them for accuracy, ribosome assembly and rRNA processing.

Exceptions to the domain closure model are the three error-restrictive S4 mutant strains isolated by Bjorkman in *Salmonella typhimurium* (6). These three error-restrictive S4 mutants Q53L, ΔV200, and E201* (contains a premature stop codon at position 201) could reverse error-restrictive phenotype conferred by S12 mutations (6). Recently Agarwal *et al.* isolated E201* and six other C-terminal truncation mutants in *E.coli*, by targeting *rpsD* for random mutagenesis (7). Interestingly the *E.coli* E201* mutant strain showed an error-prone phenotype in contrast to the error-restrictive phenotype in *Salmonella* as described by Bjorkman (6). In this project, we reconstructed the E201* and ΔV200 mutations *de novo* in *E.coli* and *Salmonella* and tested the accuracy phenotype of the mutant strains.

4.3 Materials and Methods

4.3.1 Bacterial Strains and Plasmids

E.coli MC361 strain (F^- *ara Δ(gpt-lac)5 thi prfB* [from *E.coli* B]) that carries the fully active A246 RF2 (8) was used to reconstruct classical C-terminal deletion mutants D12, D14, and D16 and Fg2 (isolated by Dr. Michael O'Connor). The reconstructed MC361 D12 was used to isolate temperature insensitive mutants. MC361 *ΔaroE721::kan* (closely linked to *rpsD*) was used for reconstruction of temperature insensitive mutants in MC361. Plasmids p34-11 UGA and p12-6 UAG, carrying a UGA or UAG stop codon in the 5'coding region of the l*acZ* coding sequence respectively, were used to monitor stop codon readthrough (9). Plasmids pKD46, pKD3 and pKD4 were used for recombineering (10). MC323 (F^- λ *lacZ521* [Tn10 linked] *rph-1*) was used as the host strain for construction of *E.coli* ΔV200 and E201*. Reconstruction was carried out in MC361.

Salmonella typhimurium MS72 (LT2 *pro::Tn10/* F` *lacZ* UGA, pro^+) was used as a host strain for the construction of *Salmonella* ΔV200 and E201* using recombineering method. Reconstruction was carried out in *Salmonella* LT2.

4.3.2 Isolation and Construction of *rpsD* Mutants

Wild-type O17 and O17 D12, D14, and D16 was a gift from Dr. Monica Ryden-Aulin. The *rpsD* alleles present in O17 D12, D14, D16, and Fg2 were reconstructed in MC361 using P1-mediated transduction of MC361 *ΔaroE721::kan.* $AroE^+$ transductants were selected and sequenced for specific alterations in *rpsD*. The strains were also tested for their characteristic temperature sensitivity. MC361 D12 was grown overnight at 37˚C and streaked on LB agar plate at 42˚C to select for temperature insensitive mutants. Selected mutants were reconstructed by P1-mediated transduction.

4.3.3 Isolation and Construction of *rpsQ* Mutants

As alterations in *rpsQ* are correlated with neamine resistance (11), a 70 μg/ml neamine concentration was used to select for *rpsQ* mutations. The purified *rpsQ* fragment containing an E62K substitution or *rpsQ* amplified with Mutazyme (Agilent Technologies, Santa Clara), an error-prone, thermostable DNA polymerase, was electroporated directly into MC361 expressing λ Red recombinase. The transformants were plated on LB-neamine (70 μg/ml) for 24 hours at 37˚C. The selected neamine resistant colonies were purified and the *rpsQ* gene was sequenced.

Deletion of *rpsQ* was attempted using recombineering methods discussed by Datseno (10). Briefly, using plasmids pKD4 and pKD3 containing a kanamycin resistance cassette and a chloramphenicol resistance cassette respectively as templates, the antibiotic cassettes were amplified using 70-mer long oligos of which 50 nucleotides were complementary to 5' or 3' *rpsQ* flanking regions and 20 nucleotides were the priming sequence for pKD3 or pKD4. The amplified fragments were transformed into MC361 and selected on LB-kanamycin or LB-chloramphenicol. *rpsQ* amplified from selected antibiotic resistant colonies were tested on an agarose gel to determine the presence of antibiotic cassette *(rpsQ::kan).*

4.3.4 Reconstruction of *rpsD* Mutants

Strains D12, D16 and five of the temperature insensitive mutants (D12-1, D12-2, D12-3, D12-4, and D12-13) carried an additional *rpsQ* E62K alteration. Reconstruction of these mutant strains was carried out by the recombineering method (10). A 22-mer oligo with the C528-A532 deletion was used to amplify *rpsD* wild-type gene linked to a kanamycin cassette at the 3' end and electroporated into MC361 expressing λ Red

recombinase. Kanamycin resistant colonies were selected and sequenced to detect the presence of the 5 nucleotide deletion in *rpsD* and absence of alterations in *rpsQ*. Other mutant strains were also reconstructed in a similar fashion using mutation-specific oligos (supplemental Table S4.1). The kanamycin cassette was removed by transient expression of the Flp recombinase, and the *rpsD* gene in the kanamycin sensitive strain was resequenced to confirm the presence of the specific mutation. The *rpsQ* gene was also sequenced to confirm the absence of any mutations.

4.3.5 Construction of E201* and ΔV200

E.coli rpsD wild-type containing a kanamycin cassette at 3'end of the stop codon was used as a template for PCR. Amplification was done using either a 30-mer oligo with the V200 deletion or a 27-mer oligo with E201 substituted with an amber stop codon (TAG) at the 5' end and 20-mer oligo containing sequences flanking the 3' end of *rpsD* (supplemental Table S4.1). MC323 expressing λ Red recombinase was electroporated with the amplified fragment. MC323 carries a premature UGA mutation in the *lacZ* gene which in the presence of near-cognate decoding produces a low level of β-galactosidase activity. This activity can be detected as pale blue colonies on LB-X-Gal-IPTG plates. E201* and ΔV200 have been previously shown to display error-prone phenotypes and hence dark blue colonies were selected and sequenced. Reconstruction was carried out in MC361 by electroporation of the purified *rpsD*-kan fragment containing ΔV200 or E201* mutation. The kanamycin cassette was removed by transient expression of the Flp recombinase, and the *rpsD* gene in the kanamycin sensitive strain was resequenced to confirm the presence of the desired mutation.

The E201* and ΔV200 mutations in *Salmonella* were constructed using the same method as above. A purified fragment, amplified using a 30-mer with V200 deletion or a 27-mer oligo with TAG substitution for E201*, that anneals to the *rpsD* coding sequence at the 5'end and a 21-mer oligo that anneals to *rpsD* 3' flanking sequence (supplemental Table S4.1) was obtained. The purified fragment was electroporated into MS72 expressing λ Red recombinase. The kanamycin resistant colonies were amplified and sequenced to detect the presence of *rpsD* ΔV200 or E201TAG truncation (E201*). Reconstruction was carried out in LT2 using KB1 phage. The kanamycin resistant transductants were sequenced to detect the presence of the desired *rpsD* mutation and absence of any other mutations in the *rpsD* region.

4.3.6 Growth Rate and Antibiotic Sensitivity Determination, Enzyme Assays, and rRNA Processing and Ribosome Analyses

Temperature sensitivity was analyzed on solid media by plating 10-fold serial dilutions of overnight cultures and incubating them at 20˚C, 37˚C, and 42˚C for 24 to 48 h. Detergent lysates of cells grown logarithmically at 37˚C and 42˚C were prepared as previously described (12), in a buffer containing 25 mM Tris-HCl pH 8.0/60 mM KCl/10 mM $MgCl_2$. The lysates were loaded onto a linear 10 to 40% sucrose gradient (in 25mM TrisHCl, pH 7.8/50mM KCl/ 10mM $MgCl_2$/ 3mM DTT) and subjected to centrifugation in a Beckman SW28 for 18h at 38,191 x g. The ribosomal subunits and 70S ribosomes separated in the sucrose gradient after centrifugation were then analyzed on an ISCO gradient fractionator connected to an ISCO UV6 detector. At least two different lysates from each mutant or wild type strain were analyzed on sucrose gradients.

Isolation and analysis of total RNA from cells growing logarithmically at 37˚C and 42˚C were carried out on 0.7% agarose–0.9% Synergel, as described by Wachi *et al.* (13). The agarose-synergel system can separate 23S rRNA from 16S rRNA and its precursors (17S, 16.5S, and 16.3S). In addition, RNAs were also isolated from wild-type strains treated with chloramphenicol (final concentration of 60 mg/liter) for 30 min. Chloramphenicol is known to inhibit rRNA processing resulting in accumulation of 17S precursors of 16S rRNA (14). RNA lysates from at least 3 independent cultures of each mutant or wild type strains were analyzed.

The effect of alteration on the accuracy phenotype was determined using two *lacZ* reporter constructs containing premature UGA (p34-11UGA) or UAG (p12-6 UAG) codons. Logarithmically growing cells at 37˚C and 42˚C were treated with O-nitrophenly-β -D-galactoside and assayed for β-galactosidase activity. At least 3 independent cultures for each mutant and wild type strain were tested and the activity was expressed in Miller units (15).

4.4 Results

4.4.1 Isolation and Construction of *rpsD* Mutants

Wild type S4 is a 205 amino acid long protein. The classical S4 mutants D12, D14, and D16 have C-terminal truncations as shown in Table 4.1. D12 has a 5 nucleotide deletion (C528 – A532) that results in a premature termination to form a 180 amino acid protein. The D14 mutant has an insertion of Cytosine (C) at G535 and forms a 182 amino acid protein truncated at the C-terminal. Fg2 has an insertion of Thymine (T) after G535, similar to D14 mutant that leads to premature termination to form a 182 amino acid long protein. The last four amino acids in all three mutant strains are changed with the last three changes being Arginine, Tyrosine, and Valine. In D16, a change of G509 to A509 results in the alteration of Tyrosine Y170 to TAA ochre stop codon forming a 169 amino acid long S4 protein (5). All the four C-terminal truncated mutants were reconstructed by P1-mediated transduction in MC361 *ΔaroE721::kan* before being used for further characterization.

Temperature insensitive mutants were isolated by streaking overnight grown cultures of temperature sensitive D12 at 42˚C and 13 temperature insensitive mutants were obtained. Of the 13 colonies sequenced, 9 carried different intragenic mutations (Table 4.1) in the *rpsD* gene with 6 strains having unique mutations and 3 having repeat mutations. As the 6 selected mutant strains contained unique intragenic *rpsD* mutations, no other genes were sequenced for these strains. Four strains (D12-6, D12-9, D12-11and D12-12) had no intragenic changes. These mutant strains contained the Δ5 deletion present in the original D12 mutant and were temperature insensitive. These mutant strains were sequenced for alterations in genes encoding S5, S12 and S17 and all four showed the presence of a specific *rpsQ* alteration affecting ribosomal protein S17 (E62K).

The sequences of the six temperature insensitive mutants carrying intragenic changes are shown in Table 4.1. All the six mutants have the C528-A532 deletion as in the D12 parent strain. Four of the mutants (D12-2, D12-3, D12-4, and D12-13) have one additional nucleotide deletion in *rpsD* that restores the reading frame to form a 204 amino acid long protein. D12-1 has a 7 nucleotide deletion whereas D12-5 has a 4 nucleotide deletion, resulting in a total of 12 and 9 nucleotide deletions, forming a 202 and 203 amino acid long proteins respectively. All the temperature insensitive mutants have a restored C-terminal region with at least one amino acid different from wild type S4 protein. The largest number of changes in the restored C-terminal region is seen in D12-4 with 10 amino acid changes followed by 8 amino acid changes in D12-2. These mutant strains containing additional intragenic mutations were reconstructed into a new strain by P1-mediated transduction in MC361 *ΔaroE721::kan.*

Table 4.1 Alterations in the C-terminal *rpsD* mutant strains

Strain	*rpsD* gene sequence starting from base 480 corresponding to amino acid 161	Alteration	Number of amino acids
WT	GAG CAG CGT GAA AAG CCA ACC TGG CTG GAA GTT GAT GCT GGC AAG ATG GAA GGT ACG TTT AAG CGT AAG CCG GAG CGT TCT GAT CTG TCT GCG GAC ATT AAC GAA CAC CTG ATC GTC GAG CTT TAC TCC AAG TAA	None	205
D12	GAG CAG CGT GAA AAG CCA ACC TGG CTG GAA GTT GAT GCT GGΔT GGA AGG TAC GTT **TAA**	Δ5	180
D12-1	GAG CAG CGT GAA AAG CCA ACC TGG CTG GAA GT# G## G## ##Δ TG GAA GGT ACG TTT AAG CGT AAG CCG GAG CGT TCT GAT CTG TCT GCG GAC ATT AAC GAA CAC CTG ATC GTC GAG CTT TAC TCC AAG TAA	Δ5 + Δ7	202
D12-2	GAG CAG CGT GAA AAG CC#A CCT GGC TGG AAG TTG ATG CTG GΔTG GAA GGT ACG TTT AAG CGT AAG CCG GAG CGT TCT GAT CTG TCT GCG GAC ATT AAC GAA CAC CTG ATC GTC GAG CTT TAC TCC AAG TAA	Δ5 + Δ1	204

Strain	*rpsD* gene sequence starting from base 480 corresponding to amino acid 161	Alteration	Number of amino acids
D12-3	GAG CAG CGT GAA AAG CCA ACC TGG CTG GAA GTT GAT GC#G GΔTG GAA GGT ACG TTT AAG CGT AAG CCG GAG CGT TCT GAT CTG TCT GCG GAC ATT AAC GAA CAC CTG ATC GTC GAG CTT TAC TCC AAG TAA	Δ5 + Δ1	204
D12-4	GAG CAG CGT G#AA AGC CAA CCT GGC TGG AAG TTG ATG CTG GΔTG GAA GGT ACG TTT AAG CGT AAG CCG GAG CGT TCT GAT CTG TCT GCG GAC ATT AAC GAA CAC CTG ATC GTC GAG CTT TAC TCC AAG TAA	Δ5 + Δ1	204
D12-5	GAG CAG CGT GAA AAG CCA ACC TGG CTG GAA GTT GA#G## G#ΔTG GAA GGT ACG TTT AAG CGT AAG CCG GAG CGT TCT GAT CTG TCT GCG GAC ATT AAC GAA CAC CTG ATC GTC GAG CTT TAC TCC AAG TAA	Δ5 + Δ4	203
D12-13	GAG CAG CGT GAA AAG CCA ACC TGG CTG GAA GTT GAT GCT GGΔT GGA AGG TAC G#TT AAG CGT AAG CCG GAG CGT TCT GAT CTG TCT GCG GAC ATT AAC GAA CAC CTG ATC GTC GAG CTT TAC TCC AAG TAA	Δ5 + Δ1	204

Strain	*rpsD* gene sequence starting from base 480 corresponding to amino acid 161	Alteration	Number of amino acids
D14	GAG CAG CGT GAA AAG CCA ACC TGG CTG GAA GTT GAT GCT GGC AAG ATG GCA AGG TAC GTT **TAA**	1 base ins	182
D16	GAG CAG CGT GAA AAG CCA ACC **TAG**	Sub	170
Fg2	GAG CAG CGT GAA AAG CCA ACC TGG CTG GAA GTT GAT GCT GGC AAG ATG GTA AGG TAC GTT **TAA**	1 base ins	182

Δ: Represents the 5 base deletion present in D12 and its derivatives
#: Represents the additional deletions in temperature insensitive derivatives of D12
The amino acids changed due to frame-shift are underlined
Premature stop codons are shown in bold

4.4.2 Growth and Temperature Sensitivity of S4 C-terminal Mutant Strains

D12, D14, D16, and Fg2 grew well on solid media at 37˚C and 20˚C but showed reduced to no growth at 42˚C. Four mutant strains (D12-1, D12-3, D12-5, and D12-13) showed complete recovery of the temperature sensitive phenotype and grew well at all the three temperatures. Two of the mutant strains D12-2 and D12-4 showed partial recovery of growth at 42˚C and additionally showed reduced growth at 20˚C (Figure 4.1).

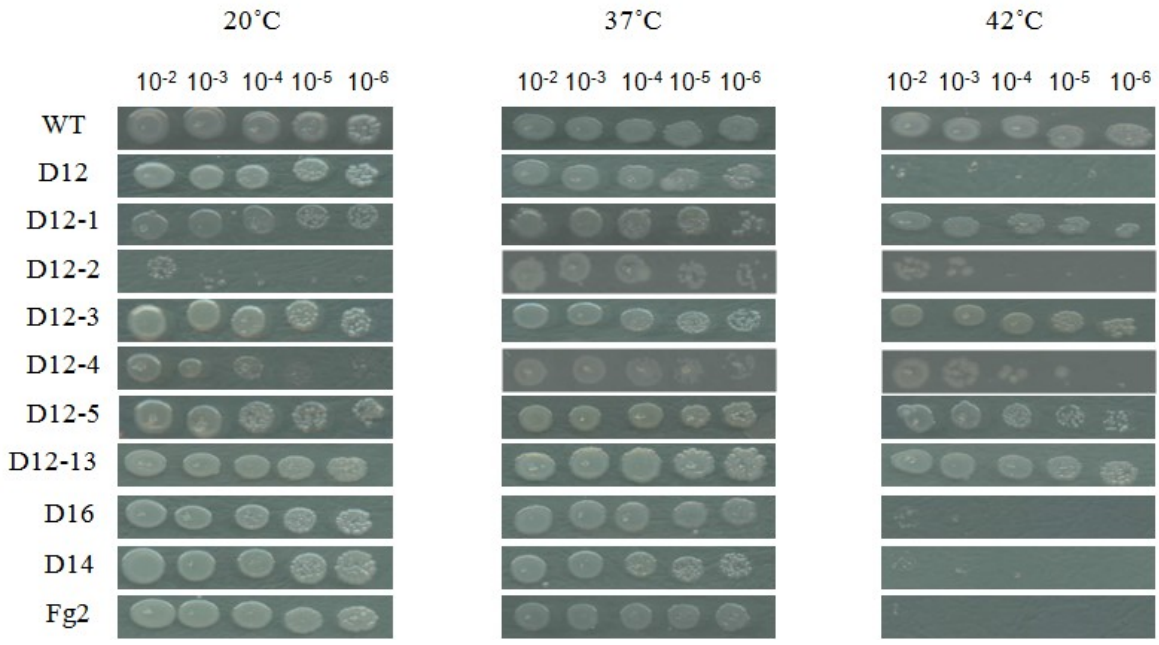

Figure 4.1 Effects of ribosomal proteins S4 mutations on growth at 20°C, 37°C and 42°C on solid media. Three-microliter aliquots of serially diluted (10^{-2} to 10^{-6}) overnight cultures were spotted onto antibiotic-free LB plates and incubated for 24 to 48 h. WT, wild type.

4.4.3 Miscoding Properties of S4 C-terminal Mutant Strains

The β-galactosidase-based UGA and UAG readthrough assays rely on decoding of the stop codon by a wild-type tRNA. It reports on defects in either the decoding or the termination process and was used to determine the miscoding properties of mutants at 37˚C and 42˚C. All the mutants showed increased readthrough of UGA codons at both temperatures compared to wild-type (Figure 4.2). The strongest effect was seen in D12 with 3.49 and 5.62 fold increase at 37˚C and 42˚C respectively, in the UGA readthrough assay. All the six temperature insensitive mutants show reduced miscoding at both temperatures compared to D12, but still, have higher miscoding levels than wild type. Similar results were

obtained in the UAG readthrough assay at 37˚C. UAG readthrough assay at 42˚C was not done.

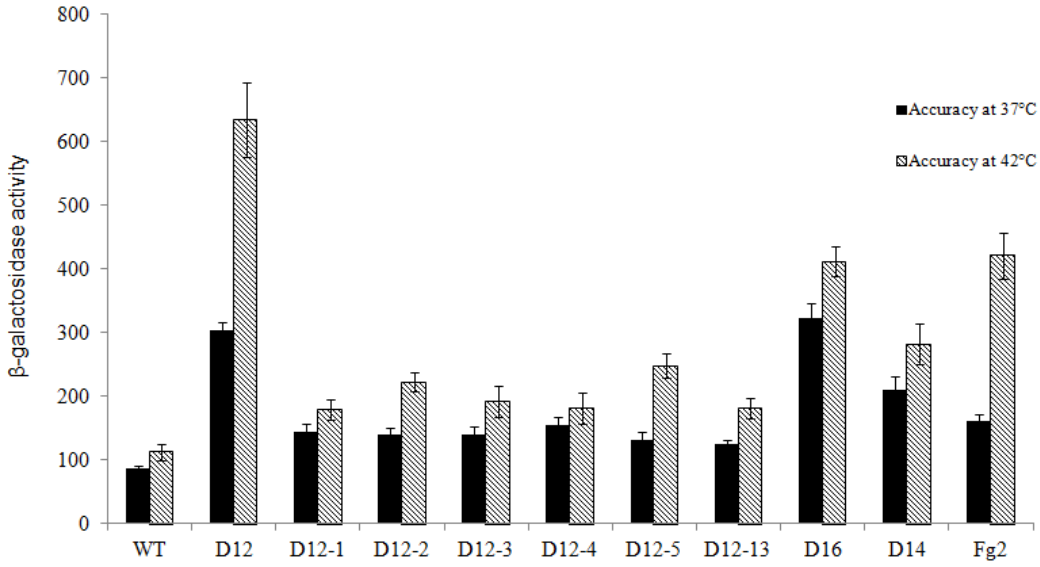

Figure 4.2 Effects of altered ribosomal protein S4 on UGA readthrough. Readthrough levels were measured in strains transformed with p34-11 a *lacZ* plasmid carrying a UGA mutation in the 5' end of the β-galactosidase coding region. Bars represent (Miller) units of β-galactosidase activity. Each bar represents the average of at least three independent assays ± SE. WT, wild type.

4.4.4 Effect of C-terminal Deletions on Ribosome Biogenesis and rRNA Processing

S4 is a primary binding protein and alterations in this protein can lead to defects in the assembly. Lysates obtained by growing each of the mutants at 37˚C and 42˚C were analyzed by sucrose gradient centrifugation. The ribosome profile of all the mutants grown at 37˚C was similar to wild type ribosome profiles (Figure 4.3A). However, the profile of

the mutants grown at 42˚C showed pronounced defects. All the C-terminal deletion mutants, D12, D16, D14, and Fg2, showed a substantial increase in the levels of 50S subunits with reduced or no 70S and 30S peaks respectively (Figure 4.3B). Interestingly, the D12 temperature insensitive mutants (D12-1, D12-2, D12-3, D12-4, D12-5, and D12-13) showed varying degree of recovery from the assembly defects, with profiles closer to wild type. The D12-4 mutant strain showed the least degree of recovery compared to other temperature insensitive mutants (Figure 4.3B). Aliquots corresponding to the 30S, 50S, and 70S peaks were collected and tested on an agarose-synergel to confirm the identities of the relevant peaks.

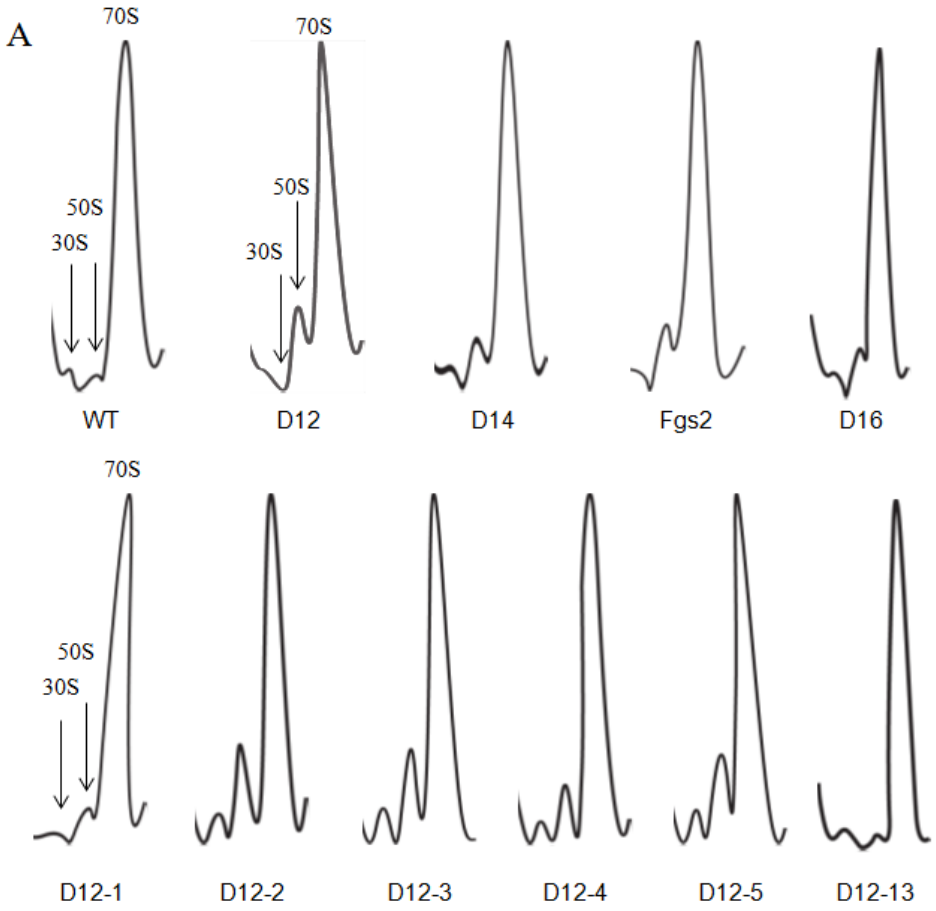

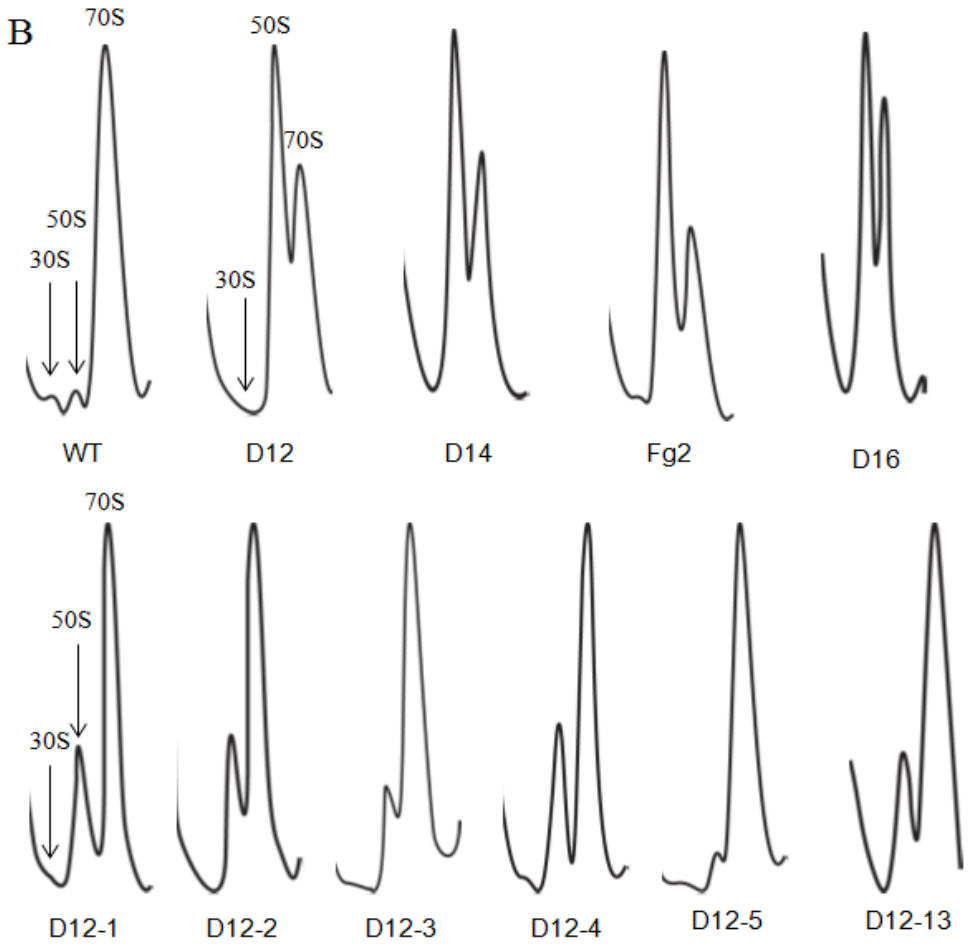

Figure 4.3 Ribosome profiles of a wild-type and S4 mutant strains grown at 37°C and 42°C. A) Gradient profiles obtained from lysates grown at 37˚C B) Gradient profiles obtained from lysates grown at 42˚C. The positions of the 30S and 50S subunits and 70S ribosomes are indicated on the profile of the wild-type strain.

Lysates from each of the mutants obtained at 37˚C and 42˚C were also analyzed for the 16S rRNA processing using the agarose-Synergel system. None of the lysates obtained from mutants grown at 37˚C showed any processing defects. Lysates of D12, D16, D14 and Fg2 obtained at 42˚C showed substantial accumulation of 16S rRNA precursors (Figure 4.4). All the C-Terminal restored mutants showed moderate to a substantial level of accumulation of 16S rRNA precursors.

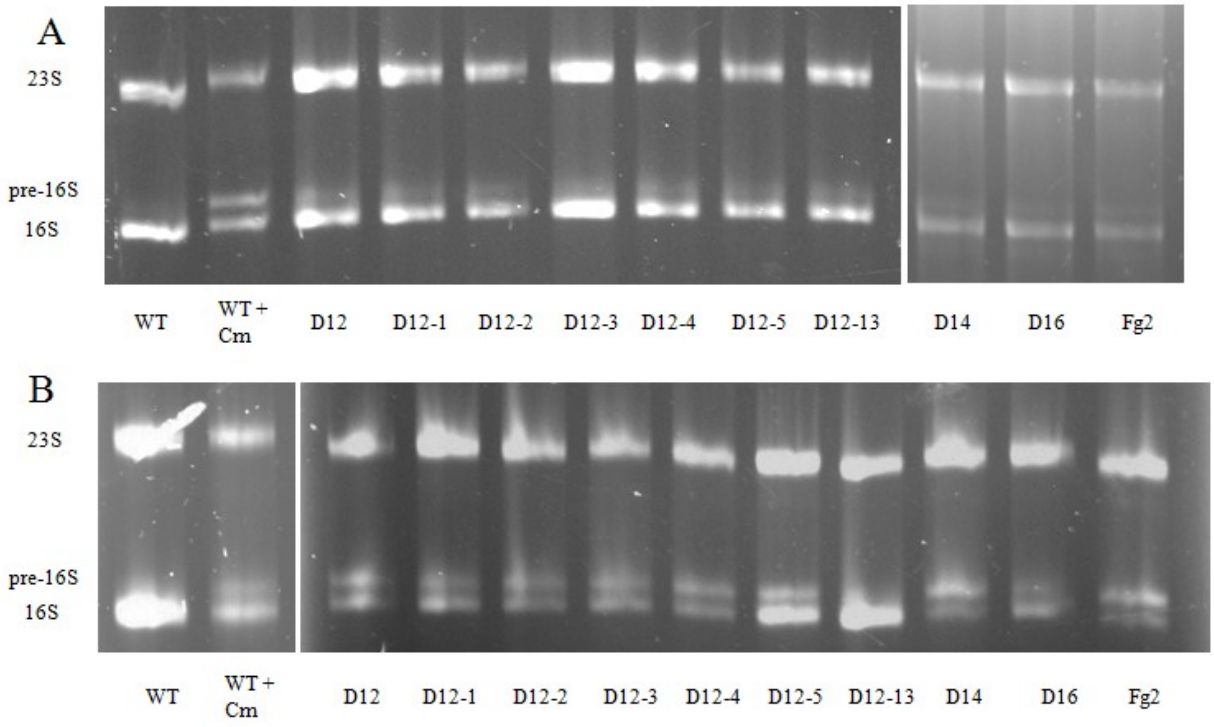

FIG 4.4 rRNA processing in wild type and S4 mutant strains at 37˚C and 42˚C.
A) Total RNA from strains grown at 37˚C. B) Total RNA from strains grown at 42˚C. Total RNAs from logarithmically growing wild type and mutant strains were extracted and electrophoresed on agarose/Synergel gels containing ethidium bromide. The second lane from the left contains RNAs extracted from wild type cells treated with chloramphenicol for 30 min., leading to the accumulation of unprocessed 17S rRNA precursors.

Overall these analyses show that restoration of the C-terminal region has a major influence on the phenotype of the mutants at 42˚C. The D12 temperature insensitive mutant strains show pronounced recovery in ribosome assembly defects at 42˚C and also incomplete recovery of the miscoding properties at 42˚C.

4.4.5 Isolation and Construction of *rpsQ* Mutants

Four of the mutant strains (D12-6, D12-9, D12-11 and D12-12) isolated during the initial screen had no intragenic mutation but contained a S17 E62K alteration. With the aim of understanding the contribution of S17 in recovery from the temperature sensitive phenotype in D12, we undertook the reconstruction of the E62K mutation in S17 and the isolation of additional mutations in S17. Alteration in *rpsQ* has been shown to confer neamine resistance in *E.coli* and hence this antibiotic resistance was used for selection of strains containing *rpsQ* mutations. MC361 wild type expressing λ Red recombinase was electroporated with a *rpsQ* PCR fragment amplified from D12 containing the E62K alteration and plated on LB medium containing 70 μg/ml neamine. From 3 different electroporation incubated at 37˚C and one electroporation incubated at 30˚C, 174 neamine resistant transformants were obtained. The ten mutants sequenced had a wild type *rpsQ* sequence. In a continued effort to reconstruct S17E62K, we amplified the wild type *rpsD* gene linked to a kanamycin resistance cassette. A strain carrying the D12 Δ5 deletion and S17 E62K, expressing λ Red recombinase was electroporated with the amplified fragment. From 7 electroporation 154 colonies were obtained, of which 4 were sequenced for alterations in the *rpsD* and *rpsQ* genes. Sequencing of *rpsQ* showed the presence of the E62K alteration in 3 strains. Sequencing of S4 in these 3 strains showed the presence of D12 Δ5deletion, and an extra nucleotide deletion (2 were identical to D12-13). One mutant

strain showed wild type sequence in both S17 and S4. Thus, we were not able to reconstruct *rpsQ* E62K alteration in strains containing wild type *rpsD* by either of the above two methods.

In order to isolate and identify new S17 alterations which can rescue temperature sensitivity, the wild type *rpsQ* was amplified with an error-prone polymerase (mutazyme). A D12 strain expressing λ Red recombinase was electroporated with the purified *rpsQ* fragment and selected for growth at 42˚C. From 4 different electroporations, 103 transformants were obtained, of which 4 were sequenced for alterations in the *rpsD* and *rpsQ* genes. Sequencing of *rpsQ* showed the presence of only the E62K alteration in all 4 strains. Sequencing of *rpsD* showed 2 strains with the expected 5 base deletion present in the original D12 mutant, whereas 2 of them also had an extra single nucleotide deletion, one if which was identical to D12-3. An attempt to delete *rpsQ* gene, with the aim of determining its influence on D12 was also unsuccessful. Overall we were not able to obtain a deletion of or recover *rpsQ* alterations other than E62K, by any of the methods discussed above.

4.4.6 Presence of Altered S17 Protein in D12 and D12 Derived Strains

The consistent isolation of only the *rpsQ* E62K alteration in all the strains made us go back and sequence the *rpsQ* gene in D12 and other strains. Surprisingly, the *rpsQ* E62K alteration was present in D12. *rpsD* is separated from *rpsQ* by approximately 7.5 Kb. Due to the proximity of the two genes and use of P1 mediated transduction for reconstruction, the *rpsD*, *rpsQ* and other genes in between them could have been transferred into the newly reconstructed strains together, instead of just *rpsD*. Sequencing other mutant strains isolated and studied in this project showed the presence of *rpsQ* E62K alteration in D16, D12-1,

D12-2, D12-3, D12-4, and D12-13. Only one temperature insensitive strain (D12-5) and D14 and Fg2 did not have the *rpsQ* alteration. MC185 and MC187 strains were derived from O17, the initial *rpsD*$^{+}$ strain used to reconstruct the original D12 mutant. Sequencing of the *rpsQ* gene in these two strains showed they had wild type *rpsQ* gene. As the strain containing the *rpsQ* E62K alteration was used for obtaining temperature insensitive mutants 5 of the 6 temperature insensitive mutants (D12-1, D12-2, D12-3, D12-4, and D12-13) contained the *rpsQ* E62K alteration. The other 4 temperature insensitive mutant strains (D12-6, D12-9, D12-11, and D12-12) that did not contain intragenic mutations but contained *rpsQ E62K* alteration and likely have an additional extragenic mutation rescuing the temperature sensitive phenotype.

4.4.7 Effect of *rpsQ* E62K Alteration in the D12 and D12 Derived Strains

To understand if the S17 alteration affected the phenotypic characterization, we attempted to reconstruct all the S4 mutant strains carrying the E62K alteration in S17 (D12, D12-1, D12-2, D12-3, D12-4, D12-13 and D16) in MC361 carrying a wild type *rpsQ* gene. Specific oligos (Table S4.1) for each of the alterations (Table 1) were used to amplify the *rpsD* gene and the linked kanamycin resistance cassette in the intergenic spacers between *rpsD* and *rpoA*. MC361 cells expressing λ Red recombinase were electroporated with the purified fragment and kanamycin resistant colonies were selected and sequenced. Only two mutant strains (D12 and D12-4) were successfully constructed. The other 5 *rpsD* mutations strains could not be reconstructed in a wild type *rpsQ* strain for unknown, presumably technical reasons.

On solid media the reconstructed D12 showed growth similar to wild type at 20˚C and 37˚C whereas showed little to no growth at 42˚C. This is consistent with the results

obtained for D12 even in presence of the S17 E62K alteration. Reconstructed D12-4 grew similar to wild type at all temperatures (Figure 4.5). In contrast, D12-4 containing S17 E62K alteration showed reduced growth at both 20˚C and 42˚C

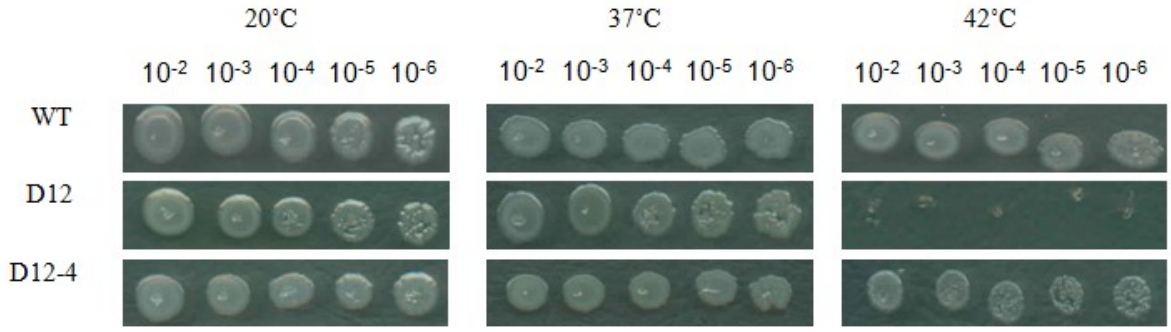

FIG 4.5 Effects of reconstructed altered ribosomal protein S4 (containing wild type S17) on growth on solid media at 20ºC, 37ºC, and 42ºC. 3 µl aliquots of serially diluted (10^{-2} -10^{-6}) overnight cultures of the D12 and D12-4 containing wild type *rpsQ* gene were spotted onto antibiotic-free LB plates and incubated for 24-48 hrs.

In the reconstructed D12 strains UGA miscoding at 37˚C for D12 showed a 4.89 increase compared to the wild type and 1.68 for D12-4. At 42˚C D12 showed a 5.68 fold increase and D12-4 showed a fold increase of 2.08. Similar results were observed for UAG readthrough. The absence of S17 alteration did not exert a pronounced influence on the miscoding properties (Figure 4.6).

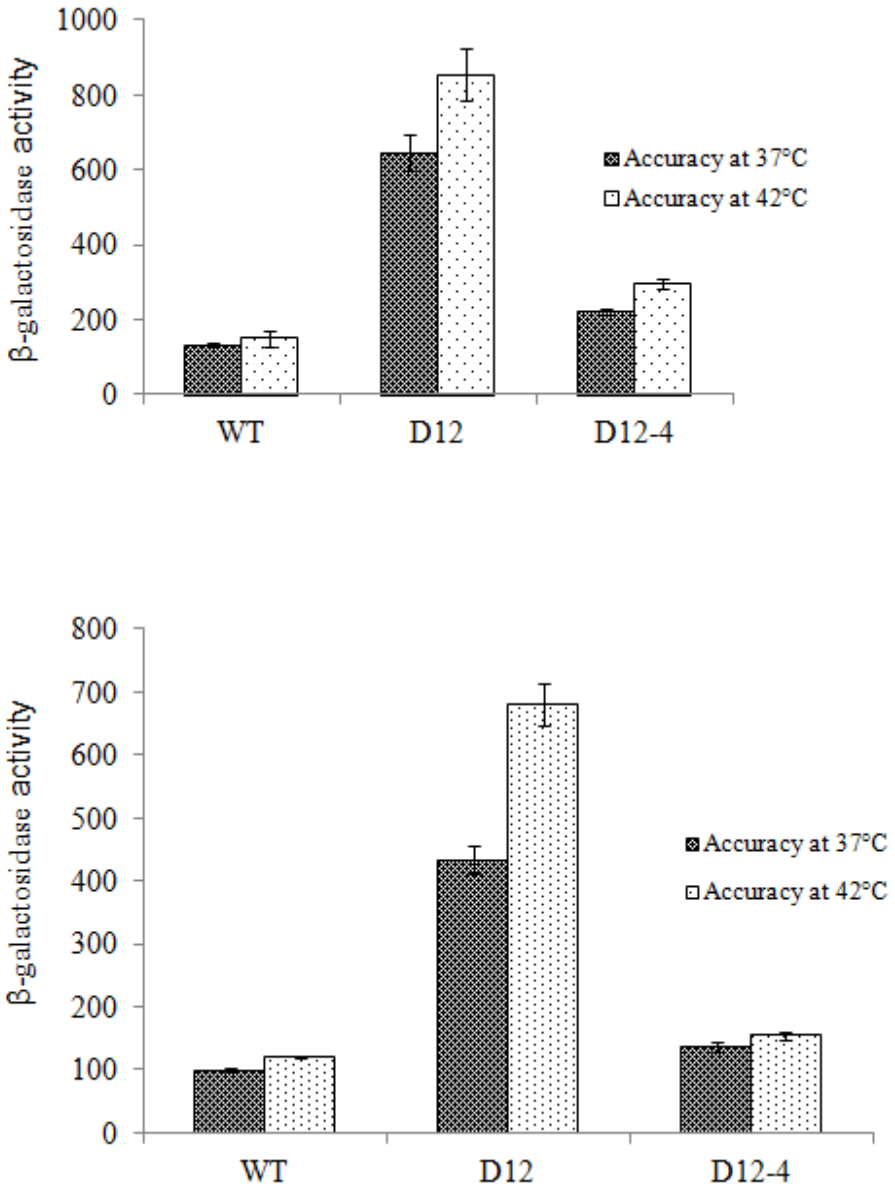

Figure 4.6 Effects of reconstructed altered ribosomal proteins S4 (containing wild-type S17) on UGA (top) and UAG (bottom) readthrough. Readthrough levels were obtained from reconstructed D12 and D12-4 with wild type S17 along with wild type strain transformed with the *lacZ* plasmid p34-11 UGA, and p12-6 UAG carrying a UGA or UAG mutation in the 5' end of the β-galactosidase coding region. Bars represent (Miller) units of β-galactosidase activity.

Ribosome gradient profiles of cultures of reconstructed D12 and D12-4 strains with wild type S17 grown at 37˚C were similar to wild type. Ribosome profiles from D12 and D12-4 cells grown at 42˚C showed assembly defects with increased 50S subunit levels. Although an assembly defect is observed in D12 even in the absence of an S17 alteration, it is less pronounced than when the S17 alteration is also present (Figure 4.7).

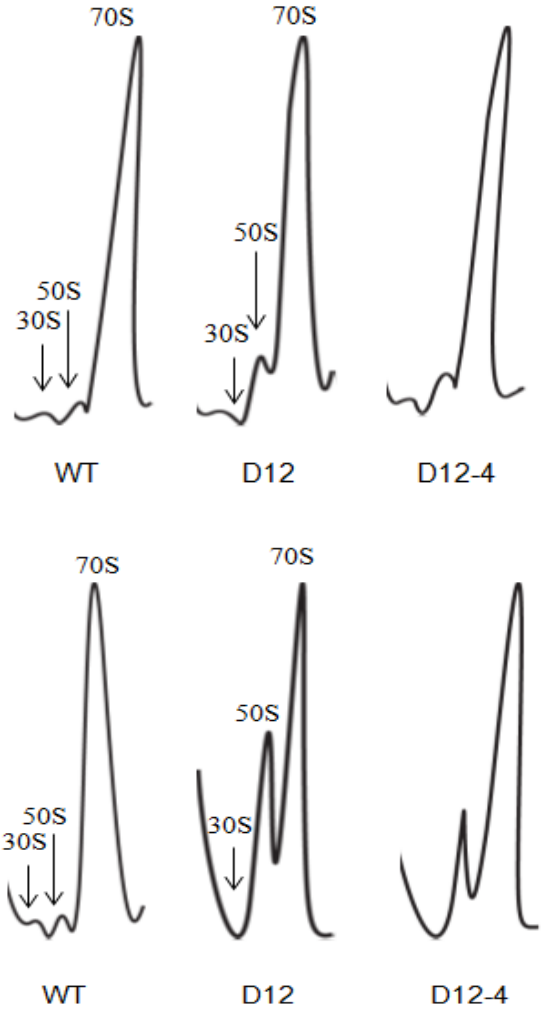

Figure 4.7 Ribosome profiles of a wild-type strain and reconstructed S4 mutant strains (containing wild-type S17) grown at 37˚C (top) and 42˚C (bottom). The positions of the 30S and 50S subunits and 70S ribosomes are indicated on the profile and the direction of sedimentation is from left to right.

RNA lysates from D12 and D12-4 obtained at 37˚C and 42˚C were analyzed for processing defects using the agarose-Synergel system. No accumulation of precursor was observed at 37˚C. D12 showed substantial accumulation at 42˚C, whereas D12-4 showed slight to moderate accumulation of the precursor (Figure 4.8). Overall, the analyses of D12 and D12-4 indicates that *rpsQ* E62K alteration can aggravate ribosome assembly at 42˚C

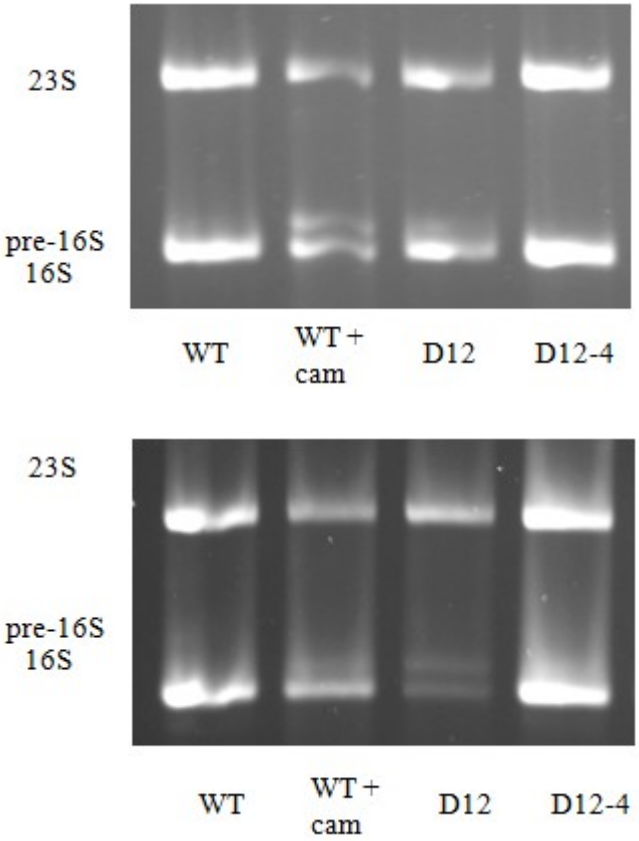

FIG 4.8 rRNA processing in wild-type and reconstructed S4 mutant strains (containing wild-type S17) grown at 37˚C (top) and 42˚C (bottom). Total RNAs from logarithmically growing wild type and mutant strains were extracted and electrophoresed on agarose/synergel gels containing ethidium bromide. The second lane from the left contains RNAs extracted from wild type cells treated with chloramphenicol for 30 min., leading to the accumulation of unprocessed 17S rRNA precursors.

4.4.8 Characterization of ΔV200 and E201*

Björkman *et al.*, (6) isolated 7 streptomycin independent (SmI) mutants in *Salmonella* containing mutations in *rpsD*. Of the 7 mutant strains, three *rpsD* mutants Q53L, ΔV200 and E201*, showed error-restrictive phenotypes whereas previously C-terminal S4 mutants in *E.coli* showed the error-prone phenotype. Recently Agarwal and coworkers (7) isolated E201* in *E.coli* using an accuracy altering screen, with E201* showing the error-prone phenotype. In this paper, we reconstructed ΔV200 and E201*, in *E.coli* and *Salmonella*, using mutation-specific oligos to further explore this discrepancy.

Miscoding properties of the mutants were tested using UGA and UAG readthrough assays at 37˚C. The ΔV200 and E201* mutant strains in both *E.coli* and *Salmonella* showed increased miscoding in readthrough assays when compared with respective wild-type strain (Figure 4.9). Ribosome profiles for ΔV200 and E201* showed no assembly defect in either of the strains (Figure 4.10). RNA lysates from each of the mutants were analyzed for 16S rRNA processing defects in the agarose-Synergel system. None of the mutants showed accumulation of 16S rRNA precursors (not shown). The mutant *E.coli* and *Salmonella* strains containing ΔV200 and E201* showed an error-prone phenotype consistent with the domain closure model.

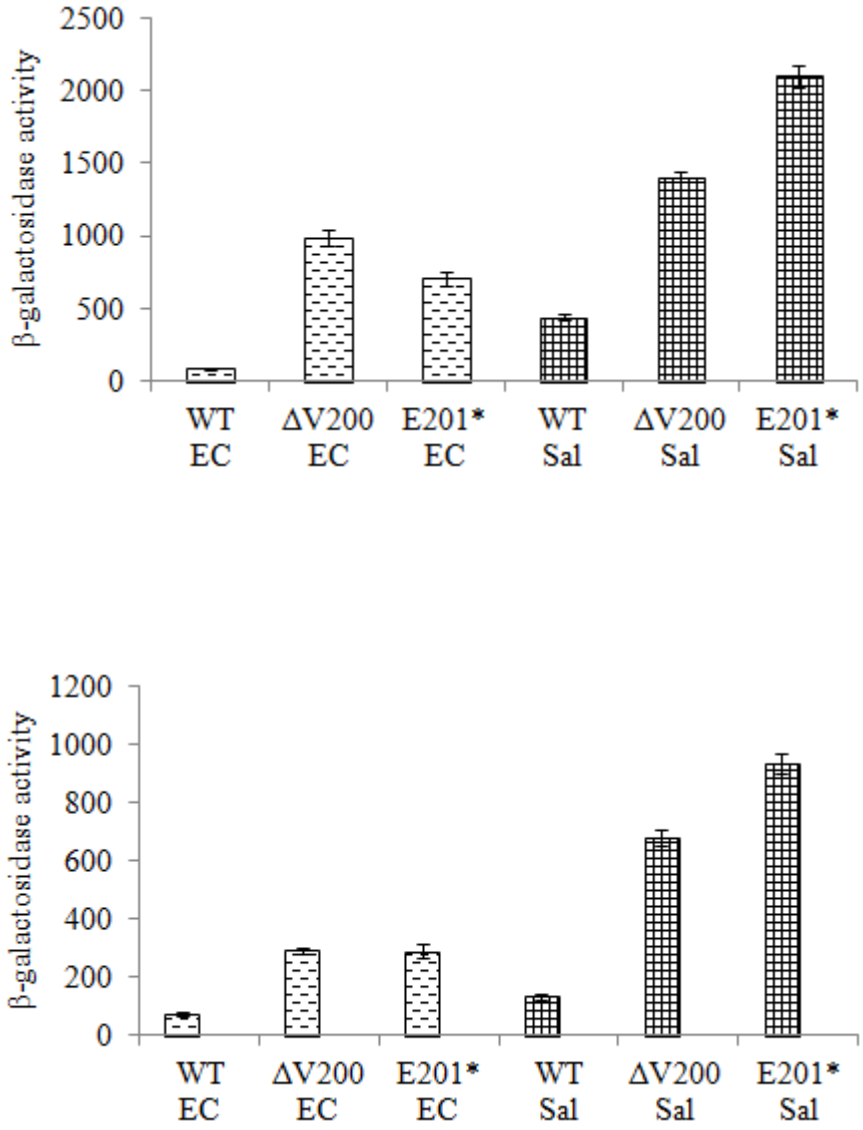

Figure 4.9 Effects of altered *E.coli* and *Salmonella* ribosomal protein S4 on UGA (top) and UAG (bottom) readthrough. Readthrough levels were obtained from strain transformed with the *lacZ* plasmid p34-11 UGA, and p12-6 UAG carrying a UGA or UAG mutation in the 5' end of the β-galactosidase coding region. Bars represent (Miller) units of β-galactosidase activity. EC- *E.coli;* Sal- *Salmonella*

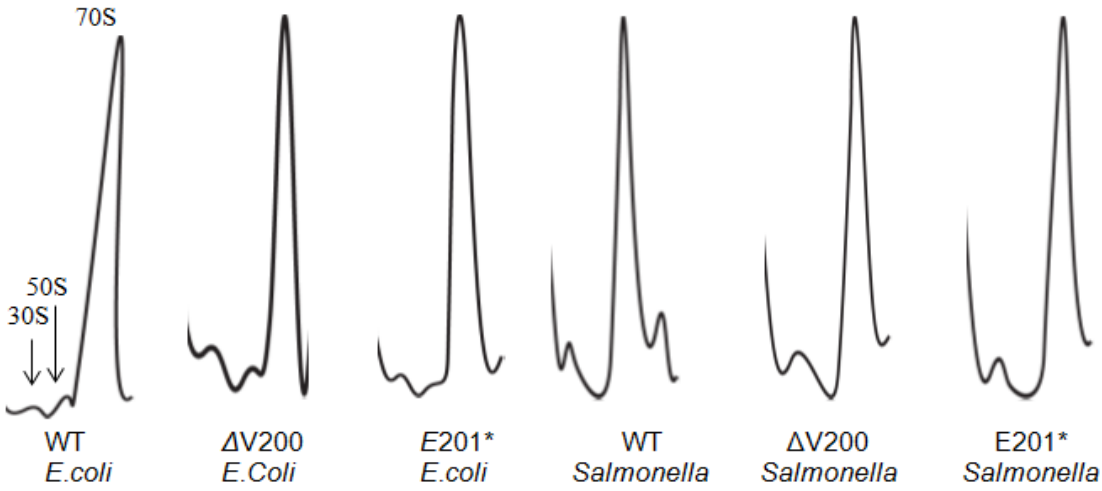

Figure 4.10 Ribosome profiles of a wild-type strain and S4 mutants at 37˚C for *E.coli* and *Salmonella*. The positions of the 30S and 50S subunits and 70S ribosomes are indicated on the profile of the wild type strain and the direction of sedimentation is from left to right.

4.5 Discussion

S4 is a 205 amino acid long ribosomal protein located at the neck of the 30S subunit, close to S3, S5, and S12 (16). The interaction between ribosomal proteins S4 and S5 is critical for stringent tRNA selection process by the transition of the small subunit from an open to a closed conformation (domain closure). Several S4 mutants were initially isolated as suppressors that could reverse the error-restrictive phenotype of *rpsL* alterations. These S4 mutants displayed error-prone phenotypes. Three such mutants D12, D14, and D16 isolated as error-prone suppressors, encoded C-terminal truncated S4 proteins. These mutants were temperature sensitive and error-prone. The S4 C-terminal region is considered to be important for interactions with S5 and is also suggested to be involved in 16S rRNA binding (5). Truncation of the S4 C-terminal region can result in an error-prone accuracy phenotype mainly due to the disruption of the S4-S5 interface or S4-16S rRNA interactions. The main goal of this project was to analyze how the restoration of the C-terminal region can effect miscoding, 16S rRNA processing, and ribosome assembly.

Our work shows that the 3 truncation mutants along with Fg2 isolated in the lab by Dr. Michael O'Connor have a miscoding phenotype at both 37˚C and 42˚C. At 37˚C, the ribosome assembly profiles and rRNA processing profiles were similar to wild type. At 42˚C, however, the 4 C-terminal truncated mutants had defective ribosome assembly profiles with little or no free 30S subunit, increased 50S subunits and low 70S ribosome levels.

The temperature sensitive D12 mutant was used to isolate temperature insensitive revertants. Some of these temperature insensitive mutants had additional intragenic deletions that restored the C-terminal region to form a nearly full-length S4 protein. The restored C-

terminal region had at least one amino acid different compared to the C-terminal region of the wild type protein. The miscoding phenotype of the C-terminal restored mutants at both 37˚C and 42˚C was substantially lower compared to D12 but was higher compared to wild type. The restoration of the C-terminal region thus could rescue the miscoding phenotype only partially. Presumably, the altered amino acids present in the temperature insensitive revertants contribute to the increased miscoding seen in these mutants. Ribosome assembly and rRNA processing profiles at 37˚C were similar to wild type and D12 in the temperature insensitive mutants. The predominant effect of C-terminal restoration was the near complete rescue of ribosome assembly defects at 42˚C.

Protein S4 binds to the 16S rRNA and initiates the 30S assembly process. Temperature sensitivity and the ribosome assembly defect of D12 have been previously shown to result from the lowered affinity of S4 for its binding site on 16S rRNA (17). The absence of the C-terminal region probably further hinders the ribosome subunit association at higher temperatures, resulting in a pronounced assembly defect and temperature sensitivity. Also, mutant ribosomes show a decreased ability to proofread *in vitro* (17). The restoration of the C-terminal region in the temperature insensitive mutants shows reduced assembly defects even though 16S rRNA processing is still defective. Consistent with this previous studies from our lab (7) have shown that there is no strict correlation between 16S rRNA processing and defective ribosome assembly defect.

In order to understand the how S17 can influence D12 temperature sensitivity, miscoding, and ribosome assembly defect, we attempted to obtain different *rpsQ* alterations and deletion. However, we failed to generate and isolate any S17 alteration or *rpsQ* deletion in D12 by the methods used.

To further gain insights as to how S17 can influence D12 temperature sensitivity, miscoding, and ribosome assembly defect, we successfully reconstructed D12 and one temperature insensitive mutant D12-4 to have wild type *rpsQ* gene. Comparison of phenotypes for D12 and D12-4 with and without S17 E62K alteration showed that the S17 E62K did not influence miscoding properties at 37˚C or 42˚C. Interestingly, D12-4 had near complete recovery for growth at 42˚C with wild type *rpsQ,* compared to partial recovery with the S17 E62K alteration. In the presence of wild type S17, D12 showed a reduced ribosome assembly defect, compared to D12 with S17 E62K alteration. The temperature insensitive mutant D12-4 also showed reduced assembly defect in presence of wild type S17, compared to D12-4 with S17 E62K. Although absence of the S17 E62K did not completely abolish ribosome assembly defect, it did reduce the scale of assembly defect.

S4 and S17 are both primary binding proteins and bind to the 5' region of the 16S rRNA to form the body of the small subunit ribosome. Green and Kurland in 1971 showed that altered S4 protein binds to 16S rRNA with lower affinity compared to wild-type S4 and can lead to a defect in 30S assembly (18). Deletion of the C-terminal region could significantly hinder the binding of S4 protein to 16S rRNA and thereby lead to the slow assembly at higher temperatures. An additional mutation in S17 can further hinder the assembly process leading to a more pronounced assembly defect as seen from the data.

Farabaugh *et al.* (19), using the yeast two-hybrid system, proposed that the residues that interact with the S4-S5 interface may also interact with the 16S rRNA. Noller in 1989 showed that protein-rRNA interaction is essential for the mature conformation of 16S rRNA in a 30S subunit (20). *Ram* mutations that are affected in the C-terminal region as described in this work may hinder proper folding of the 30S particle and have reduced intra-30S

subunit contacts (21). Restoration of the C-terminal region with changes has therefore rescued the assembly defect. The S4 C-terminal region is thus important for accuracy as well as ribosome assembly.

As an extended part of understanding the C-terminal region of S4, we investigated a discrepancy found in the literature. *Salmonella* ΔV200 and E201* were identified as suppressors that could restore the error-restrictive phenotype due to *rpsL* alteration. Interestingly, ΔV200 and E201* showed an error-restrictive phenotype in *Salmonella* (6). Recent work from our lab shows that E201* alterations in *E.coli* show an error-prone phenotype (7). Simultaneous construction and analysis of ΔV200 and E201* in *E.coli* and *Salmonella* shows that these alterations exhibit an error-prone phenotype in both organisms consistent with the open-closed model.

4.6 References

1. **Ogle JM, Carter AP, Ramakrishnan V.** 2003. Insights into the decoding mechanism from recent ribosome structures. Trends in Biochemical Sciences **28:**259-266.

2. **Gorini L, Jacoby GA, Breckenridge L.** 1966. Ribosomal ambiguity. Cold Spring Harb Symp Quant Biol **31:**657-664.

3. **Ogle JM, Brodersen DE, Clemons WM, Jr., Tarry MJ, Carter AP, Ramakrishnan V.** 2001. Recognition of cognate transfer RNA by the 30S ribosomal subunit. Science **292:**897-902.

4. **Ogle JM, Murphy FV, Tarry MJ, Ramakrishnan V.** 2002. Selection of tRNA by the ribosome requires a transition from an open to a closed form. Cell **111:**721-732.

5. **Dahlgren A, Ryden-Aulin M.** 2000. A novel mutation in ribosomal protein S4 that affects the function of a mutated RF1. Biochimie **82:**683-691.

6. **Bjorkman J, Samuelsson P, Andersson DI, Hughes D.** 1999. Novel ribosomal mutations affecting translational accuracy, antibiotic resistance and virulence of Salmonella typhimurium. Mol Microbiol **31:**53-58.

7. **Agarwal D, Kamath D, Gregory ST, O'Connor M.** 2015. Modulation of decoding fidelity by ribosomal proteins S4 and S5. J Bacteriol **197:**1017-1025.

8. **O'Connor M.** 2015. Interactions of release factor RF3 with the translation machinery. Mol Genet Genomics **290:**1335-1344.

9. **Sun Q, Vila-Sanjurjo A, O'Connor M.** 2011. Mutations in the intersubunit bridge regions of 16S rRNA affect decoding and subunit-subunit interactions on the 70S ribosome. Nucleic Acids Res **39:**3321-3330.

10. **Datsenko KA, Wanner BL.** 2000. One-step inactivation of chromosomal genes in Escherichia coli K-12 using PCR products. Proc Natl Acad Sci U S A **97:**6640-6645.

11. **Delcuve G, Cabezon T, Herzog A, Cannon M, Bollen A.** 1978. Resistance to the aminoglycoside antibiotic neamine in Escherichia coli. A new mutant whose NeaR phenotype results from the cumulative effects of two distinct mutations. Biochem J **174:**1-7.

12. **Qin D, Fredrick K.** 2013. Analysis of polysomes from bacteria. Methods Enzymol **530:**159-172.

13. **Wachi M, Umitsuki G, Shimizu M, Takada A, Nagai K.** 1999. Escherichia coli cafA gene encodes a novel RNase, designated as RNase G, involved in processing of the 5' end of 16S rRNA. Biochem Biophys Res Commun **259:**483-488.

14. **Harvey RJ, Koch AL.** 1980. How partially inhibitory concentrations of chloramphenicol affect the growth of Escherichia coli. Antimicrob Agents Chemother **18:**323-337.

15. **O'Connor M, Thomas CL, Zimmermann RA, Dahlberg AE.** 1997. Decoding fidelity at the ribosomal A and P sites: influence of mutations in three different regions of the decoding domain in 16S rRNA. Nucleic Acids Res **25:**1185-1193.

16. **Ban N, Nissen P, Hansen J, Moore PB, Steitz TA.** 2000. The complete atomic structure of the large ribosomal subunit at 2.4 A resolution. Science (New York, NY) **289:**905:920.

17. **Tapio S, Isaksson LA.** 1990. Antisuppression by mutations in elongation factor Tu. Eur J Biochem **188:**339-346.

18. **Green M, Kurland CG.** 1971. Mutant ribosomal protein with defective RNA binding site. Nat New Biol **234:**273-275.

19. **Vallabhaneni H, Farabaugh PJ.** 2009. Accuracy modulating mutations of the ribosomal protein S4-S5 interface do not necessarily destabilize the rps4-rps5 protein-protein interaction. RNA **15:**1100-1109.

20. **P.N. Allen, Noller HF.** 1989. Mutations in ribosomal proteins S4 and S12 influence the higher order structure of 16S ribosomal RNA. J Mol Biol **208:**457-468.

21. **Olsson MO, Isaksson LA.** 1979. Analysis of rpsD mutations in Escherichia coli. III. Effects of rpsD mutations on expression of some ribosomal protein genes. Mol Gen Genet **169:**271-278.

4.6 Supplemental Information

Table S4.1 Oligoneucleotide used in chapter 4

Oligo name	Oligo sequence (5` - 3`)	Application
rpsD-drug 5’	GTCCAGGCCGCGAATCTACT	To amplify S4 gene
rpsD-drug 3’	ACGCTCTAAAGGCTCAAGGG	To amplify S4 gene
S17deletion 5’	CGCGATGTCGCACGCGTTAAGACTT TACTGAACGAGAAGGCGGGTGCGT ATGTAGGCTGGAGCTGCTTCG	For deletion of *rpsQ* (S17) using recombineering
S17deletion 3’	TAAACGGCTCATTTCTGAGCCGTTT ATTCGTATTGAGAGAGTGTACTGTA CATATGAATATCCTCCTTAG	For deletion of *rpsQ* (S17) using recombineering
S17 insertion 5’	AGACTAAATCCTGGACGCTGGTTCG CGTTGTAGAGAAAGCGGTTCTGTA ATGTAGGCTGGAGCTGCTTCG	For insertion of antibiotic cassette 3’ of *rpsQ* (S17) using recombineering
S17PCRfrwd	TGCGTGAGCAGTTCAACCTGCG	To amplify S17 gene
S17PCRrev	ATAACACCGCTTCAAGGATATGG	To amplify S17 gene
S17seq1	GCAAGTGGCCAGCTGCAACAG	To sequence S17 gene
PrimerD125’	TTGATGCTGGTGGAAGGTAC	For reconstruction of D12 to get rid of S17 mutation (E62K)

Oligo name	Oligo sequence (5` - 3`)	Application
PrimerD1215’	GGCTGGAAGTGGTGGAAGGTAC	For reconstruction of D12-1 to get rid of S17 mutation (E62K)
PrimerD1225’	GTGAAAAGCCACCTGGCTGGAAGT TGATGCTGGTGGAAGGTAC	For reconstruction of D12-2 to get rid of S17 mutation (E62K)
PrimerD1235’	AAGTTGATGCGGTGGAAGGTAC	For reconstruction of D1-3 to get rid of S17 mutation (E62K)
PrimerD1245’	GAGCAGCGTGAAAGCCAACCTGGC TGGAAGTTGATGCTGGTGGAAGGT AC	For reconstruction of D12-4 to get rid of S17 mutation (E62K)
PrimerD12135’	TTGATGCTGGTGGAAGGTACGTTAA GCGTAA	For reconstruction of D12-13 to get rid S17 mutation (E62K)

CHAPTER 5

INDIRECT INTERACTIONS OF S4 AND S5 RIBOSOMAL PROTEINS AFFECTING TRANSLATIONAL FIDELITY

5.1 Abstract

The fidelity of bacterial translation is maintained by the coordinated efforts from a wide array of bacterial components. Identification of genes and proteins involved in maintaining the accuracy of bacterial strains can be obtained by mapping compensatory mutations that can either improve the fitness of the slow growing mutant strain or change the accuracy phenotype. Here, we obtained secondary mutations that could reverse the accuracy phenotype of either error-prone or error-restrictive S4 mutant strains. The accuracy phenotype of an error-restrictive S4 G86C could be reversed directly by alterations in *rpsL* or indirectly by *tusB* encoding TusB (a tRNA modification enzyme), whereas error-prone phenotype of S4 I199N could be revered indirectly by *gltB* gene encoding glutamate synthase. Thus, translational fidelity is not only affected by alteration in the ribosomal proteins, but is also affected indirectly by other genes that affect tRNA modification or amino acid pools.

5.2 Introduction

The bacterial translation process is not only critical in maintaining the fitness of the bacteria but is also a highly energetically expensive process for the cell (1). Although bacterial translation is stringently regulated, mutations in the components of the translational machinery or chemicals can affect fidelity of translation accuracy. These alterations and perturbations however, do give insights into the workings of the bacterial ribosomes and the elongation cycle (2, 3).

tRNA selection is influenced by proteins S4, S5, S12 and 16S rRNA in the decoding center (4, 5). Recent genetic studies also indicate a role for r-proteins residues away from the decoding center that can affect the accuracy phenotype (6). Ribosomal proteins S4 and S5 were initially identified as *ram* mutant proteins that could reverse the error-restrictive phenotype of *rpsL* alterations (7). Primary mutations can influence the type of secondary compensatory mutations that restore the bacterial fitness (8, 9). Genetic selections can aid in identifying a wide array of secondary mutations and provide insights into the other regions of the ribosome that may indirectly affect accuracy (10).

We wanted identify secondary suppressor mutations that can either reverse the accuracy phenotype or improve fitness of some of the novel S4 and S5 mutants recently isolated in our lab (11). We mapped a secondary mutation that arose in an error-restrictive S4 I199N strain, which was originally error-prone. We also identified secondary mutations that reversed the error-restrictive phenotype of S4 G86C. Interestingly, we not only obtained an alteration in *rpsL,* but also identified the *gltB* and *tusB* genes indirectly affecting accuracy.

5.3 Materials and Methods

5.3.1 Transposition and Isolation of Tn10 Linked to Suppressors

Overnight cultures of the strain containing the original mutation and the suppressor (i.e donor bacteria) were grown to a mid-log phase in LB containing 10% maltose at 37˚C. These cells were concentrated by centrifugation and resuspended into 1/10 volume of LB containing 0.01M $MgSO_4$. A Tn10kan containing phage λNK1316 at MOI of 0.1-1 phage/cell was allowed to adsorb on the donor bacterial cells for 15 mins at 37˚C without aeration. This mix was diluted with 1ml of LB and incubated for 90 mins at 37˚C to allow expression of kanamycin resistance. The infected cell mix was then plated on LB-kanamycin (25 μg/ml) and incubated overnight at 42˚C to inactivate temperature sensitive λ CI repressor and thereby prevent formation of lysogens. After overnight incubation, plates showing kanamycin resistant colonies were scraped off, pooled, diluted 1:10 times and used for preparation of P1 lysates.

P1 lysates were prepared from the kanamycin resistant colonies obtained after transposition containing independent transpositions of Tn10 at various regions in the chromosome. A recipient strain (suppressor free) was transduced with this P1 lysate and kanamycin resistant transductants showing a suppressor phenotype were selected and purified.

Linkage of the transposon to the suppressor was determined by using kanamycin resistant transductants showing a suppressor phenotype as donors and transducing them in suppressor free recipient cells. The linkage was determined by the co-transduction frequency which is the ratio of transductants that co-inherited both markers (Tn10kan and suppressor phenotype) divided by total number of kanamycin resistant transductants. Kanamycin

resistant colonies were selected, purified and were used for further experiments designed to identify the transposon insertion location (12-14). The above method is summarized in Figure 5.1.

5.3.2 Identification of Genomic Location of Tn10Kan Cassette Insertion and Gene Analysis

Transposon insertion locations were determined by one or more of the procedures described below.

Arbitrary PCR: Location determination of the insertion was initially attempted by rapid inverse PCR (14). As the rapid inverse PCR was not successful we used the arbitrary PCR method. This method employs two rounds of amplification using a pair of separate primers for each cycle. Briefly, chromosomal DNA containing Tn10kan insertion was amplified at low annealing temperature using a primer unique to one end of the Tn10 transposon elements in combination with an arbitrary primer (ARB1) that can hybridize to an arbitrary sequence (NNNNNNN) and has a 5'GC clamp. The products of this amplification were used as templates for a second round of PCR using a nested transposon specific primer in combination with the arbitrary primer (ARB2) containing 5' region identical to the 5'end of ARB1. The amplified fragment was purified and sequenced. The gene amplified was identified by using NCBI BLAST (15).

Cloning: Chromosomal DNA containing Tn10kan was digested with restriction enzymes and ligated to plasmid pTZ18U or pTZ19U digested with the same restriction enzyme. The ligated mixture was transformed into host bacteria. Selection was initially based on the suppressor phenotype conferred by the plasmid and ampicillin resistance

followed by selection of kanamycin resistant colonies. The colonies were purified and sequenced using plasmid specific universal primers (16).

Complementation: EcoRI and HindIII generated genomic libraries prepared on a wild-type *E.coli* strain were used to transform suppressor Tn10 kanamycin strains and plated on LB-ampicillin (100 μg/ml). Ampicillin resistant colonies were selected and purified based on their ability to reverse the phenotype contributed by the suppressor. The plasmid DNA from the selected colonies was sent for sequencing after amplification using plasmid specific universal primers (16).

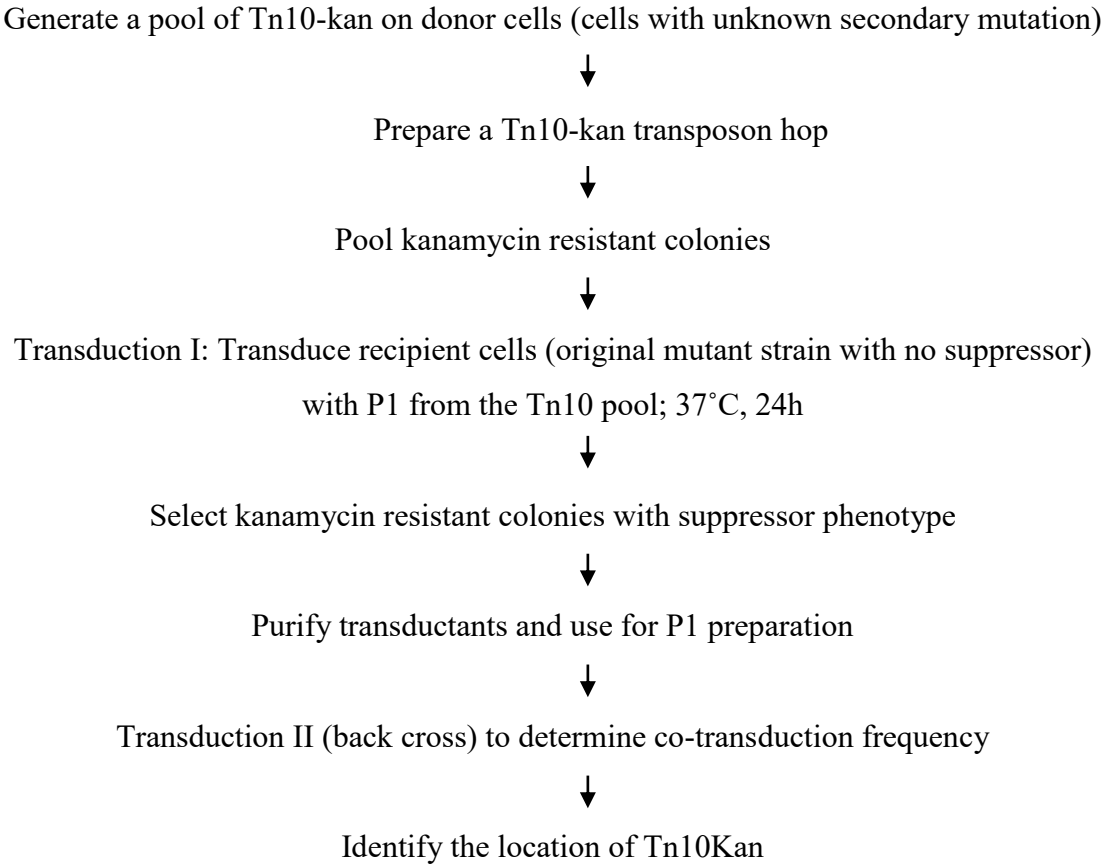

Figure 5.1 Transposition and isolation of Tn10 linked to suppressors. A pool of Tn10kan transposon hop on donor cell (cells with unknown secondary mutation) was transduced into the recipient cells (cells with original mutation) to select for Tn10kan linked transductants. A second transduction was carried out to determine the linkage of Tn10kan to the unknown secondary mutation. Identification was carried out using arbitrary PCR, cloning and complementation with genomic library.

5.4 Results

5.4.1 Isolation of Secondary Mutation in an Error-prone Mutant Strain

The *rpsD* mutation generating an I199N substitution was identified as an error-prone mutant strain, obtained by mutagenesis of the *rpsD* gene in *E.coli* MC323 (details in chapter 2). Unexpectedly, after reconstruction using P1-mediated transduction, it showed an error-restrictive phenotype in the *lacZ* miscoding assay using pLG ¾ UGA plasmid, indicating the presence of additional mutations in the genome. The error-restrictive secondary mutation was designated hypo sixteen suppressor (*hss*) and the genes encoding r-proteins known to affect accuracy (S5, S12, S17, L6, L7/L12, L14, and L19) were sequenced. As none of the genes sequenced showed any alteration, Tn10 transposon mapping was used to identify the unknown secondary mutation. Table 5.1 describes the strains used during this project

Table 5.1 Characteristics of the strains used for isolation of secondary mutation in an error-prone mutant strain

Strain	Characteristics
S4 I199N	S4 containing I199N substitution; Error-prone
Hss	Strain containing I199N and unknown secondary mutation (*hss)*; Error-restrictive
JW3179	*gltB::kan*
JW3180	*gltD::kan*
JW3181	*gltF::kan*

The kanamycin cassette from *hss* was removed by transient expression of the Flp recombinase. The *rpsD* mutation was sequenced to confirm presence of the I199N mutation and the error-restrictive phenotype was confirmed using the *lacZ* assay.

Transposon mapping was carried out as described to identify the location of the unknown secondary mutation (suppressor). *Hss* was used as the donor cell and MC323 *rpsD* I199N and MC323 *rpsD* wild type as the recipient cells. Kanamycin resistant transductants showing an error-restrictive (pale blue color) phenotype on LB-X-Gal-IPTG were selected and purified. P1 lysates prepared on the selected pale blue colored transductants were used to transduce the recipient strains to determine the co-transduction frequency. The *hss* gene was determined to be 85% co-transducible. The HssTn10kan and S4 I199N were then transferred in MC41 strain by P1-mediated transduction, to quantify miscoding using the pSG ¾ UGA *lacZ* reporter plasmid. Hss Tn10kan showed an error-restrictive phenotype whereas *rpsD* I199N showed an error-prone phenotype when compared to MC41 wild type. This was used as a confirmatory test to determine the presence of the suppressor mutation in Hss Tn10kan.

The location of the Tn10kan insertion site in *hss* was determined using three different methods. (i) Arbitrary PCR was performed using Hss chromosomal DNA as the template. (ii) Gene linked to the Tn10kan cassette was cloned into plasmid pTZ18U. (iii) Complementation studies using *E.coli* plasmid EcoRI and HindIII genomic libraries. In the plasmid complementation experiment, ampicillin resistant colonies that restored the phenotype from restrictive to *ram* (pale blue to dark blue) were selected, purified and sequenced (Figure 5.2). The sequences were tested for similarity using the Basic Local Alignment Search Tool (BLAST) program. The first two methods did not yield a definite

identity. The gene fragment in the plasmid library that restored the error-restrictive phenotype of S4 I199N was determined to be part of the *gltB* (glutamate synthase large subunit). Figure 5.3 summarizes the process of isolation of the secondary mutation in Hss.

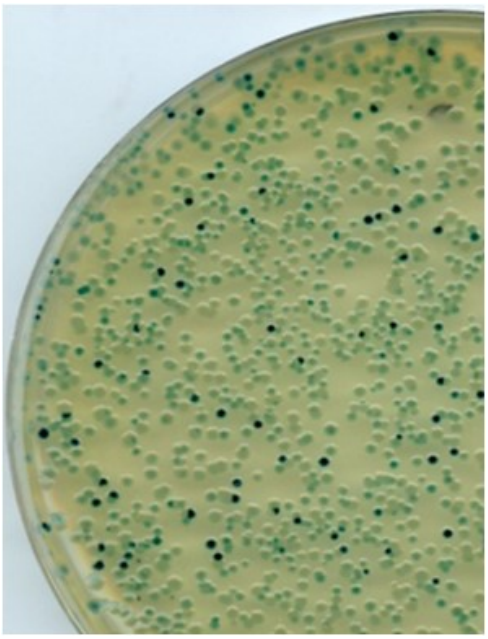

Figure 5.2 Complementation experiment using *E.coli* genomic libraries. Hss Tn10 was transformed with an *E.coli* wild-type genomic library. Colonies showing error-prone (dark blue) phenotype should have a wild-type copy of the *hss* gene as it restores the error-prone phenotype of S4 I199N.

The *gltB* gene encodes for glutamate synthase enzyme that catalyzes the formation of two glutamate molecules from glutamine and α-ketoglutarate (17). Sequencing of the *gltB* encoding gene showed wild type sequence hinting probable affect on expression of *gltB,* due to effect on transcription factors or promoter activation, causing indirect affect on accuracy.

The *gltB* gene is part of the *gltBDF* operon that codes for the large subunit (*gltB*) and the small (*gltD*) subunit of the glutamate synthase enzyme. *gltF* is considered to play a role in regulation of the operon (17). We obtained *gltB::kan*, *gltD::kan* and *gltF::kan* strains

from the *E.coli* stock center. P1 lysates from each of the gene deletions were used to transduce *rpsD* I199N and selected on LB-kan-X-Gal-IPTG. A change in the *rpsD* I199N error-prone phenotype to error-restrictive phenotype would indicate that *gltBDF* operon affects accuracy by unknown mechanisms. Since we obtained very few transductants we could not conclusively determine if the *gltBDF* operon had any effect on accuracy. *gltB* may indirectly influence accuracy by affecting the amino acid pool in the bacteria.

MC323 *rpsD* I199N (error-prone); isolated in the S4-S5 project (chapter 2)

↓

Reconstruction by P1-mediated transduction gave *rpsD hss* (error-restrictive)

↓

No second-site mutation in genes encoding for S5, S12, S17, L6, L7/L12, L14, and L19

↓

Generate *hss* linked to Tn10kan

↓

Back cross to determine co-transduction frequency

Hss is 85% co-transducible

↓

Identify the location of transposition

↓

i) Arbitrary PCR	ii) Cloning	iii) Complementation
-Template used: Chromosomal DNA from Hss	-Digested plasmid pTZ18U and chromosomal DNA -Ligated -Transformed MC323 -Selected KanR and AmpR -Amplified and sequenced using plasmid universal primers.	Transformed Hss using plasmid genomic libraries generated by HindIII and EcoRI -Selected colonies that showed restoration of error-prone phenotype from error-restrictive phenotype -Amplified and sequenced using plasmid universal primers
Gene identified: None	Gene identified: None	Gene identified: *gltB*

Figure 5.3 Isolation and identification of unknown secondary mutation in Hss. Reconstruction of S4 I199N (error-prone) unexpectedly gave a error-restrictive mutant strain Hss. Tn10kan transposon mapping was carried out to identify *hss.*

5.4.2 Isolation of Secondary Mutations in an Error-restrictive Strain

The *rpsD* mutation generating G86C substitution was obtained by mutagenesis of *rpsD* gene in *E.coli* MC323 (details in chapter 2). S4 G86C is an error-restrictive strain that was used to determine if the restriction of misreading can be reversed by additional ribosomal mutation. MC279 (leu UGA), a leu^- strain that grows in absence of leucine due to a leaky UGA mutation, was transduced with a P1 lysate carrying the *rpsD* G86C mutation linked to a kanamycin cassette and kanamycin resistant transductants were selected on LB-kanamycin (25 µg/ml). The kanamycin resistant transductants were purified and tested for growth on minimal medium (MM) in presence and absence of leucine. The leu^- phenotype is expected for error-restrictive mutations such as S4 G86C that restrict near cognate UGA decoding. The transductants that did not show any growth in absence of leucine were incubated for 7 days at 37˚C to obtain strains with compensatory mutations (suppressors). A total of 12 colonies (suppressors) obtained after 7 days were retested for their ability to grow in absence of leucine and were sequenced to confirm the presence of the *rpsD* G86C alteration. Three of the 12 suppressors were tested for miscoding using the *lacZ* plasmid p34-11 UGA. MC323 S4 G86C and MC279 wild-type were also tested simultaneously. The three suppressors tested showed an error-prone phenotype, while S4 G86C showed error-restrictive phenotype compared to the wild type. The three suppressor strains selected were designated as Sup1, Sup2 and Sup3. The identification of the second site suppressor was initially carried out by sequencing genes known to contribute to the accuracy process (S5, S12, S17, L6, L7/L12, L14, and L19). The genes encoding for $tRNA^{trp}$ and RF1 were also sequenced as alterations in $tRNA^{trp}$ and RF1 mutation can affect the leakiness of the UGA codon. Sup1 showed an E61K alteration in *rpsL* gene encoding r-protein S12 whereas Sup2

and Sup3 had no alteration in any of the genes sequenced. We carried out Tn10 transposon mapping to narrow down the location of the secondary mutation in Sup2 and Sup3. Table 5.2 describes the strains used and their characteristics.

Table 5.2 Characteristics of the strains used for isolation of secondary mutation in an error-restrictive mutant strain

Strain	Characteristics
S4 G86C	S4 containing G86C substitution; Error-restrictive
Sup1	S4 containing G86C substitution and S12 E62K substitution; Error-prone
Sup2	S4 containing G86C substitution and an unknown secondary mutation (*sup2)*; Error-prone
Sup3	S4 containing G86C substitution and an unknown secondary mutation (*sup3)*; Error-prone
JW3305	*tusB::kan*

Tn10 transposon mapping was carried out as described using Sup2 and Sup3 as donor cells and kanamycin sensitive MC323 S4 G86C and MC323 wild-type as recipient cells. Kanamycin resistant transductants showing an error-prone phenotype on LB-kan-IPTG-X-gal plates were selected and purified. The co-transduction frequency was tested by using P1 from the lysates of error-prone kanamycin resistant colonies and was determined to be 95% for *sup2* and 94% for *sup3*.

The location of the Tn10kan insertion site in Sup2 and Sup3 was determined using three different methods. (i) Arbitrary PCR was performed as described in the methods using chromosomal DNA of Sup2 and Sup3 as the template. (ii) By cloning the kanamycin linked gene in plasmid pTZ18U plasmid (iii) Complementation using a wild type *E.coli* genomic plasmid library generated using EcoRI and HindIII. In the plasmid complementation experiment, ampicillin resistant colonies that restored the phenotype from error-prone to error-restrictive (dark blue to pale blue) were selected, purified and sequenced using universal plasmid primers. The BLAST program was used to determine the identity of the sequences obtained from the three methods used. The first two methods did not yield any conclusive results on identification of the genes. Identification of the gene fragment of the plasmid genomic library that restored the error-prone phenotype of S4 G86C suggested that sup2 was near *prfA* (encoding RF1) while the sup3 complementing plasmid clone carried the *tusB* gene (encoding tRNA 2- ThioUridine synthesizing protein). Figure 5.5 summarizes the isolation of the unknown secondary mutation in Sup2 and Sup3.

The *prfA* gene encoding RF1 did not show any alterations in Sup2 and Sup3 strains, indicating that the expression of *prfA* might be affected leading to change in the accuracy phenotype or that another (unidentified) adjacent gene is affected in these strains. *tusB* is part of the *tusDCB* operon, which mediates the sulfur transfer from TusA to TusE. Proteins encoded by genes in this operon *tusABCDE* are involved in the mnm_5S_2U modification of tRNA (18). *tusABCDE* operon mutants are known to be sensitive to hydroxyurea, which is a known DNA replication inhibitor (19). Therefore, we tested Sup1, Sup2 and Sup3 for sensitivity to hydroxyurea along with MC323 wild type, MC323 S4 G86C and MC279. We found that MC323 S4 G86C along with Sup1, Sup2 and Sup3 show some degree of

sensitivity to 7.5 μM hydroxyurea (Figure 5.4). The original error-restrictive S4 G86C and the 3 error-prone suppressor strains show similar degrees of sensitivity to hydroxyurea, indicating the G86C alteration present in the 3 error-prone suppressor strains may be responsible for hydroxyurea sensitivity. To confirm that the error-prone phenotype of sup3 was due to a mutation in tusB, we obtained Δ*tusB::kan* strains from the *E.coli* stock center. P1 lysates from the gene deletion were used to transduce MC323 S4 G86C and the transductants were selected on LB-X-Gal-IPTG. A change in the S4 G86C accuracy phenotype from error-restrictive to error-prone indicates that *tusB* may be the identity of the secondary mutation in sup3.

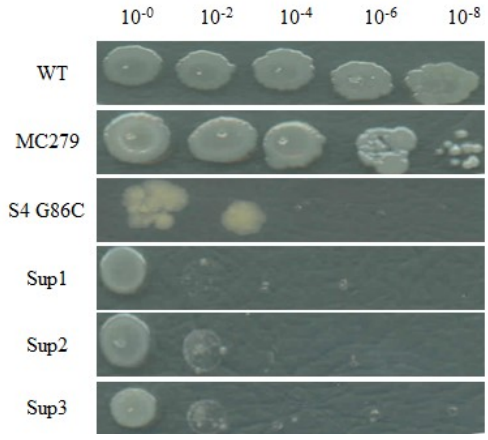

Figure 5.4 Hydroxyurea sensitivity testing. *tusB* genes are known to confer hydroxyurea sensitivity. We tested the sensitivity of the suppressor strains to 7.5 μM hydroxyurea to determine if *tusB* is altered in Sup2 and Sup3.

rpsD G86C (error-restrictive); isolated in the S4-S5 project (chapter 2)

↓

Transduce MC279 (leu UGA; leaky for leu) with P1 containing *rpsD* G86C

↓

Select kanamycin resistant, non-leaky leu^- transductants (no growth on MM without leucine)

↓

Incubate at 37˚C for 7 days to obtain leu^+ suppressors

↓

Purify and perform *lacZ* accuracy assay: Sup1, Sup2, Sup3 (ram; leu^+)

↓

No second-site mutation in S5, S12, S17, L6, L7/L12, L14, L19, tRNAtrp and RF1 for Sup2 and Sup3; *rpsL* E61K alteration in Sup1

↓

Generate *sup2* and *sup3* linked to Tn10kan

↓

Back cross to determine co-transduction frequency

sup2 and *sup3* are 95% and 94% co-transducible respectively

↓

Identify the location of transposition

↓

i) Arbitrary PCR	ii) Cloning	iii) Complementation
-Template used: Chromosomal DNA from Sup2 and Sup3	-Digested plasmid pTZ18U and chromosomal DNA -Ligated -Transformed MC323 -Selected KanR and AmpR -Amplified and sequences using plasmid universal primers.	Transformed sup2 and sup3 using plasmid genomic libraries generated by HindIII and EcoRI -Selected colonies that showed restoration of error-prone phenotype from error-restrictive phenotype -Amplified and sequences using plasmid universal primers
Gene identified: None	Gene identified: None	Gene identified: near *prfA* for *sup2* and *tusB* for *sup3*

Figure 5.5 Isolation and identification of unknown secondary mutation in Sup2 and Sup3. Leu^+ strains containing unknown secondary mutations that revere the error-restrictive phenotype of S4 G86C were designated Sup1, Sup2, and Sup3. *rpsL* E61K was identified as the secondary mutation in Sup1. Tn10kan transposon mapping was carried out to identify the unknown secondary mutation.

5.4.3 Isolation of Secondary Mutations that Increases Fitness/Experimental Evolution

Two mutant strains, one S4 and one S5 that showed reduced growth at either 20˚C or 42˚C were selected from the S4-S5 project (chapter 2) to obtain secondary mutations that can improve the fitness of these strains. MC323 S4-kan R69P showed reduced growth at both the temperatures whereas MC323 S5-kan L80Q showed reduced growth at 20˚C. The two mutant strains were subcultured at 37˚C for 10 consecutive days and each overnight culture was streaked on LB-kan and incubated at three different temperatures (20˚C, 37˚C,

and 42˚C), along with control strains that were not subcultured. A final count of 12 revertants from S4 R69P and 7 from the S5 L80Q were obtained, of which 8 from S4 and 10 from S5 were sequenced to detect the presence of the original S4 or S5 mutations (Figure 5.6). Three mutants from S4 and four from S5 had the original mutation, whereas rest of the strains gave wild type S4 or S5 sequences. One revertant strain obtained from S4, designated as Evo4 and one from S5 designated as Evo5 were pursued further. Evo4 and Evo5 were sequenced for alteration in known accuracy altering genes (S4/S5, S12, S17, L6, L7/L12, L14, and L19). As none of the known genes showed any alteration, we carried out Tn10 transposon mapping to narrow down the location of the secondary mutation. Table 5.3 describes the strains used and their characteristics.

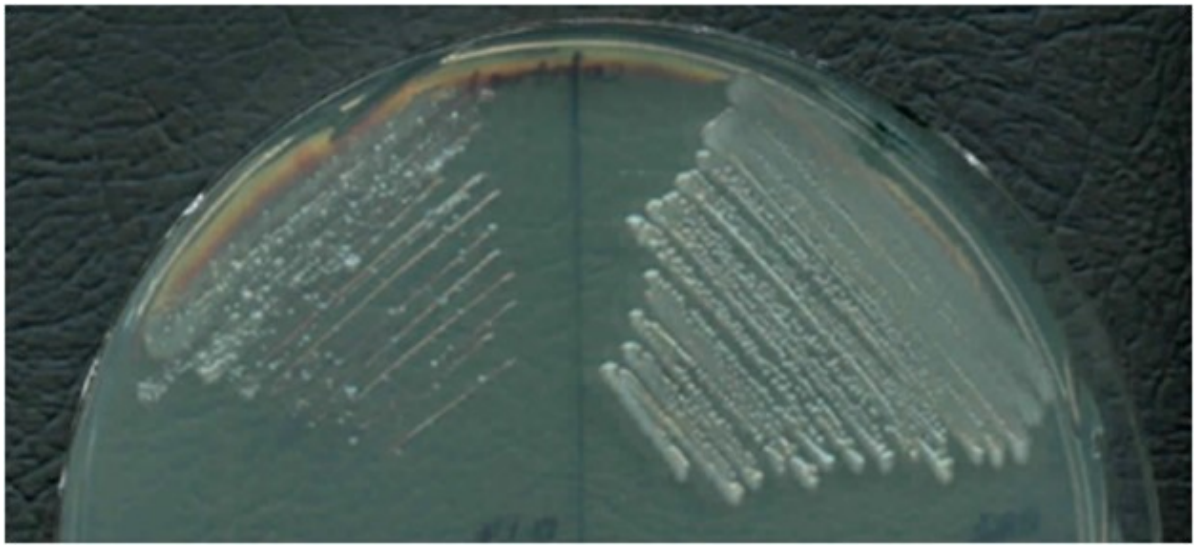

Figure 5.6 Isolation of suppressor of cold sensitivity. S5 L80Q shows reduced growth at 20˚C. By carrying out experimental evolution we obtained suppressor colonies (left) that could grow at 20˚C. Wild type MC323 (right) for comparison of growth at 20˚C

Table 5.3 Characteristics of the strains used for isolation of secondary mutations that increase the fitness of the selected mutant strain

Strain	Characteristics
S4 R69P	S4 containing R69P substitution; reduced growth at 20˚C and 42˚C
S5 L80Q	S5 containing L80Q substitution; reduced growth at 42˚C
Evo4	S4 containing R69P and unknown secondary mutation, better growth at 20˚C and 42˚C compared to S4 R69P
Evo5	S5 containing L80Q and an unknown secondary mutation, better growth at 42˚C compared to S5 L80Q

Tn10 transposon mapping was carried out as described in the methods section using Evo4 and Evo5 as donor cells and kanamycin sensitive MC323 S4 R69P and S5 L80Q as recipient cells respectively. Kanamycin resistant transductants showing improved growth at 20˚C for Evo4 transductions and improved growth at 42˚C for Evo5 transductions were selected and purified. P1 from the lysates of these transductants were transduced onto the recipient strains to test the co-transduction frequency. *evo4* and *evo5* genes were determined to be 93% and 96% co-transducible.

The location of the Tn10kan insertion in Evo4 and Evo5 was determined using following three methods. (i) Arbitrary PCR was performed as described using chromosomal DNA from Evo4 and Evo5 as the template. (ii) The kanamycin cassette linked gene was cloned in pTZ18U. (iii) Complementation using *E.coli* genomic library generated using EcoRI and HindIII. The transformants showing improved fitness were selected, purified, amplified and sequenced using plasmid universal primers (supplemental Table S5.1). The

identity of the sequences was determined using BLAST program. None of the sequences obtained from the aforementioned methods yielded a definite identity. The growth defect used to differentiating the original strain and the suppressor containing strain was subtle and insufficient to be used for mapping and hence these mutants were not pursued further. Figure 5.7 summarizes the description of the methods and results for isolation of secondary mutations that increase fitness.

MC323 *rpsD* R69P (reduced growth at 20˚C/42˚C) & *rpsE* L80Q (reduced growth at 42˚C);
Isolated in the S4-S5 project (chapter 2)

↓

Subculture for 10 consecutive days at 37˚C

↓

Streak out colonies from each overnight culture, along with non-subcultured strains as control and incubate at 20˚C, 37˚C and 42˚C

↓

Select kanamycin resistant colonies with improved fitness (S4 R69P that grows better at 20˚C and 42˚C; S5 L80Q that grows better at 20˚C)

↓

No second-site mutation in genes encoding S4/S5, S12, S17, L6, L7/L12, L14, and L19

↓

Generate *evo4* and *evo5* linked to Tn10kan

↓

Back cross to determine co-transduction frequency
evo4 and *evo5* are 93% and 96% co-transducible

↓

Identify the location of transposition

i) Arbitrary PCR	ii) Cloning	iii) Complementation
-Template used: chromosomal DNA from Evo4 and Evo5	-Digested plasmid pTZ18U and chromosomal DNA, -Ligate -Transformed MC323 -Selected KanR and AmpR -Amplified and sequences using plasmid universal primers.	Transformed Evo4 and Evo5 using plasmid genomic libraries generated by HindIII and EcoRI -Selected colonies that showed improved fitness -Amplified and sequences using plasmid universal primers
Gene identified: None	Gene identified: None	Gene identified: None

Figure 5.7 Isolation and identification of unknown secondary mutation in Evo4 and Evo5. Tn10kan transposon mapping was carried out to identify the unknown secondary mutation that conferred improved fitness.

5. 5 Discussion

Ribosomes undergo complex conformational changes during the translation process as a means of communication between the distant functional sites. This communication between different function sites of the ribosome facilitates the next steps of translation. During the elongation cycle the proteins S4, S5, and S12 play a role in transition of the open to closed conformation of the 30S subunit on recognition of the cognate aa-tRNA. Domain closure then leads to GTP hydrolysis and peptide bond formation (4, 5). S4, S5, and S12 along with the 16S rRNA contribute residues to the decoding center that determine the correctness of the codon-anticodon interactions (20).

Recent structural and genetic studies have shown that apart from the contributions of S4, S5, S12, and 16S rRNA, other regions of the ribosome also can influence translational accuracy directly or indirectly (2, 6, 21, 22). In order to explore the interactions of S4 and S5 with other regions of the ribosome we looked to obtain compensatory mutation that could restore or change the accuracy phenotype of the mutant strain.

We mapped compensatory mutation in strains derived from S4 I199N (error-prone) and S4 G86C (error-restrictive) mutants that displayed different accuracy phenotypes compared to the original strains. Of the 4 suppressor strains we studied we identified an *rpsL* alteration in one strain, and *tusB* and *gltB* in other two strains.

S12 encoded by *rpsL* gene was identified as the secondary mutation that resulted in a change from an error-restrictive phenotype of S4 G86C to error-prone. The S12 alteration was determined to be E61K. This alterations is unique in that it was not previously identified by classical genetics or present among the 40 different accuracy-altering S12 mutations by recombineering methods (23). Although we have not reconstructed and characterized this

alteration, it would be interesting to determine it accuracy phenotype and the effect it can have on its own and on other S4 alterations.

The other secondary mutation (error-prone) mapped in the suppressor strain obtained from S4 G86C (error-restrictive) was identified to be the *tusB* gene, part of the *tusBCD* operon. TusB is required for 2-thiolation of 5-methlyaminomethly-2-thiouridine (mnm_2S_2U) at wobble positions in the tRNA, required for strong codon-anticodon pairing interactions, accurate decoding and normal cell growth (18). *tusABCDE* are all important in the 2-thio modification. In *E.coli* the 2-thio modification of mnm_5S_2U confers efficient ribosome binding for $tRNA^{Lys}$ by stabilizing the weak A-U, G-U base interactions at the wobble positions. It aids in recognition of glutamine-tRNA synthetase in $tRNA^{Glu}$ (24) and enhances binding of $tRNA^{Gln}$ and $tRNA^{Arg}$ (25). Thus mutation in *tusB* gene or alteration in expression could enhance near-cognate codon recognition at wobble position and thereby increase miscoding.

In *E.coli,* mnm_5S_2U hypomodification in $tRNA^{Glu}$, $tRNA^{Lys}$ and/or $tRNA^{Gln}$ can suppress the temperature sensitive phenotype of RF1 mutant strains (26). Mutations in the genes that are important for thio modification of tRNA were shown to confer sensitivity to hydroxyurea. Sensitivity to hydroxyurea is speculated to occur due to repression of RNR (Ribonucleotide reductase) enzyme that catalyzes the formation of deoxyribonucleotides from ribonucleotides and effect the intracellular redox state and translation indirectly (19).

During the reconstruction of S4 I199N (error-prone) we unexpectedly isolated an error-restrictive strain containing a secondary suppressor mutation. The gene responsible for the error-restrictive phenotype was identified as *gltB,* part of the *gltBDF* operon. Sequencing of *gltB* did not show any alteration, indicating regions outside the coding region of the gene

may be affected. *E.coli* derives its nitrogen atom for its nitrogenous compounds mainly from glutamate. Glutamate synthase encoded by the *gltB* gene transfers amino group from glutamate to α-keto acid to form a corresponding amino acid and α-ketoglutarate (27). *gltB* mutants in *E.coli* are unable to utilize substrates such as arginine or proline as nitrogen substrates (28). Mutations in the *gltB* gene or alteration in expression may therefore directly or indirectly affect the amino acid pool. Insufficient availability of the amino acids can prolong the elongation and thereby affect the translation process.

By employing experimental evolution methods, we identified genes that may be influencing the accuracy phenotype of S4 mutants. The unexpected results obtained indicate that interactions of the mutant S4 protein with can be reversed by genes affecting not just ribosomal components (*rpsL)* but also indirectly by genes involved in maintaining the amino acids pools and tRNA modifications. Apart from the suppressors tested we have a collection of other uncharacterized stains with unmapped secondary mutations. These suppressor strains can be initially tested for alterations in the genes determined in this work or can be subjected to genomic sequencing in near future.

5.6 References

1. **Reynolds NM, Lazazzera BA, Ibba M.** 2010. Cellular mechanisms that control mistranslation. Nat Rev Microbiol **8:**849-856.

2. **VanNice J, Gregory ST, Kamath D, O'Connor M.** 2016. Alterations in ribosomal protein L19 that decrease the fidelity of translation. Biochimie **128-129:**122-126.

3. **Ogle JM, Murphy FV, Tarry MJ, Ramakrishnan V.** 2002. Selection of tRNA by the ribosome requires a transition from an open to a closed form. Cell **111:**721-732.

4. **Ogle JM, Carter AP, Ramakrishnan V.** 2003. Insights into the decoding mechanism from recent ribosome structures. Trends in Biochemical Sciences **28:**259-266.

5. **Ogle JM, Ramakrishnan V.** 2005. Structural insights into translational fidelity. Annu Rev Biochem **74:**129-177.

6. **Kirthi N, Roy-Chaudhuri B, Kelley T, Culver GM.** 2006. A novel single amino acid change in small subunit ribosomal protein S5 has profound effects on translational fidelity. RNA **12:**2080-2091.

7. **Gorini L, Jacoby GA, Breckenridge L.** 1966. Ribosomal ambiguity. Cold Spring Harb Symp Quant Biol **31:**657-664.

8. **Hummel H, Piepersberg W, Bock A.** 1980. 30S subunit mutations relieving restriction of ribosomal misreading caused by L6 mutations. Mol Gen Genet **179:**147-153.

9. **Wilson DN.** 2014. Ribosome-targeting antibiotics and mechanisms of bacterial resistance. Nat Rev Microbiol **12:**35-48.

10. **Maisnier-Patin S, Paulander W, Pennhag A, Andersson DI.** 2007. Compensatory evolution reveals functional interactions between ribosomal proteins S12, L14 and L19. J Mol Biol **366:**207-215.

11. **Agarwal D, Kamath D, Gregory ST, O'Connor M.** 2015. Modulation of decoding fidelity by ribosomal proteins S4 and S5. J Bacteriol **197:**1017-1025.

12. **Halling SM, Simons RW, Way JC, Walsh RB, Kleckner N.** 1982. DNA sequence organization of IS10-right of Tn10 and comparison with IS10-left. Proc Natl Acad Sci U S A **79:**2608-2612.

13. **Miller JH.** 2009. A Short Course in Bacterial Genetics: A Laboratory Manual and Handbook Fo Rescherichia Coli and Related Bacteria. Cold Spring Harbor Laboratory Press.

14. **Miller J.** 1972. Experiments in molecular genetics. Cold Spring Harbor Laboratory Press.

15. **Das S, Noe JC, Paik S, Kitten T.** 2005. An improved arbitrary primed PCR method for rapid characterization of transposon insertion sites. J Microbiol Methods **63:**89-94.

16. **Singer M, Baker TA, Schnitzler G, Deischel SM, Goel M, Dove W, Jaacks KJ, Grossman AD, Erickson JW, Gross CA.** 1989. A collection of strains containing genetically linked alternating antibiotic resistance elements for genetic mapping of Escherichia coli. Microbiol Rev **53:**1-24.

17. **Castano I, Bastarrachea F, Covarrubias AA.** 1988. gltBDF operon of Escherichia coli. J Bacteriol **170:**821-827.

18. **Ikeuchi Y, Shigi N, Kato J, Nishimura A, Suzuki T.** 2006. Mechanistic insights into sulfur relay by multiple sulfur mediators involved in thiouridine biosynthesis at tRNA wobble positions. Mol Cell **21:**97-108.

19. **Nakayashiki T, Saito N, Takeuchi R, Kadokura H, Nakahigashi K, Wanner BL, Mori H.** 2013. The tRNA thiolation pathway modulates the intracellular redox state in Escherichia coli. J Bacteriol **195:**2039-2049.

20. **Gregory ST, Connetti JL, Carr JF, Jogl G, Dahlberg AE.** 2014. Phenotypic interactions among mutations in a Thermus thermophilus 16S rRNA gene detected with genetic selections and experimental evolution. J Bacteriol **196:**3776-3783.

21. **Yaguchi M, Wittmann HG, Cabezon T, De Wilde M, Villarroel R, Herzog A, Bollen A.** 1975. Cooperative control of translational fidelity by ribosomal proteins in Escherichia coli. II. Localization of amino acid replacements in proteins S5 and S12 altered in double mutants resistant to neamine. Mol Gen Genet **142:**35-43.

22. **Haft RJ, Keating DH, Schwaegler T, Schwalbach MS, Vinokur J, Tremaine M, Peters JM, Kotlajich MV, Pohlmann EL, Ong IM, Grass JA, Kiley PJ, Landick R.** 2014. Correcting direct effects of ethanol on translation and transcription machinery confers ethanol tolerance in bacteria. Proc Natl Acad Sci U S A **111:**E2576-2585.

23. **Agarwal D, Gregory ST, O'Connor M.** 2011. Error-prone and error-restrictive mutations affecting ribosomal protein S12. J Mol Biol **410:**1-9.

24. **Kurata S, Weixlbaumer A, Ohtsuki T, Shimazaki T, Wada T, Kirino Y, Takai K, Watanabe K, Ramakrishnan V, Suzuki T.** 2008. Modified uridines with C5-methylene substituents at the first position of the tRNA anticodon stabilize U.G wobble pairing during decoding. J Biol Chem **283:**18801-18811.

25. **Hou YM, Gamper H, Yang W.** 2015. Post-transcriptional modifications to tRNA--a response to the genetic code degeneracy. RNA **21:**642-644.

26. **Isak G, Ryden-Aulin M.** 2009. Hypomodification of the wobble base in tRNAGlu, tRNALys, and tRNAGln suppresses the temperature-sensitive phenotype caused by mutant release factor 1. J Bacteriol **191:**1604-1609.

27. **Goss TJ, Perez-Matos A, Bender RA.** 2001. Roles of glutamate synthase, gltBD, and gltF in nitrogen metabolism of Escherichia coli and Klebsiella aerogenes. J Bacteriol **183:**6607-6619.

28. **Reitzer LL.** 2003. Nitrogen assimilation and global regulation in Escherichia coli. Annual review of microbiology **57:**155-176.

5.7 Supplemental Information

Table S5.1 Oligoneucleotide used in chapter 5

Oligo name	Oligo sequence (5` - 3`)	Application
rpsD-drug 5’	GTCCAGGCCGCGAATCTACT	To amplify S4 gene
rpsD-drug 3’	ACGCTCTAAAGGCTCAAGGG	To amplify S4 gene
rpsEdrug3’	CTGTGGGTAAAGCTGTCGCT	To amplify S5 gene
rpsEdrug 5’	GTGACCAATACGACGCAGAC	To amplify S5 gene
S17PCRfrwd	TGCGTGAGCAGTTCAACCTGCG	To amplify S17 gene
S17PCRrev	ATAACACCGCTTCAAGGATATGG	To amplify S17 gene
rpsLmutamp5'	CAGATGCCTTACGCCGCGAAC	To amplify S12 gene
rpsLmutamp3'	GCATTACGACGAACCGGACGG	To amplify S12 gene
rplF5’PCRfrwd	TAAAGGTGTTATGACTGATCGTGCA	To amplify L6 gene
rplF3’PCRrev	CCAGAACTTCAGAACCGTTCGGTGC	To amplify L6 gene
rplL5’	GGC TGC TGT ACG CGA TGC GA	To amplify L7/L12 gene
rplL3’	GTG TGA AAC GCT ACT GGC GC	To amplify L7/L12 gene
L14PCRfrwd	CGAATAAACGGCTCAGAAATGAGC	To amplify L14 gene
L14PCRrevanti	GACAGGACATTCTTAACTTTACCGC G	To amplify L14 gene
rplS3’new	TGG CGG AGT TCA AAA CGG AA	To amplify L19 gene
rplS5’new	CGC AGT GGT GAT TAC TAC CC	To amplify L19 gene

Oligo name	Oligo sequence (5` - 3`)	Application
RF1 3’	GACTAACCGCTTCATCCATGCGCC	To amplify RF1 gene
gltBP35’	GGAAGTGGGGTTCCCGCAGA	Forward primer for GltB from start codon
gltBP33’	CACCACGTCCGGGTTGTAGG	reverse primer for GltB near stop codon
gltBP45’	CACCCATGCGATTGCCAAAG	Forward primer for GltB from seq in the center
gltBP43’	ATAAACATTCTGACTCATTG	Reverse primer for GltB near stop codon
gltBseqP15’	GGA ACT GCG TGC CTT CTT TG	5’ primer for sequencing of GltB
gltBseqP25’	CTG GCC CGA TGG TGG CGC TC	5’ primer for sequencing of GltB
gltBseqP13’	CCA GTC GGC GGA CGT TTT TC	3’ primer for sequencing of GltB
gltBseqP23'	GTC GTG AGC TGT TTG AAA TC	3’ primer for sequencing of GltB
gltBseqP33’	CAG CTC GCG GGT TTC ACG GG	3’ primer for sequencing of GltB
gltBseqP43’	GGG TTG CCG CAC GAC AGG CA	3’ primer for sequencing of GltB

Oligo name	Oligo sequence (5` - 3`)	Application
P1rightextern	TTATACCCATATAAATCAGCATCC	Arbitrary PCR primer for Tn10 kan transposon
P2rightintern	CAACTCTGGCGCATCGGGCTTCCC	Arbitrary PCR primer for Tn10 kan transposon
P1leftextern	ATGGAACTGCCTCGGTGAGTTTTC	Arbitrary PCR primer for Tn10 kan transposon
P2leftintern	AGGGGAAATTAATAGGTTGTATTG	Arbitrary PCR primer for Tn10 kan transposon
ARB1	GGCCAGGCCTGCAGATGATGNNNNNNNNNNGTAT	Arbitrary PCR primer for Tn10 kan transposon (ARB1+ARB2)
ARB2	GGCCAGGCCTGCAGATGATG	Arbitrary PCR primer for Tn10 kan transposon
ARB3	GGCCACGCGTCGACTAGTCANNNNNNNNNNAGCTG	Arbitrary PCR primer for Tn10 kan transposon (ARB3+ ARB4)
ARB4	GGCCACGCGTCGACTAGTCA	Arbitrary PCR primer for Tn10 kan transposon
Univ17merfrwd	GTAAAACGACGGCCAGT	Universal primer for plasmids
Univ16merrev	AACAGCTATGACCATG	Universal primer

Oligo name	Oligo sequence (5` - 3`)	Application
tusB5’	ACGCCGCGAACTCGCCAACT	To amplify TusB gene
tusB3’	GGACGCCGAATTTTAGGGCG	To amplify TusB gene
tusC5’	CGGAAGCCTCGCTGACCTGT	To amplify TusC gene
tusC3’	GAGCAGACGCAGCAGCGCAG	To amplify TusC gene
tusD5’	TCTCCAAACACACTGTCTAT	To amplify TusD gene
tusD3’	GCATCTAAACCTTCCCGGCC	To amplify TusD gene

CHAPTER 6

CONCLUSIONS AND FUTURE DIRECTIONS

6.1 Conclusions

The accuracy of the elongation cycle depends on the ability of the ribosomes to decode the mRNA into the corresponding amino acids. The stringency and speed with which the ribosome can select the correct cognate amino acyl-tRNAs and reject the non-cognate tRNA determines the quality and efficiency of the translation process. Accuracy can be altered by mutations not only in the proteins at the decoding center, but also by mutations in the r-RNA, other translational factors, and antibiotics.

The 30S small ribosomal subunit houses the decoding center that determines the correctness of the incoming codon-anticodon interactions, and is made up by parts of proteins S4, S5, S12, and 16S rRNA. Ribosomal proteins S4 and S5 not only participate in the decoding process but are also important in the assembly process and interactions with antibiotics. S4 is an essential primary ribosomal binding protein that binds to the 16S rRNA, initiates nucleation and subunit assembly, whereas S5 is an essential component of the small ribosomal subunit that is involved in subunit assembly, maintenance of translational fidelity and the ribosome's response to the antibiotic spectinomycin.

Intact interactions between the S4-S5 interfaces help maintain the open conformation of the 30S ribosomal subunit. Disruption of the S4-S5 interface results in a transition from an open to closed conformation (domain closure) which then leads to GTP hydrolysis and peptide bond formation. Alterations at the S4-S5 interface that facilitate domain closure,

result in an error-prone phenotype and alterations that restrict domain closure result in an error-restrictive accuracy phenotype. Most of the S4 and S5 mutations studied are found to be clustered near the S4-S5 interface and decrease the accuracy of the translation.

One of the main aims of this work was to investigate the diverse ways in which S4 and S5 proteins contribute to translational accuracy. S4 and S5 mutations previously isolated were selected as secondary mutations that reversed the error-restrictive phenotype conferred by alteration in *rpsL* and were found at the interface. To understand the range of S4 and S5 residues that can influence the decoding fidelity, we carried out random mutagenesis of genes encoding S4 and S5. We obtained a wide array of mutants that were distributed throughout the S4 (19 mutants) and S5 (13 mutants) proteins and these included novel mutations as well as mutations that have been previously reported in either *E.coli* or some other bacteria. Of the 33 mutant strains characterized only 4 showed an error-restrictive phenotype, whereas the rest of the mutant strains showed an error-prone phenotype. Although all the mutants had an altered accuracy phenotype, only a fraction of the mutations affected 16S rRNA processing and/ ribosome assembly. The altered S4 and S5 residues can be predicted to influence accuracy based on their location and interaction in the *E.coli* 70S ribosome.

1) Residues near the S4-S5 interface may affect domain closure directly.

2) Residues buried but close to the interface may affect domain closure indirectly

3) Residues away from the S4-S5 interface but near the 16S rRNA interface and may affect protein-16S rRNA interactions

4) Residues that interact with other ribosomal proteins indicate the importance of proper organization of S4 and S5 for accurate decoding.

The S4 and S5 alterations that confer 16S rRNA processing defect and/or ribosome assembly defects in this project are not preferentially located to any specific region, and can near or away from the interface.

In a continued effort to understand the influence of S4 and S5 protein, we investigated the effects of mutations in specific regions of the S4 and S5 proteins that have been previously discussed in the literature but have not been explored.

The S5 G27D mutation in the loop 2 regions of the S5 protein, is away from the S4-S5 interface, is cold-sensitive, confers spectinomycin resistance and has an error-prone phenotype. The accuracy phenotype of G27D can be explained by an altered 16S RNA 5' processing mechanism that affects ribosome conformation and therefore affects fidelity. To investigate the effect of different alterations in the loop 2 region of S5 and their role in modulation of accuracy, spectinomycin resistance, rRNA processing and ribosome assembly, we generated a collection of 21 mutants using recombineering method. Of the 21 mutants, only 2 mutations conferred an error-restrictive phenotype, whereas the rest of the mutations conferred an error-prone phenotype. Only a fraction of the mutants showed 16S rRNA processing and/or ribosome assembly defects indicating that the mechanism by which the mutations studied in this project affect accuracy is distinct from the altered 16S rRNA processing model. As these mutations are away from the interface, they do not directly influence domain closure, and hence may affect accuracy through some other unknown mechanisms.

The C-terminal region of the S4 protein was investigated in detail as the C-terminal region of S4 makes extensive contacts with S5 at the S4-S5 interface. Classical C-terminal truncation mutants D12, D14, and D16 are temperature sensitive, error-prone, and have

ribosome assembly defects. Yeast two-hybrid studies show the miscoding phenotype for these mutants is due to disruption of the S4-S5 interface. We obtained temperature insensitive mutants from D12 that restored the C-terminal region with at least one change in the amino acid sequence. Restoration of the C-terminal region rescued miscoding partially, but showed near-complete rescue of the ribosome assembly defect at higher temperatures. The restored C-terminal mutants did not show any rescue of the 16S rRNA processing defect. As S4 is a primary binding protein and initiates 30S assembly process, the absence of the C-terminal region may have hindered the ribosome subunit assembly at a higher temperature in D12 and was rescued with the restoration of the C-terminal region in the temperature insensitive mutants. Separately, comparison of D12 and D12-4 with and without S17 E62K showed that presence of E62K S17 alteration aggravated the assembly defect caused by the S4 alteration.

A previous discrepancy in the literature about two S4 protein alteration, ΔV200 and E201* was addressed in this project. The *E.coli* S4 E201* mutation isolated in the first part of this project displayed error-prone phenotype and was consistent with the domain closure model as shown in the yeast two-hybrid system using C-terminal truncated mutants. *Salmonella* E201* and ΔV200 displayed an error-restrictive phenotype and conflicted with the domain closure model. We generated both the mutants de novo in *E.coli* and *Salmonella*, and determined that the accuracy phenotype conferred by the mutations in both the bacteria was error-prone, thus agreeing with the domain closure model.

In the process of investigating the interactions of S4 and S5, not only with each other but also with other regions of the ribosome, we mapped secondary mutations that could reverse the accuracy phenotype of the mutant strain used. We isolated a *gltB* gene encoding

glutamate synthase and the *tusB* gene encoding TusB involved in thio modification of tRNA bases. Isolation of these genes shows that accuracy can be indirectly affected by genes that affect tRNA modification as well as amino acids pools.

16S rRNA is essential for assembly of the ribosomal small subunit and for decoding. Ribosome structure is important as the ribosome undergoes a series of conformational changes to maintain the stringency of tRNA selection. As 16S rRNA processing and ribosome assembly are an integral part of the decoding process, one of our aims has been to determine the correlation, if any, between accuracy, 16S rRNA processing, and ribosome assembly. From the mutants studied in this work, we do not see any strict correlation between 16S rRNA processing and ribosome assembly, or with accuracy.

6.2 Future Directions

In order to continue understanding the diverse mechanism by which of S4 and S5 interaction influence accuracy, the following experiments need be carried out.

1) Study the effect of S4 mutations on 16S rRNA binding: As S4 binds to 16S rRNA and initiates the ribosome assembly process; studying the effects of known S4 mutations will help gain insights into the binding dynamics of S4-16S rRNA

2) Study the interaction of S4-S5 with 16S rRNA: Although S5 does not directly bind to the 16S rRNA during ribosome assembly, it interacts with residues of the 16S rRNA in the 70S ribosome. Studying the effect of S4-S5 alteration on its interaction with 16S rRNA will aid in understanding the interactions between the r-proteins, 16S rRNA and accuracy.

3) Identify key residues in the S4-S5 interaction: By mutating known S5 residues and introducing these fragments in *E.coli* containing specific S4 mutations to select combination

of mutants that can restore wild type phenotype, will enable us to identify key residues in the S4-S5 region.

4) Experimental evolution: We obtained compensatory mutations that reversed the accuracy phenotypes conferred by S4 alteration. We can similarly identify functional sites that can indirectly affect accuracy by obtaining compensatory mutations to different S4, S5, and S12 alterations.

VITA

Divya Kamath was born in Bangalore, India. In May of 2005 Divya graduated from University of Mumbai, India with her Bachelor's in Microbiology. She received her Master's in Microbiology in May of 2007 from University of Mumbai, India. Divya worked as a Junior Research Fellow at Piramal Life Sciences, Mumbai India before coming to University of Missouri-Kansas City (UMKC) in 2011. She received her Master's degree in Molecular Biology and Biochemistry in May of 2013 at UMKC.